ชีววิทยาเชิงสังเคราะห์ด้วยไซยาโนแบคทีเรีย: ความสามารถทางพันธุกรรมในการผลิตเพปไทด์ต้านจุลชีพและ*ทรานส์*-เรสเวราทรอลใน *Synechocystis* sp. PCC 6803

นางสาวสุภาลักส์ แท่นทอง

วิทยานิพนธ์นี้เป็นส่วนหนึ่งของการศึกษาตามหลักสูตรปริญญาวิทยาศาสตรดุษฎีบัณฑิต
สาขาวิชาเทคโนโลยีชีวภาพ
คณะวิทยาศาสตร์ จุฬาลงกรณ์มหาวิทยาลัย
ปีการศึกษา 2558

SYNTHETIC BIOLOGY WITH CYANOBACTERIA: GENETIC CAPACITY TO PRODUCE ANTIMICROBIAL PEPTIDES AND *trans*-RESVERATROL IN *Synechocystis* sp. PCC 6803

Miss Supaluk Tantong

A Dissertation Submitted in Partial Fulfillment of the Requirements
for the Degree of Doctor of Philosophy Program in Biotechnology
Faculty of Science
Chulalongkorn University
Academic Year 2015

Thesis Title	SYNTHETIC BIOLOGY WITH CYANOBACTERIA: GENETIC CAPACITY TO PRODUCE ANTIMICROBIAL PEPTIDES AND *trans*-RESVERATROL IN *Synechocystis* sp. PCC 6803
By	Miss Supaluk Tantong
Field of Study	Biotechnology
Thesis Advisor	Assistant Professor Supaart Sirikantaramas, Ph.D.
Thesis Co-Advisor	Professor Peter Lindblad

Accepted by the Faculty of Science, Chulalongkorn University in Partial Fulfillment of the Requirements for the Doctoral Degree

.....Dean of the Faculty of Science
(Associate Professor Polkit Sangvanich, Ph.D.)

THESIS COMMITTEE

.....Chairman
(Associate Professor Teerapong Buaboocha, Ph.D.)
.....Thesis Advisor
(Assistant Professor Supaart Sirikantaramas, Ph.D.)
.....Thesis Co-Advisor
(Professor Peter Lindblad)
.....Examiner
(Associate Professor Chanpen Chanchao, Ph.D.)
.....Examiner
(Professor Aran Incharoensakdi, Ph.D.)
.....External Examiner
(Somnuk Bunsupa, Ph.D.)

สุภาลักส์ แท่นทอง : ชีววิทยาเชิงสังเคราะห์ด้วยไซยาโนแบคทีเรีย: ความสามารถทางพันธุกรรมในการผลิตเพปไทด์ต้านจุลชีพและ*ทรานส์*-เรสเวราทรอลใน *Synechocystis* sp. PCC 6803 (SYNTHETIC BIOLOGY WITH CYANOBACTERIA: GENETIC CAPACITY TO PRODUCE ANTIMICROBIAL PEPTIDES AND *trans*-RESVERATROL IN *Synechocystis* sp. PCC 6803) อ.ที่ปรึกษาวิทยานิพนธ์หลัก: ผศ. ดร.ศุภอรรจ ศิริกันทรมาศ, อ.ที่ปรึกษาวิทยานิพนธ์ร่วม: ศ. ปีเตอร์ ลินด์บลาด, 174 หน้า.

ไซยาโนแบคทีเรียที่มีความสามารถสังเคราะห์ด้วยแสง ได้รับความสนใจสำหรับการผลิตเอนไซม์และสารออกฤทธิ์ชีวภาพหลายชนิด เนื่องจากไม่นานมานี้ ได้รับการพัฒนาในออกแบบและพันธุวิศวกรรมเพื่อใช้เป็นแหล่งผลิตต้นแบบ งานวิจัยนี้ได้ประเมินความสามารถในการใช้ไซยาโนแบคทีเรียเป็นแหล่งผลิตดีเฟนซินจากพืช ซึ่งเป็นกลุ่มหนึ่งในเพปไทด์ต้านจุลชีพและ*ทรานส์*-เรสเวอราทรอล โดยใช้โปรโมเตอร์สองชนิดคือ P*trc*1Ocore และ P*trc*1O

การวิเคราะห์ทางคอมพิวเตอร์และโครงข่ายการแสดงออกร่วมของยีนถูกนำมาใช้เพื่อระบุ *Os*DEF7 และ *Os*DEF8 จากข้าวที่มีการแสดงออกร่วมกับยีนตอบสนองต่อเชื้อโรค ยีนทั้งสองนี้เมื่อถูกผลิตใน *Escherichia coli* พบว่าอยู่ในรูปไดเมอร์ ที่สามารถยับยั้งเชื้อจุลชีพก่อโรคในพืชได้อย่างมีนัยสำคัญ แม้ว่าจะตรวจพบการแสดงออกยีนทั้งสองในไซยาโนแบคทีเรีย *Synechocystis* PCC 6803 แต่ไม่สามารถตรวจพบรีคอมบิแนนท์เพปไทด์

การแสดงออกในเซลล์เจ้าบ้านต่างชนิดของเอนไซม์ที่เกี่ยวข้องในการผลิต*ทรานส์*-เรสเวอราทรอล ได้แก่ ไทโรซีนแอมโมเนียไลเอส คูมาโรอิวโคเอไลเกส และสติลบีนซินเทส ใน *Synechocystis* PCC 6803 ยีนดังกล่าวมีการแสดงออกและแปลรหัสเป็นโปรตีนที่สามารถละลายได้จากโปรโมเตอร์ทั้งสองชนิด พบว่ามีการผลิตกรดคูมาริกจากปฏิกิริยาในหลอดทดลองและในเซลล์ แต่ไม่สามารถตรวจสอบการผลิต*ทรานส์*-เรสเวอราทรอลได้ แต่กระนั้นก็ตามงานวิจัยนี้ชี้ให้เห็นข้อมูลที่มีคุณค่าต่อการพัฒนาไซยาโนแบคทีเรียเพื่อเป็นเจ้าบ้านทางเลือก

สาขาวิชา เทคโนโลยีชีวภาพ ลายมือชื่อนิสิต .....

ปีการศึกษา 2558 ลายมือชื่อ อ.ที่ปรึกษาหลัก .....

ลายมือชื่อ อ.ที่ปรึกษาร่วม .....

5472888623 : MAJOR BIOTECHNOLOGY
KEYWORDS: SYNECHOCYSTIS PCC 6803, DEFENSIN, RICE, COEXPRESSION NETWORK ANALYSIS, TRANS-RESVERATROL

SUPALUK TANTONG: SYNTHETIC BIOLOGY WITH CYANOBACTERIA: GENETIC CAPACITY TO PRODUCE ANTIMICROBIAL PEPTIDES AND *trans*-RESVERATROL IN *Synechocystis* sp. PCC 6803. ADVISOR: ASST. PROF. SUPAART SIRIKANTARAMAS, Ph.D., CO-ADVISOR: PROF. PETER LINDBLAD, 174 pp.

Phototrophic cyanobacteria are attractive candidates for heterologous production of numerous enzymes and bioactive products due to the recent progress in design and genetic engineering of selected model strains. In this study, the capability of cyanobacteria for producing plant defensin, a class of antimicrobial peptide, and *trans*-resveratrol production was evaluated using the two different promoters P*trc*1Ocore and P*trc*1O.

The in silico and gene coexpression network analyses were performed to identify rice defensins, *Os*DEF7 and *Os*DEF8 that are coexpressed with pathogen-responsive genes. Both recombinant peptides were heterologously produced in *Escherichia coli* as dimer that exhibited significant inhibitory activities against several plant pathogens. Although their gene expressions were detected in *Synechocystis* PCC 6803, the recombinant peptides were not found.

The heterologous expression of enzymes involved in the *trans*-resveratrol production, namely tyrosine ammonia-lyase, coumaroyl CoA ligase, and stilbene synthase, were also performed in *Synechocystis* PCC 6803. The respective genes were expressed and translated to soluble proteins under both promoters. *p*-Coumaric acid was detected in both in vitro and in vivo reactions. However, *trans*-resveratrol could not be detected. Nevertheless, these results provide valuable information toward developing cyanobacteria as an alternative host.

Field of Study: Biotechnology Student's Signature .....
Academic Year: 2015 Advisor's Signature .....
Co-Advisor's Signature .....

ACKNOWLEDGEMENTS

I would like to express my sincere appreciation to my advisor, Assist. Prof. Supa-art Sirikantaramas, Ph.D. for his guidance, supervision throughout the course of this research.

I would like to express my deepest gratitude to my co-advisor, Prof. Peter Lindblad for his provision of experimental facilities in Angstrom Laboratory, Department of Chemistry, Uppsala University, Sweden.

I would like to thank Assoc. Prof. Onanong Pringsulaka, Ph.D. for providing the laboratory facilities for activity assay in this research.

I would like to acknowledge Chulalongkorn University graduate scholarship to commemorate the 72nd anniversary of his majesty king Bhumibol Aduyadej, The 90th anniversary of Chulalongkorn University fund (Ratchadaphiseksomphot Endowment Fund), and the overseas research experience scholarship from Chulalongkorn University for their financial support on my work.

My deep thanks to Rui Miao, and members of Angstrom laboratory for their friendship, kind assistance and suggestion during working in Sweden, also the member of plant biotechnology laboratory (708) for their friendship.

Finally, I would like to express my wholehearted gratitude and the deepest appreciation to Assoc. Prof. Tikamporn Yongvanich, my parents, my sisters, and Weerasak Thakernkarnkit for their morale support, understanding, assistance and strong encouragement throughout my entire education.

CONTENTS

Page

THAI ABSTRACT iv

ENGLISH ABSTRACT v

ACKNOWLEDGEMENTS vi

CONTENTS vii

LIST OF TABLES xii

LIST OF FIGURES xiii

CHAPTER I INTRODUCTION 1

CHAPTER II LITERATURE REVIEWS 4

2.1 AMP 4

2.1.1 Types and structures of plant AMPs 5

2.1.2 Biological activity and mechanism of AMPs 10

2.1.3 Productions of plant AMPs 12

2.1.4 Application of plant AMPs 13

2.2 *Trans*-resveratrol 15

2.2.1 Biosynthetic pathway of *trans*-resveratrol 15

2.2.2 Activity benefits of *trans*-resveratrol 17

2.2.3 Productions of *trans*-resveratrol 19

2.2.3.1 Productions of *trans*-resveratrol in microorganisms 19

2.2.3.2 Productions of *trans*-resveratrol in plant cells 21

2.2.4 Applications of *trans*-resveratrol 23

2.3 Cyanobacteria as a plant genes expressing host 24

CHAPTER III MATERIALS AND METHODS 25

3.1 Equipments 25

3.2 Chemicals 26

3.3 Bacterial and fungal strains 26

3.4 Restriction enzymes 28

3.5 Molecular enzymes 28

3.6 Commercial plasmids 29

Page

3.8 Synthetic oligonucleotides and genes 29
3.9 Purification column 29
3.10 Miscellaneous 30
3.11 Research methodology 30
3.11.1 Analysis of the genes of plant bioactive products; AMPs and *trans*-resveratrol 30
3.11.1.1 In silico analyses of DEFs 30
3.11.1.2 Selection of genes involved in *trans*-resveratrol production 32
3.11.2 Production of *Os*DEFs and *trans*-resveratrol 33
3.11.2.1 Cloning of genes involved in *Os*DEFs and *trans*-resveratrol production 33
3.11.2.1.1 Cloning of *OsDEFs* for expression in *E. coli* 33
3.11.2.1.2 Cloning of *OsDEFs* and genes involved in *trans*-resveratrol production for *Synechocystis* expression 34
3.11.2.2 Expression of *OsDEFs* and enzymes involved in *trans*-resveratrol production 35
3.11.2.2.1 The recombinant peptide in *E. coli* 35
3.11.2.2.2 The recombinant peptide in *Synechocystis* 36
3.11.2.3 Homology study 38
3.11.2.4 Transcript detection 38
3.11.2.4.1 RNA extraction 38
3.11.2.4.1.1 Bacterial RNA 38
3.11.2.4.1.2 Cyanobacterial RNA 38
3.11.2.4.2 Reverse transcription (RT)-PCR 39
3.11.2.5 Protein purification 40
3.11.2.5.1 Purification of GST-tagged protein 40
3.11.2.5.2 Purification of strep-tagged protein 40
3.11.2.6 Protein determination 40
3.11.2.6.1 Protein concentration 40
3.11.2.6.2 SDS-PAGE analysis 41

Page

3.11.2.6.3 Western blot analysis 41
3.11.2.6.3.1 Strep-tagged proteins 41
3.11.2.6.3.2 Flag-tagged proteins 42
3.11.2.7 The activity determination 43
3.11.2.7.1 Determination of the antimicrobials activity of *Os*DEFs expressed from *E. coli* 43
3.11.2.7.1.1 Bioassay of antibacterial activity 43
3.11.2.7.1.2 Bioassay of antifungal activity 43
3.11.2.8 Product determination by LC-MS analysis 44
3.11.3 Determination of growth rate and chlorophyll *a* content of *Synechocystis* 45
3.11.3.1 Growth rate 45
3.11.3.2 Chlorophyll *a* content 46
3.11.4 Optimization conditions for the production of *Os*DEFs and *trans*-resveratrol in *Synechocystis* 46
3.11.4.1 Genetic manipulations 46
3.11.4.1.1 Promoters 46
3.11.4.1.2 Bicistronic design variants 47
3.11.4.1.3 Tag terminus 47
3.11.4.1.4 Homologous recombination 48
3.11.4.2 Substrate concentrations and growth condition for *trans*-resveratrol production 48
3.11.5 In vitro production of *trans*-resveratrol 49
CHAPTER IV RESULTS 50
4.1 AMP production 50
4.1.1 In silico analyses of AMPs 50
4.1.2 Expression of *OsDEFs* in *E. coli* 62
4.1.2.1 Antimicrobial activities of *OsDEFs* 63
4.1.2.2 Homology modeling of *Os*DEFs 66
4.1.3 Expression of *OsDEFs* in *Synechocystis* 68

Page

4.2 *trans*-resveratrol production 73
4.2.1 Gene analysis of genes involved in *trans*-resveratrol production 73
4.2.2. Cloning and expression of genes encoding enzymes involved in *trans*-resveratrol production in *Synechocystis* 74
4.2.3. The expression level of enzymes involved in *trans*-resveratrol production from *Synechocystis* 80
4.2.4 The effects of enzymes involved *trans*-resveratrol production on *Synechocystis* 83
4.2.4.1 The effects on the growth rate 83
4.2.4.2 The effects on the chl *a* content 86
4.2.5 Estimation of the *trans*-resveratrol production in *Synechocystis* 88
4.2.5.1 Metabolites detection from the *Synechocystis* expressed enzymes involved in *trans*-resveratrol production 88
4.2.5.2 Optimization conditions of *trans*-resveratrol production 90
4.2.5.3 In vitro production of *trans*-resveratrol 96
CHAPTER V DISCUSSION 100
5.1 AMPs production 100
5.1.1 In silico analyses of AMPs 100
5.1.2 Production of *OsDEFs* in *E. coli* 103
5.1.2.1 Antimicrobial activities and homology structures of *Os*DEFs .. 104
5.1.3 Production of *Os*DEFs in *Synechocystis* 106
5.2 *Trans*-resveratrol production in *Synechocystis* 108
5.2.1 Expression of genes involved in *trans*-resveratrol biosynthetic pathway 108
5.2.2 Optimization of *trans*-resveratrol production in *Synechocystis* 112
CHAPTER VI CONCLUSION 117
6.1 AMP production 117
6.2 *Trans*-resveratrol production 118
6.3 *Synechocystis* as an alternative expression host 119
REFERENCES 120

Page

APPENDIX A Additional data 142
APPENDIX B General information 150
APPENDIX C Primer lists 156
APPENDIX D Reagent preparations 161
APPENDIX E Methods 169
APPENDIX F Protein determinations 171
APPENDIX G Calculation methods 173
VITA 174

LIST OF TABLES

Page

Table 2-1 Main class of antimicrobial peptides……...10

Table 2-2 Microorganisms used for the production of *trans*-resveratrol…..…….23

Table 4-1 The information of DEF genes in database analyzed by in silico analyses……53

Table 4-2 Partial list of genes coexpressed with *OsDEF7* and *OsDEF8*……....55

Table 4-3 MIC assays of *Os*DEF7 and *Os*DEF8……...……..64

Table 4-4 Bioinformatics information of genes involved in *trans*-resveratrol production……73

Table B-1 Plant DEFs ……..…….150

Table C-1 The list of oligonucleotide sequences used …….……156

Table F-1 Standard curve BSA…….….172

LIST OF FIGURES

Page

Fig. 2-1 Biosynthetic pathway of *trans*-resveratrol……...……..17

Fig. 4-1 Gene coexpression network analysis of *OsDEF7* and *OsDEF8* …….....58

Fig. 4-2 Organ-specific expression profiles of selected *OsDEFs*……...…….59

Fig. 4-3 Phylogenetic relationships of *Os*DEF7 and *Os*DEF8 within the *Os*DEF family…….…...60

Fig. 4-4 Phylogenetic relationships of *Os*DEF7 and *Os*DEF8 with other plant DEFs……...……61

Fig. 4-5 SDS–PAGE analysis of GST-*Os*DEF7 and -*Os*DEF8 fusion protein expressed in *E. coli Rosetta-gami* (DE3)…….....63

Fig. 4-6 The antifungal activities of *Os*DEF7 and *Os*DEF8 against *F. oxysporum* and *H. oryzae*……65

Fig. 4-7 The homology modeled structures of *Os*DEF7 and *Os*DEF8……....67

Fig. 4-8 RT-PCR of *OsDEFs* expressed in DH5αZ1……...68

Fig. 4-9 RT-PCR of *OsDEFs* expressed in *Synechocystis* …….……69

Fig. 4-10 RT-PCR of *OsDEFs* from homologous recombination in *Synechocystis*....70

Fig. 4-11 Growth rate of engineered *Synechocystis* transformed by pEERM and pEERM_ *OsDEFs* ……....71

Fig. 4-12 Chlorophyll *a* content of engineered cells *Synechocystis* with pEERM and pEERM_ *OsDEFs*……72

Fig. 4-13 Western blot analysis of the engineered cells expressing enzymes involved in *trans*-resveratrol pathway under the control of either P*trc*1Ocore or P*trc*1O in DH5αZ1…….……...76

Page

Fig. 4-14 RT-PCR of *PAL* expressed under P*trc*1Ocore and P*trc*1O, and *STS* expressed by BCD constructs in DH5αZ1……..…….76

Fig. 4-15 Western blot analysis of the engineered cells expressing the enzymes involved in the *trans*-resveratrol pathway under the control of P*trc*1O in DH5αZ1...77

Fig. 4-16 Expression analysis of the enzymes involved in *trans*-resveratrol production in *Synechocystis* under two different promoters……78

Fig. 4-17 Expression analysis of *PAL* in *Synechocystis* under two different promoters and *STS* expressed by BCD constructs…….79

Fig. 4-18 RT-PCR analysis of *PAL* expressed under P*trc*1Ocore and P*trc*1O and BCD_*STS* in *Synechocystis*……..80

Fig. 4-19 Protein purification of recombinant enzymes involved in the *trans*-resveratrol biosynthetic pathway from *Synechocystis* PCC 6803 using P*trc*1O promoter...……...…82

Fig. 4-20 Production yield of purified recombinant enzymes in engineered *Synechocystis* PCC 6803……..……...…….…...83

Fig. 4-21 Growth rate of engineered cells of *Synechocystis* PCC 6803 expressing the enzymes of the *trans*-resveratrol biosynthetic pathway under two promoters P*trc*1Ocore and P*trc*1O……..……...……..……85

Fig. 4-22 Chlorophyll *a* content of engineered *Synechocystis* PCC 6803 expressing the enzymes of the *trans*-resveratrol biosynthetic pathway……..…..87

Fig. 4-23 LC-MS analysis of *Synechocystis* PCC 6803 expressing TAL under controlled of P*trc*1Ocore and P*trc*1O…….....89

Fig. 4-24 Production of *p*-coumaric acid in *Synechocystis* PCC 6803 expressing TAL under controlled of P*trc*1Ocore and P*trc*1O…….90

Page

Fig. 4-25 Expression analysis of expressed STS in *Synechocystis* PCC 6803 using two different promoters……..……..91

Fig. 4-26 Production yield of expressed STS in *Synechocystis* PCC 6803 using two different promoters……..……...92

Fig. 4-27 Growth rate of *Synechocystis* PCC 6803 expressing STS under two promoters P*trc*1Ocore and P*trc*1O in different growth conditions……..…94

Fig. 4-28 Chlorophyll *a* content of *Synechocystis* PCC 6803 expressing STS under P*trc*1Ocore and P*trc*1O.……..……..…...95

Fig. 4-29 LC-MS analysis of in vitro production of *p*-coumaric acid…….……97

Fig. 4-30 In vitro production of *p*-coumaric acid...…….…….……98

Fig. 4-31 LC-MS analysis of unknown compound from the in vitro reaction…….....99

Fig. A-1 Graphical presentation of gene coexpression network analysis of *Os*DEFs……..142

Fig. A-2 Protein sequences alignment of *OsDEFs*……147

Fig. A-3 The possible roles of rice *AMPs* ……..…147

Fig. A-4 The expression levels of *Os*AMPs in different parts of rice……...148

Fig. A-5 Dimeric configurations of NaD1.....149

Fig. B-1 GenScript OptimumGeneTM algorithm……..152

Fig. B-2 The partial nucleotide sequence of *Vv*STS optimized by GenScript OptimumGeneTM algorithm……..153

Fig. B-3 P*trc* promoters used.……153

Fig. B-4 Vectors used…….……154

Fig. F-1 Standard curve of BSA…….……...172

CHAPTER I

INTRODUCTION

1.1 Statement of problem

Cyanobacteria are photoautotroph which can be used as a low–priced expression host since they require inexpensive inputs to fuel. Because of their genetic engineering capability, *Synechocystis* PCC 6803 has been widely exploited as an expression host (Huang et al., 2010). Particularly, it has been demonstrated that plant genes were able to be expressed in the genetic modified *Synechocystis* PCC 6803 (Liu et al., 2011).

Antimicrobial peptides (AMPs) are small, naturally occurring peptides that function as host defense peptides against microbial invaders. They are widely spread throughout a variety of both prokaryotic and eukaryotic organisms (Montesinos, 2007). The AMPs in plants have been studied far less than that in animals. There have been many examples of constitutive AMP overexpression in plants that resulted in significantly improved microbial resistance. For instance, the overexpression of tomato defensin, is able to resist fungal pathogens and could be assumed multiple functions related to defense and development (Stotz et al., 2009). From previous studies, such peptides have been identified in *Arabidopsis thaliana* and *Oryza sativa* that found 825 genes and 598 genes, respectively (Silverstein et al., 2007). Therefore, many rice AMPs have not been functionally annotated.

Trans-resveratrol is a polyphenol compounds categorized as plant secondary metabolites produced under stress conditions. It has been reported to exert a number of beneficial health effects in humans, such as anti-cancer, anti-viral, neuroprotective,

anti-aging and anti-inflammatory effects. It can be biosynthesized either from phenylalanine catalyzed by phenylalanine ammonia-lyase (PAL) and coumarate 4-hydroxylase (C4H), respectively, or from tyrosine catalyzed by tyrosine ammonia-lyase (TAL) to produce the intermediate precursor, coumarate. The catalysis of coumaric acid to *trans*-resveratrol requires two additional enzymes: coumaroyl CoA ligase (4CL) and stilbene synthase (STS), respectively. From the literature, the expression of TAL from *Rhodobacter sphaeroides* (*Rs*TAL) (as the initial enzyme) in *A. thaliana* could enhance the metabolic flux in phenylpropanoid pathway leading to highly accumulation of flavonoids and phenylpropanoids (Nishiyama et al., 2010).

Hence, the goal of this research is to explore the capability of the plant antimicrobial peptides (AMPs) and *trans*-resveratrol production in *Synechocystis* PCC 6803.

1.2 Objectives

To use *Synechocystis* PCC 6803 as an expression host for the production of plant bioactive products

1.3 Scope of the study

1.3.1 To select the genes of plant bioactive products; AMPs and *trans*-resveratrol

1.3.2 To produce AMPs and *trans*-resveratrol in *Synechocystis* PCC 6803

1.3.2.1 To construct the expression vector of AMPs and enzymes involved in *trans*-resveratrol production

1.3.2.2 To express *AMPs* and genes involved in *trans*-resveratrol production in *Synechocystis* PCC 6803

1.3.2.3 To determine the expression level and activity of obtained AMPs and enzymes involved in *trans*-resveratrol production

1.3.3 To optimize the production of AMPs and *trans*-resveratrol in *Synechocystis* PCC 6803

1.4 Expected results

Synechocystis PCC 6803 could be used as a host for the productions of rice AMPs and *trans*-resveratrol.

1.5 Thesis organization

This thesis comprises six chapters as follows: Chapter 1 is the introduction. Chapter 2 gives the literature reviews. In Chapter 3, materials and methods are provided. The results can be found in Chapter 4. Chapter 5 is the discussion and the final chapter is the conclusions.

CHAPTER II

LITERATURE REVIEWS

2.1 AMP

In nature, plants possess their physical barriers; cell wall, cutin, lignin, and polysaccharides, as the first-line of defense to prevent their cells from penetrating microbes. Once infected, they produce secondary metabolites for protecting themselves from predators and microbial pathogens. Besides, plants also produce small peptides known as AMPs to eliminate microbial invasion without requiring adaptive immunity (Kulkarni et al., 2006). AMPs are small, naturally occurring peptides that function as host defense peptides against microbial invaders (Silverstein et al., 2007; De-Paula et al., 2008; Bolintineanu and Kaznessis, 2011). Thus, AMPs are any peptides that can protect host cell from infection of microbes, but not include the enzymes eliminating microbes (Maroti et al., 2011; Wu et al., 2011)

AMPs are widely spread throughout a variety of both prokaryotic and eukaryotic organisms, including microorganisms, higher plants, and animals (Montesinos, 2007). Nevertheless, AMPs are abundant among eukaryotic organisms (Kulkarni, 2006). From many literatures, the effective major sources of these peptides are reported in animal, namely: nematodes, arthropods, amphibians, fish, reptiles and mammals, including human (Kulkarni, 2006; Montesinos, 2007; Li et al., 2011; Li and Leong, 2011;Rajanbabu and Chen, 2011; Sperstad et al., 2011). In plants, they also accumulate many types AMPs in their most vulnerable tissues to anticipate and cope with attacks from different pests and pathogens. They could be induced by specific biotic or abiotic agents. AMPs can be found in various tissues of plants; seed,

root, tuber, stem, vascular tissues, bark, leaves, inflorescence, floral tissues, fruit, and shoot.

2.1.1 Types and structures of plant AMPs

In plants, a particular group of such defense-related proteins are cysteine-rich peptides (CRPs) that particularly well represented among plants. The number and arrangement of cysteine residues in the primary sequence distinguishes each AMP from the others. These cysteine residues differently form disulfide bridges in secondary structure. The patterns of disulfide formation can be used to categorize AMP class as defensin, thionin, lipid transfer protein, hevein-type peptide, knottin-type peptide, cyclotide, and snakin. The consensus sequence of cysteine of each class is shown in **Table 2-1**.

Defensin (DEF) is one of the most study AMPs. They have been reported to exhibit the inhibitory activities against fungi, bacteria and insects. They are previously known as ɤ-thionins with the approximate size of 5-10 kDa. They contain six to eight cysteines that they are extremely conserved in almost all plant DEFs (**Table 2-1**). These DEFs share a typical three dimensional folding pattern, stabilized by four disulfide bridges. They resemble a global by connecting between two positions of cysteine for connecting one α-helix to three β-sheets. These bonds crucially stabilize the structure of protein. The structures of plant DEFs are rather similar to animals' such as insect and mammalian DEFs (Tavares et al., 2008).

Thionin (THION) has small variations in amino acid length (45–48 amino acids) in which four to eight of these are cysteine residues. The patterns of

disulfide bonds are shown in **Table 2-1**. THIONs can be divided into three subgroups, α-, β- and ɤ-THIONs. They distinguish from the other group by arranging of disulfide bridges and β-sheet. However, α- and β-THIONs share the same three-dimensional structure. Most studies are γ-THIONs that they are in monomeric forms but they also are capable to form oligomers (Song et al., 2005). It also has been found that its C-termini domain is an important determinant on antifungal activity, as well basic amino acid, such as lysine and arginine (R) (Spelbrink et al., 2004).

Lipid transfer proteins (LTPs) are basic proteins with larger molecules of 70 to 93 amino acids with eight cysteine residues. LTPs are consisting of two families; LTP1 and LTP2 (Kader, 1996). They share some common characteristics, such as basic isoelectric point, low molecular weight, and the number of cysteines at conserved locations that are engaged in forming four disulfide bridges (**Table 2-1**). Several LTPs have been determined for its three-dimensional structures revealing a flexible hydrophobic tunnel within the molecule which can bind to different sizes of lipids (Lerche et al., 1997; Charvolin et al., 1999). This could be suggested that they may involve in transportation of lipids and sphingolipids through the cell membrane. These proteins have also associated with pathogen resistance (Tavares et al., 2008). Therefore, they were classified into a group of non-specific lipid transfer proteins (nsLTPs).

Hevein-type peptides (HEV) are a small chitin-binding peptide consisting of 43 amino acid residues. They structurally similar to hevein that is the peptide isolated from rubber latex (*Hevea brasiliensis*). Such peptides contain eight

cysteine residues forming four disulfide bridges at the conserved position (**Table 2-1**). Although hevein-type AMPs share certain sequence homology, they differ in the number of disulfide bonds. Like chitin binding proteins, they share a common property that is the ability to bind chitin (β 1,4-linked polymer of N-acetylglucosamine and related polysaccharides). These AMPs have been an effective fungicides or plant-responsive peptides against microorganisms and pests (Tavares et al., 2008; Odintsova et al., 2009) because the chitin is the main composition of the cell walls of fungi and the exoskeleton of invertebrates (such as insects and nematodes).

Knottin-type peptides are characterized by a triple-stranded β-sheet and the inhibitor cysteine knot (ICK) arrangement of the three disulfide bonds (Nawrot et al., 2014). The knottin type antifungal peptides have been isolated from *Mirabilis jalapa* L. (Mj-AMP1) and *Phytolacca americana* (PAFP-S) (Cammue et al., 1992; Gao et al., 2001). The structure of PAFP-S consists of a triple-stranded, antiparallel β-sheet with a long loop region connecting β-strands 1 and 2. This peptide from garden pea (PA1b) acts on insecticides through inhibition of vacuolar ATPase (Chouabe et al., 2011).

Cyclotides were originally discovered in the coffee-family plant *Oldenlandia affinis* (Rubiaceae) (Koehbach et al., 2013). They are ribosomally synthesized cysteine-rich peptides that cyclized head-to-tail backbone (hence the named as cyclo-peptides). They comprise 30 amino acids with six conserved cystine residues that are arranged in a knot topology to three disulfide-bonds (**Table 2-1**). The combination of a knotted and strongly braced structure makes them exceptionally stable (Craik, 2010). Cyclotides have their hydrophobic face

located on different regions of the surface, this may result from membrane disruption by the hydrophobic cyclotides (Wang et al., 2009; Kamimori et al., 2005).

Snakins were named because of some parts of their amino acid sequences are similar to the peptide of snake venoms, snakins. They are basic antimicrobial peptides composed of 63 amino acid residues with the extreme conservation of 12 cysteines folding six potential disulfide bonds. There are not only cysteines in the homology sequence, but some amino acids are also found in the same pattern (**Table 2-1**). Their amino acid sequence alignments similar to those of the members of gibberellic acid stimulated transcript (GAST) family from tomato and the gibberellic acid stimulated in *Arabidopsis* (GASA) family from *Arabidopsis* (Segura et al., 1999; Berrocal-Lobo et al., 2002). Snakin/GASA proteins are expressed in different plant organs. However, most of these genes are regulated by plant hormones and participate in hormonal signaling pathways modulating hormonal levels and responses (Nahirñak et al., 2012). Differently, the action of these AMPs namely does not lead to leakage of cell membranes under low or high salt conditions and does not destroy lipid membranes (Caaveiro et al., 1997).

Apart from cysteine-rich molecules, a new group of plant defense molecules with activity against bacteria have been reported as the glycine-rich proteins (GRPs) which were first described as storage proteins in the plant (Mousavi and Hotta, 2005; Mandal et al., 2009). Myrosinase-binding proteins (MBPs) are the members of GRPs. They are extremely cationic, showing two disulfide bridges. They associate with hydrolysis of glucosinolates by

myrosinase enzymes. Thus, they act against fungi, bacteria and insects. Furthermore, the 2S albumin is a water-soluble storage protein, rich in glutamine. These proteins are low molecular weight and they also form disulfide bonds similar to CRPs. Structurally, they have four α-helices and four disulfide bonds as found the α -amylase/trypsin inhibitors and nsLTPs. Additionally, maize has been reported to produce the cell-penetrating peptides which derived from the proline-rich N-terminal repetitive domain. They have been shown to interact with the membrane (Veldhoen et al., 2008). The novel antibiotic peptides have reported as shepherdins, which are linear glycine/histidine-rich peptides isolated from the roots of shepherdins purse (*Capsella bursa-pastoris*). In addition, macrocyclic cystein-knot peptides were also recovered from different plants belonging from the Rubiaceae families when screening for anti-HIV compounds (Lee et al., 2012).

Table 2-1 Main class of antimicrobial peptides

Class	The number of amino acid	Consensus sequence
Defensin	35-70	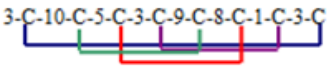
Thionin	25-55	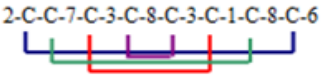
Lipid transfer protein	65-95	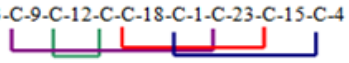
Hevein-type peptides	30-45	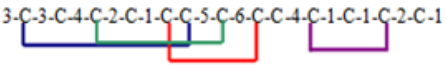
Snakin	60-90	3-C-3-C-2-RC-9-C-3-C-2-CC-2-C-2-CVP-1-G-7-CPCY-12-KCP

2.1.2 Biological activity and mechanism of AMPs

AMPs provide alternative means to eliminate invading pathogens. Their functions can be classified as direct antimicrobial activity and immune modulatory properties. However, the majority of AMPs share two features that enable them to interact with microbes by process of phospholipid membrane permeation; namely, the barrel stave (i) and the carpet mechanisms (ii) (Matsuzaki, 1999; Rotem and Mor, 2009).

(i) Barrel stave: cationic AMPs initially interact through electrostatic forces with negatively charged bacterial membranes. They modify anionic lipids or wall components to reduce the net negative charge of their envelope during infection and in response to the host environment. This mechanism is found in plant DEFs, it is believed that electrostatic binding between the arginine groups of cationic DEFs and the membranes rich in anionic phospholipids induce the permeabilization causing leakage of intracellular metabolites (Mendez-Samperio, 2008).

(ii) Carpet model: AMPs can form amphipatic structures in hydrophobic environments and thus penetrate into the bacterial phospholipid bilayer. Once inserting into membrane layers, they are formed irreversible pores or destabilized.

AMPs do not only act as a microbicide, but also cause the changes of cytoplasmic membrane formation, or inhibition of cell-wall synthesis, nucleic acid, protein and even enzymatic activity (Cho and Lee, 2011). The most interesting property of AMPs is their cell specificity by which they kill microbes but are non-toxic to mammalian cells. The relative insensitivity of eukaryotic cells to AMP is generally ascribed to the differences in lipid composition between eukaryotic and prokaryotic cell membranes (Dathe and Wieprecht, 1999; Matsuzaki, 1999). It has been proposed that the net positive charge of the AMPs accounts for their preferential binding to the negatively charged outer surface of bacteria, which is different from the predominantly zwitter ionic surface of normal mammalian cells (Devaux, 1991; Dolis et al., 1997). Relatively lower negative membrane potential in eukaryotes than in

prokaryotes is thought to play an important role in their selectivity (Matsuzaki, 1999). Therefore, these molecules can rapidly kill a broad range of bacteria (both positive and negative grams) and enhance the quality and the effectiveness of innate immune system with unique inhibitory mechanisms. In addition, these antimicrobial mechanisms differ from those of currently distributed conventional antibiotics. Therefore, AMPs are expected to be sources of new type of antibiotics. Furthermore, the selectivity of some AMP towards tumor cells has been suggested due to a higher negative membrane potential of tumor cells, than the normal cells in many types of cancer. Thus, these might be a promising anti-cancer compound (Hoskin and Ramamoorthy, 2008).

2.1.3 Productions of plant AMPs

AMPs can be obtained from the isolation of natural sources, chemical synthesis, and heterologous expression. Among these sources, the natural source extraction is a labor intensive and time-consuming process. It cannot provide a consistence quality of extract, and cannot provide peptides in large amounts. Chemical synthesis is very efficient, but it is a complex and costly process. Therefore, it is also not an ideal platform for large-scale peptide production. Comparatively, recombinant approach provides an economical means for protein manufacture. This technology therefore offers the most cost-effective means for large-scale peptide production. In general, many AMPs have been successfully obtained through recombinant production in several heterologous hosts such as microbes (Parachin et al., 2012) and plants (Ingham and Moore, 2007). Among these systems, *E.coli* has been the most widely used microbial

host(Li and Chen, 2008; Li, 2011). In *E.coli*, AMPs have been successfully expressed by different methods, which include expression as fusion proteins (Piers et al., 1993), N-terminal inclusion body forming proteins (Haught et al., 1998; Lee et al., 2000), N-terminal anionic pre-pro-region (Zhang et al., 1998), tandom repeats of an anionic complement and the AMP itself (Lee et al., 2000). These have been applied to protect them from proteolytic degradation and to mask these peptides lethal effect towards the host. Most AMPs have also been produced in plant as protective peptides. Importantly, plant-based system is considered to address drawbacks of other biological expression systems (Basaran and Rodríguez-Cerezo, 2008). The main advantage is the post translational process; proper folding, glycosylation and disulfide bond formation, which is critical for AMP activity (Ramessar et al., 2008). Plant-based platform can be widely applied ranging from cultures of cells, or tissues to transgenic plants. However, in this system, cost and time are required for production, market size of the product, production scale, and capacity of the process which are all the main disadvantages (Holaskova et al., 2015).

2.1.4 Application of plant AMPs

AMPs have attractive properties that are they illustrate a broad range of antimicrobial activities, and they mainly target microbial membranes, impeding the ability of microbes to develop resistance against them. Therefore, these peptides could be promising candidates for new antibiotics (Hancock and Sahl, 2006). However, efficacy and safety must be addressed before the peptides can be brought to clinical trials.

Recently, there are currently several animal AMPs which went through various phases of clinical trial pipeline. For example, bovine indolicine called omiganan, for the treatment of papulopustular rosacea (in phase III) (Moual et al., 2013). Although the applications of plant AMP for medical propose have been the challenging strategies. As, plant AMPs have been less studied comparing to animals'. Additionally, the plant AMP should meet the same standards of safety, quality and effectiveness offered by counterparts other AMPs.

For agricultural application, plant AMPs have been expressed in transgenic plants to reduce the need of conventional crop protection agents that is desirable and cost effective (De Bolle et al., 1996). Transgenic plants have been widely studied as their morphology unaffected. This is because after challenging these plants with bacterial or fungal phytopathogens, they demonstrated enhanced resistance against various economically important pathogens in the second generation. For instance, the gene encoding thionin from barley endosperm expressed under CaMV35S promoter in transgenic tobacco plants could resistance to *Pseudomonas syringae* pv. Tabaci 153 and *P. syringae* pv. *syringe* (Carmona et al., 1993). The transgenic plants also displayed insecticidal properties (Ponti et al., 2003). Nevertheless, the future commercial applications of plant AMPs production will mainly depend on the compatibility of AMP production strategy with the regulatory standards, agricultural value of the host plant as well as end-user needs and concerns.

2.2 *Trans*-resveratrol

Trans-resveratrol (3, 5, 4´-*trans*-trihydroxystilbene) is a plant polyphenolic compound as a member in the stilbene family. It is produced as a secondary metabolite under stress conditions, as well as the invasion of microbes and insect. This compound could be found in many botanical sources, particular in peanuts (*Arachis hypogaea*) and grape (*Vitis vinifera*). In grape, it can be found in the seed and skin of the fruits (Fernández-Mar et al., 2012). Grapevine could accumulate *trans*-resveratrol in leaves at high concentrations up to 400 µg g^{-1} fresh weight (Sbaghi et al., 1995).

2.2.1 Biosynthetic pathway of *trans*-resveratrol

Trans-resveratrol can be synthesized through phenylpropanoid pathway (**Fig. 2-1**). This is an important plant secondary metabolism pathway that involves in the synthesis of a wide variety of plant natural products including flavonoids, lignins, coumarins, and stilbenes (Zhang et al., 2011). It uses the aromatic amino acid from the shikimate pathway as the substrate; phenylalanine or tyrosine, which are catalyzed by phenylalanine/tyrosine ammonia-lyase (PAL/TAL) (EC 4.3.1.5/EC 4.3.1).

In plant, PAL is the first key enzyme that links between primary metabolism and secondary metabolism. It catalyzes the formation of *trans*-cinnamic acid in the cytosol by non-oxidative deamination of L-phenylalanine, which could be the rate-limiting step in the phenylalanine metabolism pathway. Subsequently, *trans*-cinnamic acid is hydroxylated by cinnamate-4-hydroxylase (C4H), a cytochrome P450 monooxygenase (EC 1.14.13.11) (Fahrendorf and

Dixon, 1993; Teutsch et al., 1993) to produce *p*-coumaric acid at a position close to the membrane of rough ER and the golgi apparatus (Sato et al., 2004). The *p*-coumaric acid is then activated to its coenzyme A (CoA) thioester, *p*-coumaroyl CoA by *p*-coumarate CoA ligase (4CL) (EC 6.2.1.12). Apart from plants, grasses and some species of fungi and bacteria possess another initial enzyme of phenylpropanoid pathway, TAL (Ferrer et al., 2008). It directly uses tyrosine as a substrate, thus reducing the number of enzymes to produce *p*-coumaroyl CoA from three in the general pathway to two enzymes (Ferrer et al., 2008). Finally, stilbene synthase (STS) (EC 2.3.1.95) catalyzes the sequential decarboxylative addition of three acetate units from malonyl CoA and one molecule of coumaroyl CoA to form *trans*-resveratrol (Dixon and Paiva, 1995; Halls and Yu, 2008).

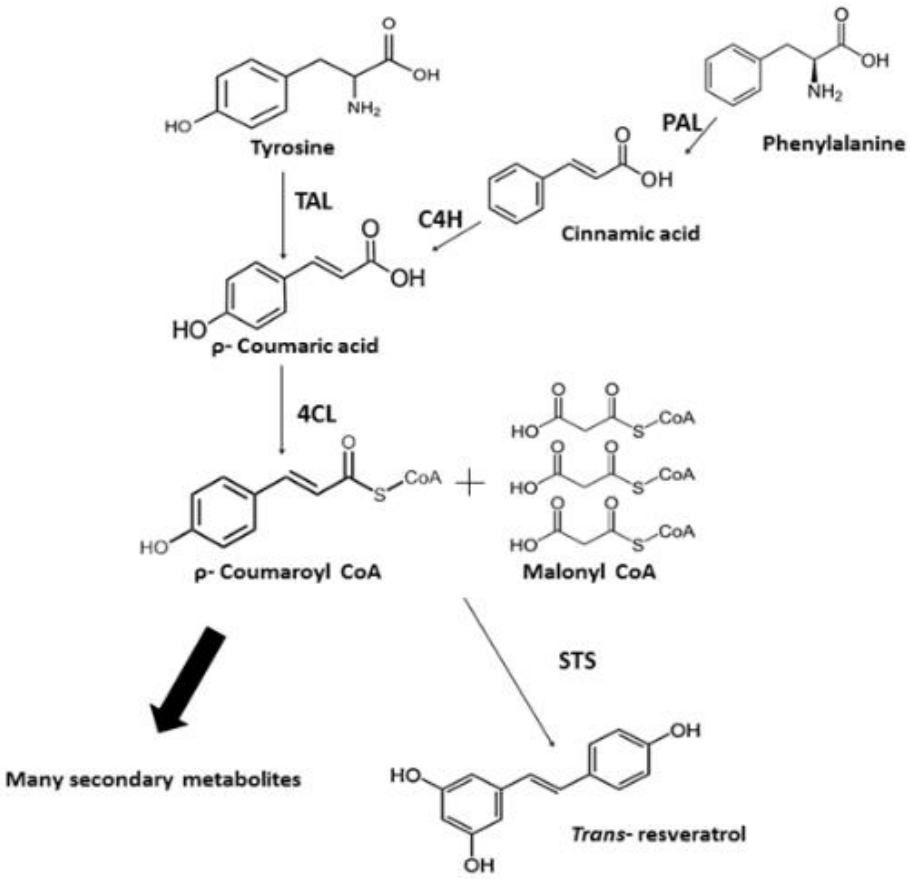

Fig. 2-1 Biosynthetic pathway of *trans*-resveratrol. TAL, tyrosine ammonia-lyase; PAL, phenylalanine ammonia-lyase; C4H, cinnamate-4-hydroxylase; 4CL, 4-coumarate CoA ligase; STS, stilbene synthase.

2.2.2 Activity benefits of *trans*-resveratrol

From the dietary information, *trans*-resveratrol could be absorbed around 70% ingestion in approximately 30 min after intake (Walle et al., 2004). *Trans*-resveratrol has been considered as no adverse side effects compound, unless extremely over dose intake. From the studies, rats were still healthy after testing with 1,000-times the content of this compound in red wine for 28 days, and 700

mg of Resvida™ (high purity *trans*-resveratrol content) /kg body weight/day for 90 days (Williams et al., 2009).

Trans-resveratrol has been studied to exert numbers of beneficial health effects in humans, such as anti-cancer, anti-viral, neuroprotective, anti-aging and anti-inflammatory effects (Bradamante et al., 2004; Anekonda, 2006; Sharma et al., 2007; Kundu and Surh, 2008). As an antioxidant, *trans*-resveratrol enhances the antioxidant capacity of blood plasma and reduce lipid peroxidation (Wenzel et al., 2005; Whitehead et al., 1995), which is strongly caused the coronary heart disease and myocardial infarction (Holvoet, 2004). Furthermore, these effects protect the cardiovascular system in a multidimensional ways; preventing platelet aggregation, decreasing the rate of triglyceride synthesis, and inhibiting the deposition of cholesterol and triglycerides (Bertelli et al., 1995; Wang et al., 2002). *Trans*-resveratrol has been studied that it could extend the lifespan of mice whose diet supplemented with such compound, and decrease the cases of the negative effects of a high-calorie diet (Baur and Sinclair, 2006). *Trans*-resveratrol could also slow the development of tumor through multiple complementary mechanisms including the induction of cell cycle arrest an apoptosis, promoting the anti-proliferative and pro-apoptotic effects of tumor cells, and inhibition of cyclooxygenase activity to reduce the risk of many cancers (Schneider et al., 2001; Garvin et al., 2006). *Trans*-resveratrol is converted to piceatannol, a compound with known anticancer, by additional aromatic hydroxy group. (Potter et al., 2002). Regarding the concentration studied, *trans*-resveratrol has been proved for the pharmacologically actives in vitro anticarcinogenic activity at doses ranging

from 5 to 100 mM, and in vivo doses for the prevention of cardiovascular disease are between 100 nM and 1 mM (Bertelli, 2007). Besides, 50 mg of *trans*-resveratrol /kg body weight could result in the direct insulin-suppressive action in the rat (Szkudelski, 2008). *Trans*-resveratrol has shown the strong neuroprotective effects, as it is able to penetrate the blood–brain barrier and potentially protect against brain damage (Dong et al., 2008). Low doses of this compound could prevent the effect of Huntington's, Parkinson's, and Alzheimer's diseases (Sinclair, 2005; Parker et al., 2005). Other properties of *trans*-resveratrol, it reportedly showed activity against various types of microorganisms such as some plant pathogenic fungi, human pathogenic bacteria and fungi, as well as the protozoan parasite Leishmania major (Zhang et al., 1998; Jung et al., 2007; Jung et al., 2005; Kukrić and Topalić-Trivunović, 2006; Lu et al., 2008; Kedzierski et al., 2007).

2.2.3 Productions of *trans*-resveratrol

As *trans*-resveratrol has several benefits, many attempts have tried to operate in microorganisms such as yeast and bacteria, and plant cell cultures in order to produce high amount of its.

2.2.3.1 Productions of *trans*-resveratrol in microorganisms

Over decades, the productions of numerous molecules have been widely used microorganism-based systems for large quantities production. For *trans*-resveratrol production, the powerful strategy has been investigated in microbes by two methods; pathway engineering and

introducing of selective genes (Donnez et al., 2009). To obtain *trans*-resveratrol from the precursors of the pathway; L-phenylalanine or L-tyrosine, engineering the genes encoded enzymes of the entire *trans*-resveratrol pathway is the most promising option. Many strains have initially been manipulated with the *PAL* such as *Saccharomyces cerevisiae, Lactococcus lactis, Aspergillus niger, and Aspergillus oryzae. TAL* from *Rhodobacler sphaeroides* was also studied. However, it could produce *trans*-resveratrol when coumaric acid added to the medium. Hence, increasing the activities of these enzymes in bacteria have been an ongoing efforts (Xue et al., 2007). Alternatively, the specific genes encoded the enzymes of biosynthetic pathway is directly introduced into the microorganisms. For instance, yeast *S. cerevisiae* and *E. coli* transformed with the 4CL gene from tobacco and STS gene from grapevine enabled them to produce 5.8 and 16 mg L^{-1} *trans*-resveratrol, respectively (Beekwilder et al., 2006). Similarly, 4CL gene from *A. thaliana* and a STS gene from *Arachis hypogea* transformed into *E. coli* were able to convert *p*-coumaric acid into *trans*-resveratrol around 100 mg L^{-1} (Watts et al., 2006). This suggested that different plant genes encoding enzymes introduced into microorganisms could show different yields of *trans*-resveratrol production. Nevertheless, the production efficacy depends on various factors, such as the species and the strain, the origin of the transferred genes, as well as other parameters of manipulation process.

2.2.3.2 Productions of *trans*-resveratrol in plant cells

The culture system of plant cells is typically carried out in a liquid medium under aseptic conditions (Namdeo, 2007). This is the most efficient way to synthesize and secrete the compounds to the medium (Zhao et al., 2005), also it is adaptable for large-scale bioreactors (Roberts and Shuler, 1997). There are two particular plant-cell model systems that currently in development; cell suspension cultures and hairy roots (Guillon et al., 2006).

Cell suspension cultures constitutively produce the compound in response to stress after elicitation. The genetic modification is therefore not required. The most common of elicitors utilized for *trans*-resveratrol production such as methyljasmonate, cyclodextrins or chitosan (Repka, 2001). They basically represent the in vitro production of *trans*-resveratrol. The amount of *trans*-resveratrol could be varied according to plant species, elicitor and culture conditions. The concentrations of *trans*-resveratrol produced from plant cell cultures could be reached up to the amount of naturally occurring in the plant (reviewed in Donnez et al., 2009). There have been reports of various cell suspensions producing *trans*-resveratrol (Kouakou et al., 2006). The grapevine has originally and widely been used for production of *trans*-resveratrol and its derivatives (Vitrac et al., 2002). Recently, a bacterial *TAL* was introduced in *A. thaliana* leading to an increased metabolite flux into phenylpropanoid pathway (Nishiyama et al., 2010).

Hairy root cultures are able to grow in liquid media and produce secondary metabolites. They are transformed the plant genes by transferring

recombinant plasmid of Ri T-DNA (from *Agrobacterium rhizogenes*), which causes a genetic modification leading to the development of roots. For the production of *trans*-resveratrol, hairy root cultures of peanut (*Arachis hypogea*) showed high amount of compound after eliciting with sodium acetate for 24 hours (Tassoni et al., 2005).

Calli are the group of dedifferentiated cells that grow on a solid culture medium. Similar to cell suspension culture, the production *trans*-resveratrol in callus cultures has been linked to the stimulation of plant defense mechanisms. Nonetheless, calli showed better capability to produce *trans*-resveratrol, as it could synthesize the aromatic compound which is the important precursor for *trans*-resveratrol biosynthesis pathway. Basically, the calli grew better, thus it could produce large amounts of the phenylalanine when the medium added with para-fluorophenylalanine (PFP) which reached the production up to 0.25% dry weight. Calli of *Vitis amurensis* have been shown to synthesize *trans*-resveratrol after treated with 0.1 mM sodium nitroprusside, up to 0.15% of dry weight (Kiselev et al., 2007). In addition, a rolB gene under the control of 35S promoter was transformed into these calli by the *Agrobacterium tumefaciens* leading the production of *trans*-resveratrol approximately 3.15% dry weight. However, large scale production in callus cultures has been the difficulties, as space requirements and culturing time have to be optimized.

Table 2-2 Microorganisms used for the production of *trans*-resveratrol (taken from in Donnez et al., 2009)

Microorganisms	Species	Introduced genes	Origin of genes	Amount of *trans*-resveratrol produced
Yeast	*Yarrowia lipolytica*	*PAL/TAL, C4H, 4CL, STS*	*Rhodotorula glutinis* (*PAL/TAL*), *Streptomyces coelicolor* (*4CL*), *Vitis* sp. (*STS*)	1.46 mg/l
	Lactococcus lactis *Aspergillus niger* *Aspergillus oryzae*	*PAL, C4H, 4CL, STS*	*Arabidopsis thaliana* (*PAL, C4H, 4CL*), *Rheum tataricum* (*STS*)	–
	Saccharomyces cerevisiae	*PAL, C4H, 4CL, STS*	*Arabidopsis thaliana* (*PAL, C4H, 4CL*), *Rheum tataricum* (*STS*)	–
		TAL, 4CL, STS	*Rhodobacter sphaeroides* (*TAL*), *A. thaliana* (*4CL*), *V. vinifera* (*STS*)	5 mg/l
		4CL, STS	*Populus trichocarpa x Populus deltoides* (*4CL*), *V. vinifera* (*STS*)	1.45 mg/l
			Nicotiana tabacum (*4CL*), *V. vinifera* (*STS*)	5.8 mg/l
Bacteria	*Escherichia coli*	*4CL, STS*	*S. coelicolor* (*4CL*),*Vitis* sp. (*STS*)	3.6 mg/l
			A. thaliana (*4CL*), *Arachis hypogaea* (*STS*)	100 mg/l
			N. tabacum (*4CL*), *V. vinifera* (*STS*)	16 mg/l
			Lithospermum erythrorhizon (*4CL*), *A. hypogaea* (*STS*)	171 mg/l
		TAL, 4CL, STS	*A. thaliana* (*4CL*), *Rhodobacter capsulatus* (*TAL*), *R. tataricum* (*STS*)	–

2.2.4 Applications of *trans*-resveratrol

Currently, the main production of *trans*-resveratrol is from the field cultures of *Polygonum cuspidatum* (syn. *Fallopia japonica*). China is the main producer of this extracts, with different degrees of purity. In the cosmetics, grapevine is the main source of *trans*-resveratrol and its derivatives, as it is the most suitable raw material for cosmetics such as facial creams. However, the main market for *trans*-resveratrol is focused on health improving proposes, as the nutraceuticals. Nowadays, the demand for *trans*-resveratrol from grapevine, in relation to the French paradox, might further increase rapidly, and new sources might soon become a necessity.

2.3 Cyanobacteria as a plant genes expressing host

The heterologous expression of plant genes in plant cells or microorganisms however has some limitations, eg; plant cell cultures need long time for cultivation, while microorganisms cannot express large amount of this plant products, owing to the difference of biomolecular systems. Particularly, the cost of microbial culture medium is a significant barrier for using them as an expression host. To produce this biologically active molecule in large scale, the biotechnology could be the powerful means applied for low cost and rapid production from the suitable sources. Therefore, photoautotrophic cyanobacteria might be an attractive candidate for heterologous expression due to their genetic engineering capability and requiring the inexpensive inputs; sunlight as fuel.

Cyanobacteria *Synechocystis* PCC 6803 (from here on refer to as *Synechocystis*) has been widely exploited as a model cyanobacterial expression host (http://genome.kazusa.or.jp/cyanobase). For instance, plant thioesterase gene was introduced into cyanobacteria making them producing feasible yield of fatty acid production (Liu et al., 2011). Relatively, the isoprene synthase gene from kudzu was optimized for codon preference and was expressed in *Synechocystis*. The result indicated that the optimized gene showed much higher expression level than that of wild type (Lindberg et al., 2010). These researches indicated that cyanobacteria could be applied as a source for biofuel production. Plant terpenoids could also be heterologously produced in cyanobateria (Pattanaik and Lindberg, 2015). This evidently shows that *Synechocystis* PCC 6803 could be the practical host for plant genes expression.

CHAPTER III

MATERIALS AND METHODS

3.1 Equipments

Agarose gel electrophoresis	(BioRad, USA)
Autoclave	(Ta Chang Medical instrument, Taiwan)
Balance	(Sartorius, Germany)
Blotting equipment	(Biorad, USA)
Centrifuge tubes	(Oxygen scientific, USA)
Digital balance	(Mettler Toledo, USA)
Digital dry bath	(Labnet International, Inc., USA)
Gel documentation	(UVP, UK)
Fridge and freezer	(Electrolux, Sweden)
High performance liquid chromatography	(Shimudzu, Japan)
Incubator	(Gallenkamp, UK)
Incubator shaker	(Kuhner shaker, Switzerland)
Laminar flow	(Thermo electron corporation, USA)
Magnetic stirrer	(KIKA Labortechnik, Malaysia)
Magnetic bar	(Lio Lab Limited Partnership)
Microcentrifuge	(Satorious, Germany)
Microplate spectrometer	(ASYS Hitech GMBH, Austria)
Microrefrigerated centrifuge	(Hettich, USA)
Microwave	(Sharp, Thailand)
Nanodrop	(Thermo Scientific, UK)

Oven	(Heraeus, Germany)
pH meter	(Mettler Toledo, USA)
Power supplier	(Amersham Bioscience, Sweden)
Refrigerated incubator shaker	(New Brunswick Scientific Co., Ltd, China)
Rotary shaker	(IKA Labortechnik, Germany)
Shaker	(Multitron, Germany)
Slab gel electrophoresis equipment	(Biorad, USA)
Spin down centrifuge	(Bertintechnologies, Sweden)
Thermal cycler	(Biorad, USA)
UV-VIS spectrometer	(Thermo Scientific, UK)
Vortex	(Scientific industries, USA)

3.2 Chemicals

In all experiments, the analytical grade and/or molecular biological grade chemicals and reagents were purchased from various manufacturers; namely, Sigma (USA), Merck (Germany), Fluka (Switzerland), Carlo Erba (Italy), Ajax Finechem (Australia), Difco (USA), Usb (USA), Biorad (USA), Amresco (Canada), VWR Chemicals (Canada), and Invitrogen (Canada).

3.3 Bacterial and fungal strains

E. coli DH5α, (F-Ø80*lac*ZΔM15Δ (*lac*ZYA-*arg*F) U169 *deo*R *rec*A1 *end*A1 *hsd*R17(rk-, mk+) *pho*A*sup*E44 *thi*-1 *gyr*A96 *rel*A1 λ-) were used as hosts for plasmid propagation.

E. coli DH5αZ1, ((F-) supE ΔlacU169 ΔargF hsdR17 recA1 endA1 gyrA96 thi-1 relA1) were used as hosts for propagation of plasmid contained P*trc*O1core and P*trc*1O.

E. coli HB101, F-, *hsdS20* (*rB-*, *mB-*), *xyl5, l-, recA13, galK2, ara14, supE44, lacY1, rpsL20* (*strr*), *leuB6, mtl-1, thi-*, contain the helper plasmid pRL443 facilitating the cyanobacterial transformation (Elhai et al., 1998).

E. coli Rosetta (DE3), pLysS (F^- ompT $hsdS_B(R_B^- m_B^-)$ gal dcm λ(DE3 [lacI lacUV5-T7 gene 1 ind1 sam7 nin5]) pLysSRARE (Cam^R) were used as hosts for expression.

Erwinia carotovora, Kingdom: Bacteria, Phylum: Proteobacteria, Class: Gammaproteobacteria, Order: Enterobacteriales, Family: Enterobacteriaceae, Genus: Erwinia, Species: carotovora. It is a gram-negative, rod-shaped bacterium causing cell death through plant cell wall destruction by creating an osmotically fragile cell or soft rot of plant.

Fusarium oxysporum, Kingdom: Fungi, Division: Ascomycota, Class: Sordariomycetes, Subclass: Hypocreomycetidae, Order: Hypocreales, Family: Nectriaceae, Genus: Fusarium, Species: oxysporum. Their aerial mycelium first appears white, and then may change from violet to dark purple. They infect the vascular system causing lacking of water ensues such as stomata leaves.

Helminthosporium oryzae, Kingdom: Fungi Division: Ascomycota Class: Dothideomycetes Subclass: Pleosporomycetidae Order: Pleosporales Family: Pleosporaceae Genus: Helminthosporium Species: oryzae. The mycelium is brown causing the withering and yellowing of leaves or brown spot disease.

Xanthomonas oryzae, Kingdom: Bacteria, Phylum: Proteobacteria, Class: Gammaproteobacteria, Order: Xanthomonadales, Family: Xanthomonadaceae, Genus: Xanthomonas, Species: pv. *oryzae* (*Xoo*) and pv. *oryzicola* (*Xoc*). They are a gram-negative, rod-shaped, round-ended bacterium. They infect the plants leaf veins as well as the xylem causing blockage and plant wilting, or bacterial leaf blight.

The bacterial and fungal strains used in antimicrobial assays, were obtained from plant protection research and the development office, Thailand.

3.4 Restriction enzymes

*Bam*HI	Thermo Scientific (USA)
*Eco*RI	New England Biolabs (USA)
*Hin*dIII	New England Biolabs (USA)
*Pst*I	Thermo Scientific (USA)
Sal I	New England Biolabs (USA)
Spe I	Thermo Scientific (USA)
*Xba*I	Thermo Scientific (USA)

3.5 Molecular enzymes

FastAP Thermosensitive Alkaline Phosphatase	Thermo Scientific (USA)
Phusion	Thermo Scientific (USA)
Phusion Hot Start II	Thermo Scientific (USA)
T4 DNA ligase	New England Biolabs (USA)

3.6 Commercial plasmids

CloneJET PCR Cloning Kit	Thermo Scientific (USA)
pGEX-6P-3	addgene (USA)

3.7 Kits used

CloneJET PCR Cloning Kit	Thermo Scientific (USA)
Gel DNA Recovery Kit	Zymo reasearch (USA)
GeneJet RNA extraction kit	Thermo Scientific (USA)
PCR Purification Kit	Thermo Scientific (USA)
Plasmid Extraction Kit	Thermo Scientific (USA)
qScript cDNA synthesis kit	Quanta Biosciences (USA)

3.8 Synthetic oligonucleotides and genes

All synthetic oligonucleotides primers and DNA sequencing were serviced from Bio Basic Inc. (Canada) and Macrogen (Netherlands). The primers information was shown in Appendix C. The synthetic oligonucleotides were synthesized by GenScript USA Inc. (USA). Rice cDNAs were obtained from Rice Genome Resource Center, (Japan).

3.9 Purification column

Pierce Glutathione Spin Columns	Thermo Scientific (USA)
Strep-Tactin Spin Column	IBA (Germany)

3.10 Miscellaneous

TriDye ^{TM} 1 kb DNA Ladder	New England Biolabs (USA)
Prestained Protein Ladder, Broad Range	Fermentas (Canada)
6X DNA loading dye	Fermentas (Canada)

3.11 Research methodology

All experiments were performed at least in triplicates and the results were presented as mean values. The research methodology is as follows:

3.11.1 Analysis of the genes of plant bioactive products; AMPs and *trans*-resveratrol

3.11.2 Production of DEFs and *trans*-resveratrol

3.11.3 Determination of growth rate and chlorophyll *a* content of *Synechocystis*

3.11.4 Optimization of the production of DEFs and *trans*-resveratrol in *Synechocystis*

3.11.1 Analysis of the genes of plant bioactive products; AMPs and *trans*-resveratrol

3.11.1.1 In silico analyses of DEFs

The plant AMP genes have been classified into several families based on amino acid sequence homology by PhytAmps (Hammami et al., 2009[a]) (http://phytamp.pfba-lab-tun.org). This source has identified and has reported the functions of plant AMPs. However, DEF has widely been studied family. Therefore, the genes of *DEFs* and *DEF* like (*DEFL*) proteins in genome of *O. Sativa Japonica* (*Os*) were identified by two databases; Phytozome (Goodstein et al., 2012) (http://www.phytozome.net)

and Gramene (Ware et al., 2002) (http://www.gramene.org). From these data, the basic of coexpression analysis was applied to select the active *OsDEF*s that is the genes involved in the plant defense mechanism having simultaneously being expressed with the pathogen-responsive genes. The coexpressions of *OsDEFs* with resistance proteins were considered by Plantarraynet (Lee et al., 2009) (http://arraynet.mju.ac.kr) and RiceArrayNet (http://www.ricearray.org). The % cut off was set at 60% ($r_{\text{two-spots}}$ at 6.0). Moreover, the expression level in rice organs was determined by microarray database, Rice eFP browser (Jain et al., 2007). The expression profile is ranged from vegetative reference tissues/organs (seedling, root, mature leaf, and young leaf), shoot apical meristem (SAM), stages of panicle development (P1–P6), and seed developmental stages (S1–S5). These developmental stages have been categorized according to panicle length and days after pollination based on the specifications from (Itoh et al., 2005). The *OsDEFs* coexpressed with plant-responsive mechanisms were aligned for comparing the similarity within the group. Furthermore, the candidate *OsDEFs* were compared to the other plant DEFs (the gene informations shown in **Table B-1**, Appendix B) by using neighbore-joinning estimation analysis with Molecular Evolutionary Genetics Analysis (MEGA 4) with bootstrap resampling as default (Tamura et al., 2007). From in silico analyses, the full-length cDNA sequences of the candidates were selected and ordered from cDNA library (Rice Genome Resource Center, Ibaraki, Japan). The subcellular localizations and secretory signal peptide were predicted by wolfpsort (Horton et al., 2007)

and SignalP (Petersen et al., 2011), respectively. The mature peptides were predicted the calculated molecular mass by Expasy compute pI/Mw tool (Gasteiger et al., 2003) (http://web.expasy.org).

3.11.1.2 Selection of genes involved in *trans*-resveratrol production

Genes encoding enzymes involved in *trans*-resveratrol production were selected from the previous report; *PAL* (Genbank: L77912) from *Zea mays*, *TAL* (Genbank: 77464988) from *R. sphaeroides*, and *C4H* (Genbank: AM468511.2), *4CL* (Genbank: AM428701.2), and *STS* (Genbank: DQ366301) from *V. vinifera*. The subcellular localizations of these enzymes, the signals peptides as well as calculated molecular mass were analyzed. The fragments for expression vector were also designed by selecting some molecular parts from registry standard biological parts (http://parts.igem.org) such as the hybrid promoter P*trc*1O (BBa_J153001) and the terminator (B1006). To reach the highest possibility of expression in *Synechocystis*, the genes involved *trans*-resveratrol production were optimized the codon preference by the algorithm of GenScript OptimumGeneTM. The codon adaptation index (CAI) of each gene was upgraded from around 0.60 in native gene to more than 0.85 to increase the efficiency of translation in *Synechocystis*. Additionally, the frequency of the optimal codons used and GC content were also considered (see in Appendix B). These optimized individual genes and the fused genes of *TAL*, *4CL* and *STS* were synthesized by GenScript.

3.11.2 Production of *Os*DEFs and *trans*-resveratrol

3.11.2.1 Cloning of genes involved in *Os*DEFs and *trans*-resveratrol production

3.11.2.1.1 Cloning of *OsDEFs* for expression in *E. coli*

To confirm the antimicrobial activities of *OsDEFs* identified from the coexpression network analysis, the genes removed signal peptides were expressed in *E. coli*. The specific oligonucleotide primers were designed to contain the restriction sites of *Bam*HI and *Eco*RI; DEF7_F/R and DEF8_F/R (sequences shown in Appendix C). The cDNAs of *OsDEF7* and *OsDEF8* were amplified by the designed primers with Phusion DNA polymerase. The reaction was carried out in a thermocycler with the reaction condition; initial denaturation at 98^{o}C for 30 s, 30 cycles of the reaction including 98^{o}C for 10 s, 65^{o}C for 30 s, and 72^{o}C for 20 s, and final extension at 72^{o}C for 5 min. The GST containing expression vector, pGEX-6P-3 was used as the expression vector in *E. coli*. The purified PCR products and vector were digested with *Bam*HI and *Eco*RI and were ligated by molar ratio of 1:3 of vector to insertion with T4 ligase. The recombinant vectors were transformed into *E. coli* DH5α by heat shock transformation. The transformants were screened by colony PCR technique with *Taq* polymerase. Reaction condition; the initial denaturation at 94^{o}C for 3 min., 30 cycles of the reaction including 95^{o}C for 45 s, 60^{o}C for 30 s, 72^{o}C for 30 s, and final extension at 72^{o}C for 10 min. The target colonies were then extracted plasmids for the nucleotide sequences

analysis (Bio Basic Inc., Canada). Finally, the verified recombinant plasmids of pGEX-6P-3_*OsDEF7* and _*OsDEF8* were transformed into *E. coli Rosetta-gami* (DE3) for expression.

3.11.2.1.2 Cloning of *OsDEFs* and genes involved in *trans*-resveratrol production for *Synechocystis* expression

The cDNAs of *OsDEFs* and codon–optimized nucleotide sequences of genes involved in *trans*-resveratrol production were used as template. They were amplified by oligonucleotide primer that the forward primer contained orderly the molecular parts; *Eco*RI, P*trc*O1core (Camsund et al., 2014), ribosome binding sites (RBS*) (Heidorn et al., 2010), spacer and 5′ gene-specific region. The sequences of the primer were shown in Appendix C, named as gene_trcoreF. The reverse primers are in order composed of 3′ gene-specific region, Gly-Ser linker, strep tag, stop codon, terminator (BB1006), and *Pst*I site, they were named as gene_trcR. The genes fragments were amplified by the designed primers with PrimeSTAR DNA polymerase. The reaction was carried out in a thermocycler. Reaction condition; the initial denaturation at 98^{o}C for 30 s, 30 cycles of the reaction including 98^{o}C for 10 s, 55^{o}C for 5 s, 72^{o}C for 20 s for *Os*DEFs/ 1.30-2.30 min. for genes involved in *trans*-resveratrol production, and final extension at 72^{o}C for 5 min. pPMQAK1 was used as the expression plasmid of *Synechocystis*. The purified PCR products and vector were digested with *Eco*RI and *Pst*I and were

ligated at 1:3 by concentration ratio of vector to insertion with Quick ligase. The recombinant vectors were transformed into competent DH5αZ1 by heat shock transformation. The colonies were screened by colony PCR technique with Dream*Taq* polymerase. Reaction condition; the initial denaturation at 95^{o}C for 2 min., 30 cycles of the reaction including 95^{o}C for 30 s, 65^{o}C for 30 s, 72^{o}C for 30 s for *OsDEFs*/ 1.30-2.30 min. for the genes involved in *trans*-resveratrol production, and final extension at 72^{o}C for 5 min. Finally, the plasmids were extracted and analyzed the nucleotide sequences (Macrogen, Netherlands).

3.11.2.2 Expression of *OsDEFs* and enzymes involved in *trans*-resveratrol production

3.11.2.2.1 The recombinant peptide in *E. coli*

The transformants of pGEX-6P-3_*OsDEF7* and _*OsDEF8* were grown in 5mL Luria–Bertani broth (LB) containing 50 µg mL^{-1} kanamycin, 100 µg mL^{-1} tetracyclin, 100 µg mL^{-1} ampicillin, and 34 µg mL^{-1} chloramphenicol in the temperature- controlled shaker at 37^{o}C, 250 rpm overnight. 200 µL overnight medium were added into 200 mL LB and then grew at 37^{o}C, 250 rpm. When the culture density reached an OD_{600} of 0.6, it was induced by 0.1mM IPTG and was continue grown at for 24 hr. The cells were collected by centrifuging at 6000 rpm for 15 min at 4^{o}C. The cells were resuspended with 10 mM

phosphate buffer, pH 7.4. Subsequently, the cell solution was disrupted by sonicating on ice at 25% pulse with 1 s of sonication and a 15 s rest. This cycle were repeated for 45 min. The crude DEFs were obtained by centrifuging at 12000 rpm for 10 min at 4^{o}C. This was then purified by method described in 3.11.2.5.1. The protein concentration was determined according to 3.11.2.6 before testing the antimicrobial activity as in 3.11.2.7.1. The homology modeling of the protein was also studied to predict the relation of their functions and structures according to 3.11.2.3.

To estimate the capacity of expression in *Synechocystis*, the expression in *E. coli* was preliminary tested. The transformants of pPMQAK1 vector were cultured in 5 mL LB containing 50 µg mL^{-1} kanamycin in the temperature-controlled shaker at 37^{o}C, 250 rpm overnight. The cell culture were collected at same OD_{600} at 0.6 and were centrifuged at 6000 rpm for 15 min before detecting by SDS-PAGE described in 3.11.2.6.2 and Western blot analysis in 3.11.2.6.3.

3.11.2.2.2 The recombinant peptide in *Synechocystis*

The recombinant plasmids of pPMQAK1_*OsDEFs* and _ genes involved in *trans*-resveratrol production were transformed into cyanobacteria by conjugation; triparental mating adapted from Elhai and Wolk, 1988). The *E. coli* helper cell (HB101) and *E. coli* cargo (DH5αZ1) containing plasmid were grown in 4 mL LB medium supplemented with 100 µg mL^{-1} ampicillin and 50 µg mL^{-1} kanamycin,

respectively at 37°C, 250 rpm overnight. *Synechocystis* was culture till OD_{730} > 0.5. The *E. coli* culture was centrifuged at 3000 rpm for 10 min and were resuspended with 2 mL LB. They were mixed and were centrifuged at the same speed. The *E. coli* mixture was resuspended with 200 µL LB. Cyanobacteria cell culture were centrifuged at 3000 rpm for 10 min and were resuspended with 5 mL BG-11 (Stanier et al., 1971). 200 µL *E.coli* cargo/helper mixed culture and 100 µL of cyanobacterial culture was mixed and incubated at 30°C under light for 1 hr. The mixtures of three strains were then diluted to 1:10 with BG-11 before plating onto the membrane in non-antibiotic BG-11 plate and incubating for 1-2 days at 30°C with light. To screen for cyanobacteria-contained vector, the membrane of were placed onBG-11 agar supplemented with 25 µg mL^{-1} kanamycin and incubated at 30°C with light. When the transformants appeared on the membrane, they were picked to grow in 6 mL BG-11 with antibiotic in 6-well plate before screening as the method described in 3.11.2.1.2. To detect the expressed protein, 100 µL of cell culture from 6-well plate was inoculated in 20 mL BG-11 supplemented with 25 µg mL^{-1} kanamycin until OD_{730} around 0.5-0.6. The cell number was determined according to Eaton-Rye, 2004. The cells were collected by centrifuge at 5000 rpm for 5 min. and were resuspended with 2 mL phosphate buffered saline (PBS) buffer. The cell suspension was repeated centrifugation and resuspended with 200 µL PBS with 1% (v/v) protease inhibitor. The cell was freezed at -80°C and thawn at 37°C before breaking by the

glass bead. The mixture was centrifuged at 1000 rpm for 30 s to settle the bead and the supernatant was collected. The protein concentration was assayed according to 3.11.2.6.1.

3.11.2.3 Homology study

The structures of *Os*DEF7 (EMB:BAF09407) and *Os*DEF8 (EMBL:BAF10767) were compared with published plant AMPs. The protein sequence alignment was performed. Subsequently, the homology models were simulated by Discovery Studio (version 3.0). The homology modeling was implemented through the protocol of software.

3.11.2.4 Transcript detection

3.11.2.4.1 RNA extraction

3.11.2.4.1.1 Bacterial RNA

The *E.coli* transformant was grown in 5 mL LB containing antibiotic at 37^{o}C, 250 rpm till density reached an OD_{600} of 0.3-0.5. The cells were collected by centrifuging 6000 rpm for 10 min. The RNA was extracted according to the instructions of GeneJet RNA extraction kit.

3.11.2.4.1.2 Cyanobacterial RNA

Cyanobacterial cultures were grown in the same condition in 3.11.2.2.2 till OD_{730} = 0.3. The cultures were spun down at 5000 rpm for 5 min. The cell was resuspended in 0.5 mL

TRIzol and was added with 0.2 g glass bead. The cell was disrupted by bead beater for 35 s three times. The cell mixture was added with 0.1 mL chloroform and was mixed by inversion. The mixture was incubated at room temperature for 10 min. before centrifuging at 14000 rpm for 15 min at 4^{o}C. The supernatant were removed to new tube and mixed with 0.25 mL isopropanol by inversion. The solution was incubated at room temperature for 10 min. and was repeated the centrifugation at 14000 rpm for 10 min at 4^{o}C. The pellet was washed with 1 mL cold 75% ethanol and centrifuged at 14000 rpm for 5 min at 4^{o}C. before being dried at room temperature for 10 min. The dried pellet was dissolved with 50 µL nuclease-free water.

3.11.2.4.2 Reverse transcription (RT)-PCR

RT-PCR experiments were performed to study expression of individual genes, 400 ng mRNA were treated with DNaseI in 20 µL reaction volume. The reaction was carried out at 37^{o}C for 1 hr and was inactivated by adding 50 µL 10 mM EDTA and heating at 75°C for 10 min. 10 ng of treated mRNA was reverse-transcribed by qScript cDNA synthesis kit according to the instructions. RT-PCR negative controls were prepared by preparing duplicates of each sample without reverse transcriptase. RT-PCR was carried out using 1 ng of resulting cDNA as a template. The oligonucleotide primer pairs used were specific gene primer and 16sRNA which were run in parallel as positive controls.

The PCR reaction was carried out according to the protocol of Phusion Hot Start II, and the cycling conditions were 30s of initial denaturation at 98℃ for 30s followed by 25 cycles of denaturation (98℃ for 10s), primer annealing (65℃ for 30 s), and elongation (72℃ for 25 s); the final elongation step was at 72℃ for 5 min. Samples were resolved by electrophoresis in a 1% (w/v) agarose gel.

3.11.2.5 Protein purification

3.11.2.5.1 Purification of GST-tagged protein

The supernatant from 3.11.2.2.1 was subsequently purified by Pierce glutathione spin columns (Thermoscientific, USA) according to the manufacturer's instruction.

3.11.2.5.2 Purification of strep-tagged protein

The supernatant from 3.11.2.2.2 was subsequently purified by Strep-Tactin® Spin Column Kit (IBA, Germany) according to the manufacturer's instruction.

3.11.2.6 Protein determination

3.11.2.6.1 Protein concentration

The concentration of protein was determined by the method developed from Bradford (1976) using bovine serum albumin (BSA) as a standard. The standard curve was shown in Appendix F. The reaction consisted of 5 μL of sample and 295 μL of Bradford reagent

was added into microplate. The reaction was incubated at room temperature for 5 min. Finally, the absorbance of the blue solution was measured at 595 nm by microplate spectrometer.

3.11.2.6.2 SDS-PAGE analysis

A protein sample was prepared by mixing with 2X sample buffer to final concentration of 1X sample buffer. The reaction was incubated at 95°C for 5 min. The protein sample was then separated by SDS-PAGE (the protocols for SDS-PAGE described in Appendix D).

3.11.2.6.3 Western blot analysis

3.11.2.6.3.1 Strep-tagged proteins

After protein separation in SDS-PAGE, the SDS gel was transferred to Trans-Blot Turbo system (Biorad, USA). The cassette was then assembled into electroblotted kit (Trans-Blot Turbo cell). The standard protocol was selected at a constant amperes of 1 A (25 volt constant) per gel at 30 min. Subsequently, the protein-transferred membrane was incubated in 20 mL blocking buffer for 1 hr on rocker platform at room temperature and then rinsed with 20 mL phosphate buffered saline containing Tween 20 (PBST) for 5 min., three times. The membrane was incubated in 20 mL PBST supplemented with 10 µL biotin blocking buffer for 10 min. Subsequently, 10 µL of 1:100 strep tactin HPR (IBA, Germany) was added into the solution and then incubated for 1 hr on rocker

platform at room temperature. The membrane was washed with PBST and PBS for 1 min. twice, respectively. The membrane was detected by chemical detection of Immun-StarTM WesternCTM chemiluminescence kit (Biorad, USA). A membrane was incubated in the mixing solution of 3 mL luminol/ enhancer and 3 mL perioxide solution for 3-5 min. The picture was visualized by Gel DocTM XR+ and ChemiDoc TM XRS+ imager (Biorad, USA)

3.11.2.6.3.2 Flag-tagged proteins

The protein from SDS-PAGE was transferred to the membrane by the same protocol mentioned in 3.11.2.6.3.1. To detect the flag-tagged proteins, the membrane was incubated in 20 mL blocking buffer for 1.5 hr on rocker platform at room temperature and then rinsed with 20 mL tris buffered saline containing Tween 20 (TBST) for 15 min., three times. The membrane was incubated with primary antibody in 15 mL TBST supplemented with 3 µL mouse anti-flag antibody (Sigma, USA) for 1 hr. The membrane was washed with 20 mL TBST for 15 min., three times. The membrane was then incubated with secondary antibody in 15 mL TBST supplemented with 3 µL goat anti-mouse IgG (Agrisera, Sweden) for 1 hr. The membrane was washed with 20 mL TBST for 15 min., three times. The membrane was detected by the same method in 3.11.2.6.3.1.

3.11.2.7 The activity determination

3.11.2.7.1 Determination of the antimicrobials activity of *Os*DEFs expressed from *E. coli*

3.11.2.7.1.1 Bioassay of antibacterial activity

The antibacterial activity was determined by broth micro-dilution assay. The pathogens causing plant diseases, *Erwinia carotovora*, *Xoo* and *Xoc* were used as the testing strains. The antibacterial activity assay was conducted with different concentrations of the peptides to compare their effects on the bacterial growth. Antibacterial activity of peptides was examined using log phase-cultured bacteria in LB broth at 37°C. The cultures were diluted in tryptic soy medium (HiMedia Laboratories Pvt. Ltd, India) to give approximately $5x10^5$ CFU mL^{-1} 100 µL of the bacterial suspension was transferred to a 96-well plate. 100 µL of same medium containing different concentrations of purified *Os*DEFs was added to each well. The plate was incubated over night at room temperature and the absorbance measured at 600nm by a microplate reader Model 550 (Bio-Rad). 100 µL of same medium and one containing ampicillin were added to a well as a negative and positive control, respectively. The MIC was then calculated.

3.11.2.7.1.2 Bioassay of antifungal activity

The antifungal activities of the recombinant *Os*DEFs were determined by hyphae point technique (Bains and Bisht, 1995).

F. oxysporum and *H. oryzae* were grown on potato dextrose agar (PDA) plate until it formed spores. These microbes-contained PDA were drilling with the certain diameter. The disks containing fungi were applied into the PDA supplemented by various concentrations of recombinant *Os*DEFs. The inhibitory activity on fungal spore germination was determined at room temperature incubation for 8 days. The inhibitory diameter in cm was measured daily. Fresh PDA and PDA supplemented with ampicillin were used as a negative and positive control, respectively.

3.11.2.8 Product determination by LC-MS analysis

The products were extracted from cyanobacteria by mixing the cell with 1 mL 80% (v/v) methanol for 45 min at 4°C. This extracts were centrifuged at 12000 rpm for 10 min at 4°C. The supernatant was kept and evaporated. The extracts were resuspended with 100 µl methanol. 50 µL of extracted sample was diluted in 150 µL 50% (v/v) methanol and filtered through 0.2 µm filters. The metabolites was detected and quantitated by of LC-MS analysis. The sample extracts (10 µL) were analyzed using an LC-MS system equipped with an electrospray ionization (ESI) operated in negative mode. A LUNA 5 µ C18 (2) 150 × 4.6 mm column (Phenomenex, USA) was used to separate the extracted metabolites, with LC-MS grade-water with 0.1% formic acid (A) and acetonitrile with 0.1% formic acid (B) as solvents. A linear gradient from 5 to 95% B at a flow rate of 0.5 mL min^{-1} and temperature, 38°C was used. Full mass-to-charge ratio (*m/z*) was

acquired between 100–1200 at 4 scans sec^{-1}. The scans were repeated for 40 min in a single run. The data were recorded and analyzed by Agilent MassHunter Quanlitative Analysis B.06.00. Standard stock solutions were prepared in 50:50 MeOH/H_2O at a concentration of 5 mg mL^{-1} for each compound. Aliquots of this standard mixture were used for calibration. Two calibration curves were obtained by analyzing standard solutions with the optimized LC-MS method at 5 concentrations, ranging from 0.2 μg to 1 μg and at 4 concentrations, ranging from 5 μg to 20 μg.

3.11.3 Determination of growth rate and chlorophyll *a* content of *Synechocystis*

3.11.3.1 Growth rate

To study the effects of genes expressions on the growth rate of the cell, the transformant cyanobacterial cells were grown in 20 mL of BG-11 medium containing 25 μg mL^{-1} kanamycin. The initial cell concentration was calculated to an OD_{730} of 0.0025 and cultures were incubated in rotatory shaker at 120 rpm and 30°C under continuous illumination of 50 $\mu Em^{-2}s^{-1}$ cool white fluorescent lamps from two sides of the shaker. The growth rate was monitored by measuring the optical density of the culture at 730 nm with a spectrophotometer every day for 2 weeks. Another set of experiment was set by growing in 50 mL BG-11 under the same condition to study the effect on amount of chlorophyll *a* (chl *a*) and the changes of metabolites in the cell. The cells were grown till OD_{730} of cell around 0.5-0.6. The total amount of chl *a* was determined according to the

method in 3.11.3.2. The cells were collected by centrifuging at 5000 rpm for 5 min. for detecting the metabolite by LC-MS analysis in 3.11.2.8.

3.11.3.2 Chlorophyll *a* content

The cell culture was grown in 50 mL BG-11 under 50 $\mu Em^{-2}s^{-1}$ of light intensity until OD_{730} around 0.5-0.6. 1 mL of cell culture was collected and centrifuged at 13000 rpm for 1 min. Then, 90% of the liquid was removed with pipette and then add an equivalent amount of 100% methanol to the liquid pellet; yields 90% methanol final concentration. The solution was mixed vigorously on a vortex to fully suspend the pellet. The reaction was incubated in the dark at room temperature for 15 min. to extract the chl *a*. The extract was centrifuges at 1300 rpm for 5 min. and the supernatant was collected to measure the absorbency at 665 nm. The chl *a* concentration was calculated according to an extinction coefficient of 78.74 L $g^{-1}cm^{-1}$ for chl *a* in 90% methanol (Meeks and Castenholz, 1974) that was shown in Appendix G.

3.11.4 Optimization conditions for the production of *Os*DEFs and *trans*-resveratrol in *Synechocystis*

3.11.4.1 Genetic manipulations

3.11.4.1.1 Promoters

The same cloning method as 3.11.2.1.2 was tried with another promoter, P*trc*1O. The sequences of the primer were also designed in the same order with P*trc*O1core as the sequences shown in

Appendix C, named as gene_trc1OF. The reverse primers were used that of P*trc*O1core. All cloning step was similar to 3.11.2.1.2.

3.11.4.1.2 Bicistronic design variants

To improve translation, the bicistronic (BCD) constructs with double RBS were tried. The forward primer was designed according to the BCD2 sequences of Matalik et al. (2013) with adding the restriction site of *Eco*RI. The sequence of primers was shown as gene_bcdF in Appendix C. The reverse primers were used that of P*trc*O1core. All cloning step was similar to 3.11.2.1.2.

3.11.4.1.3 Tag terminus

To improve ensure the expression of protein tag, the tag was arranged to n-terminus. The forward primer contained orderly sequences of *Eco*RI, P*trc*O1core, RBS*, spacer, start codon (ATG), sequence of strep or flag tag, and 5′ gene-specific region. The sequences of the primer were shown in Appendix C, named as gene_NstrepF/gene_NflagF. The reverse primers are in order composed of 3′ gene- specific region, stop codon, terminator (BB1006), and *Pst*I site, they were named as gene_trcNR which it was used for both protein tags. All cloning step was similar to 3.11.2.1.2.

3.11.4.1.4 Homologous recombination

To increase the possibility of expression in *Synechocystis*, the integration of the genes into the genome by homologous recombination strategies was also applied. The *OsDEFs* and enzymes related in *trans*-resveratrol were cloned into vectors for homologous recombination, pEERM3+ vector which contains nickle promoter, kanamycin resistance genes. The genes were amplified by forward primer contained *Xba*I, ATG, sequence of strep tag and 5′ gene-specific region. The sequences of the primer were shown in Appendix C, named as gene_p3F. The reverse primers composed of 3′ gene-specific region and *Pst*I site. They were named as gene_p3R. The genes were amplified by the designed primers with Phusion Hot Start II DNA polymerase. The reaction was carried out in a thermocycler. The purified PCR products and vector were digested with *Xba*I and *Pst*I. The method of ligation, transformation and colony screening were similar to 3.11.2.1.2.

3.11.4.2 Substrate concentrations and growth condition for *trans*-resveratrol production

The optimal concentration of substrates and growth condition to produce *trans*-resveratrol was determined as followed. The transformant cyanobacterial, pPMQAK1_STS cells were grown in 50 mL of BG-11 medium supplemented with 25 μg mL^{-1} kanamycin and varied concentration of substrates; 0, 25, 50, 75, and 100 nM *p*-coumaroyl CoA.

The initial cell concentration was calculated to an OD_{730} of 0.0025. They were grown under the same condition as in 3.11.3.1. Another experiment was performed in the growth chamber. The cells were grown at 120 rpm and 30°C under continuous illumination of 30 $\mu Em^{-2}s^{-1}$light until the OD_{730} around 0.5-0.6. The growth temperature was then decreased to 25°C and continued culturing for 24 h. Finally, the cells were further collected by centrifuging at 5000 rpm for 5 min. to quantitate the product by LC-MS analysis describes in 3.11.2.8. Moreover, the effects of addition of *p*-coumaroyl CoA on growth rate and chl *a* content were also studied as describes in 3.11.3.1 and 3.11.3.2, respectively.

3.11.5 In vitro production of *trans*-resveratrol

The cells containing pPMQAK1_*TAL*, pPMQAK1_*4CL* and pPMQAK1_*STS* under controlled of P*trc*1O were grown in 200 mL of BG-11 under the same condition as in 3.11.2.2.2 until the OD_{730} around 0.5-0.6. The cells were collected, and three fractions were resuspened together. The cell mixtures was made up the volume to 10 mL before breaking by the glass bead. The mixture was collected and divided into the tubes 500 µL each. They were tested by treating with two concentrations of L-tyrosine; at 50 and 100 µM. The reactions were incubated at 30°C for 7 and 14 h. Finally, the mixtures were extracted before quantitating the *trans*-resveratrol by LC-MS analysis in 3.11.2.8.

CHAPTER IV

RESULTS

4.1 AMP production

4.1.1 In silico analyses of AMPs

In the genome of *O. sativa japonica*, 57 genes encoding *Os*DEFs and *Os*DEFLs were found as shown in **Table 4-1**. Hypothetically, genes involved in similar mechanisms would be coexpressed and the functions of unknown genes that coexpressed could be implied. Therefore, the gene coexpression network analysis of all *Os*DEF genes identified to investigate their involvements in pathogen response using Rice Oligonucleotide Array Database and PlantArrayNet. These databases provide the gene coexpression information from accumulated microarray data. Among all 57 rice DEF genes, 22 are present in both databases and, of those, only 11 genes are coexpressed with genes participated in plant pathogen response processes (**Table 4-1**). They are *OsDEF1* (LOC_Os01g70680), *OsDEF7* (LOC_Os02g41904), *OsDEF8* (LOC_Os03g03810), *OsDEF9* (LOC_Os04g11130), *OsDEFL9* (LOC_Os06g22919, *OsDEFL21* (LOC_Os06g48660), *OsDEFL28* (LOC_Os11g08220), *OsDEFL43* (LOC_Os12g12230), *OsDEFL48* (LOC_Os11g47120), *OsDEFL49* (LOC_Os04g31250), and *OsDEFL70* (LOC_Os10g20550). The gene coexpression networks of *OsDEF7* and *OsDEF8* are shown in **Fig. 4-1** (the gene lists were shown in **Table 4-2**). Those of the others are shown in **Fig. A-1**, Appendix A. These *OsDEF* genes are coexpressed

with groups of genes encoding plant disease resistance proteins (*Pi-ta*), thaumatins, thaumatin-like proteins (TLPs), microbe-eliminating enzymes (chitinases and β-1,3-glucanases), and AMPs in other families. In addition, some of these *OsDEF*s, namely *OsDEF1, OsDEF7, OsDEF8, OsDEF9, OsDEFL21, OsDEFL43, OsDEFL48* and *OsDEFL49*, are also coexpressed with genes involved in growth and development such as rapid alkanization factor (RALF) proteins, stigma-specific protein (Stig1) family proteins, and gibberellin regulated proteins (**Fig. 4-1** and **Fig. A-1**, Appendix A).

On the other hand, the expression levels of all *OsDEFs* were confirmed in all tissue of rice from the microarray database, Rice eFP browser. However, the expression profiles of only 14 from 57 *OsDEFs* could be found; *OsDEF1, OsDEF3, OsDEF6, OsDEF7, OsDEF8, OsDEFL1, OsDEFL9, OsDEFL12, OsDEFL31, OsDEFL50, OsDEFL56, OsDEFL79, OsDEFL80*, and *OsDEFL81* (**Table 4-1**, **Fig A-4** in Appendix A). Among these, *OsDEF7* and *OsDEF8* obviously showed the higher expression levels throughout the organs examined, while other *OsDEF*s are specifically expressed in seeds (*OsDEF1, OsDEF2, OsDEFL1,* and *OsDEFL50*), seedling root (*OsDEF9*), or late inflorescence stage (*OsDEF56*) (**Fig. 4-2**). In addition, seven out of these 57 *OsDEFs* could be expressed under stress conditions; drought, salt, and cold stress. They are *OsDEF1, OsDEF3, OsDEF6, OsDEF7, OsDEF8, OsDEFL1,* and *OsDEFL56*.

All 11 *OsDEFs* coexpressed with plant-responsive genes were compared the similarity within the group by neighbor-joining estimation. The result indicated that *OsDEF7* and *OsDEF8* could be grouped in the same distance (**Fig. 4-3**). Additionally, *OsDEF7* and *OsDEF8* were aligned to other reported

plant DEFs. The result showed that *Os*DEF7 linked with the group of peptides such as *Ta*Def, *Tu*AMPD1, *Tk*AMPD2, and *Tm*AMPD1. *Os*DEF8 was closer to other characterized antifungal *Ca*J1-2 (**Fig.4-4**). Based on these results, both *OsDEF7* and *OsDEF8* are involved with plant-responsive genes and they show high expression levels. Hence, *OsDEF7* and *OsDEF8* were selected for expression to confirm the antimicrobial activities identified from the coexpression network analysis.

Table 4-1 The information of DEF genes in database analyzed by in silico analyses. Fifty seven of *OsDEFs* were identified in *O. sativa* by two databases; Phytozome and Gramene. The coexpression with plant-responsive genes was considered by Plantarraynet and Rice Oligonucleotide Array Database. The expression level in rice organs and under stress conditions were determined by rice microarray database. The closed dots illustrate data availability for each gene in each database.

Name	Gene Symbol	Rice database		Coexpression analysis		Coexpresed with plant resistance genes	Expression level
		Phytozome	Gramene	PlanArrayNet	Rice oligonucleotide database		
OsDEF1	LOC_Os01g70680	•	•	•		•	•
OsDEF3	LOC_Os02g07600	•	•				•
OsDEF6	LOC_Os02g12060	•	•				•
OsDEF7	LOC_Os02g41904	•	•	•	•	•	•
OsDEF8	LOC_Os03g03810	•	•	•		•	•
OsDEF9	LOC_Os04g11130	•	•	•	•	•	
OsDEF12	LOC_Os04g44130	•	•	•			
OsDEFL1	LOC_Os02g07550	•	•	•			•
OsDEFL2	LOC_Os07g01700	•	•	•			
OsDEFL3	LOC_Os12g41790	•	•				
OsDEFL4	LOC_Os01g61360	•	•	•			
OsDEFL6	LOC_Os10g37290	•	•	•			
OsDEFL7	LOC_Os01g40220	•	•	•			
OsDEFL8	LOC_Os06g22880	•	•	•			
OsDEFL9	LOC_Os06g22919	•	•	•		•	•
OsDEFL11	LOC_Os06g23060	•	•				
OsDEFL12	LOC_Os06g48690	•					•
OsDEFL13	LOC_Os07g41290	•	•	•			
OsDEFL14	LOC_Os09g11790	•	•	•			
OsDEFL15	LOC_Os11g45360	•					
OsDEFL16	LOC_Os12g06750	•	•				
OsDEFL17	LOC_Os12g06760	•	•	•			
OsDEFL18	LOC_Os12g12220	•					
OsDEFL21	LOC_Os06g48660	•		•		•	
OsDEFL25	LOC_Os11g42530	•					

OsDEFL27	LOC_Os06g45320	•	•				
OsDEFL28	LOC_Os11g08220	•	•	•		•	
OsDEFL29	LOC_Os11g08240	•	•				
OsDEFL30	LOC_Os11g08250	•	•				
OsDEFL31	LOC_Os11g08260	•		•			•
OsDEFL32	LOC_Os11g08270	•	•				
OsDEFL33	LOC_Os11g08280	•					
OsDEFL34	LOC_Os11g42520	•	•				
OsDEFL35	LOC_Os01g10550	•					
OsDEFL38	LOC_Os02g56870	•	•	•			
OsDEFL40	LOC_Os03g56682	•	•				
OsDEFL43	LOC_Os12g12230	•	•	•		•	
OsDEFL44	LOC_Os11g47269	•					
OsDEFL45	LOC_Os11g08170	•	•				
OsDEFL47	LOC_Os09g02160	•		•			
OsDEFL48	LOC_Os11g47120	•	•	•	•	•	
OsDEFL49	LOC_Os04g31250	•	•	•	•	•	
OsDEFL50	LOC_Os04g15740	•					•
OsDEFL53	LOC_Os08g04520	•					
OsDEFL55	LOC_Os08g15545	•					
OsDEFL56	LOC_Os08g15550	•					•
OsDEFL69	LOC_Os10g20540	•					
OsDEFL70	LOC_Os10g20550	•	•	•	•	•	
OsDEFL71	LOC_Os02g53590	•	•	•			
OsDEFL72	LOC_Os02g20130	•		•			
OsDEFL73	LOC_Os02g49540	•	•				
OsDEFL74	LOC_Os02g53570	•	•	•			
OsDEFL75	LOC_Os02g53600	•	•	•			
OsDEFL78	LOC_Os02g07440	•					
OsDEFL79	LOC_Os11g34990	•		•			•
OsDEFL80	LOC_Os11g39910	•					•
OsDEFL81	LOC_Os10g20560	•		•			•

Table 4-2 Partial list of genes coexpressed with *OsDEF7* (A) and *OsDEF8* (B). This list includes the significance level, calculated by t test, for the correlation coefficient and the standard score, calculated based on a distribution made from the r values of all pairs of a query spot of *OsDEF7* and *OsDEF8*.

A

No.	Target Spot	Oligomer ID	MSU Gene	TAIR Locus	*r*	*P*	Z-score	Description by BLAST Analysis
1	AK105463	Os01g0914300	LOC_Os01g68589		0.827	3.45e-45	2.86	Plant lipid transfer/seed storage/trypsin-alpha amylase inhibitor domain containing protein.
2	AK108191	Os06g0691200	LOC_Os06g47600	AT1G73620	0.821	5.06e-44	2.84	Thaumatin-like protein precursor.
3	AK062516	Os06g0266800	LOC_Os06g15620	AT3G10185	0.803	7.16e-41	2.78	GAST1 protein precursor.
4	AK120044	Os01g0822900	LOC_Os01g60740	AT5G01870	0.783	1.37e-37	2.70	Lipid transfer protein.
5	AK060686	Os06g0256900	LOC_Os06g14540	AT1G70710	0.771	7.65e-36	2.66	Endo-β-1,4-glucanase precursor (EC 3.2.1.4).
6	AK105575	Os02g0786900	LOC_Os02g54560	AT4G25780	0.738	1.90e-31	2.55	PR-1a pathogenesis related protein (Hv-1a) precursor.
7	AK107438	Os07g0592000	LOC_Os07g40240	AT5G59845	0.737	2.50e-31	2.54	Gibberellin regulated protein family protein.
8	AK059681	Os01g0243700	LOC_Os01g14140	AT1G78520	0.733	6.10e-31	2.53	β-1,3-glucanase-like protein.
9	AK059324	Os05g0389000	LOC_Os05g32270	AT2G41710	0.731	1.25e-30	2.52	Pathogenesis-related transcriptional factor and ERF domain containing protein.
10	AK119692	Os11g0115100	LOC_Os11g02350	AT5G59320	0.729	1.83e-30	2.52	Lipid transfer protein.
11	AK104005	Os12g0114800	LOC_Os12g02300	AT5G59320	0.729	1.88e-30	2.52	Nonspecific lipid-transfer protein 3 precursor (LTP 3).
12	AK063684	Os10g0554800	LOC_Os10g40614	AT2G45180	0.726	5.11e-30	2.50	Plant lipid transfer/seed storage/trypsin-alpha amylase inhibitor domain containing protein.
13	AK119798	Os10g0371000	LOC_Os10g22590	AT4G08685	0.719	2.57e-29	2.48	Pollen Ole e 1 allergen and extensin domain containing protein.
14	AK101108	Os02g0733300	LOC_Os02g50040	AT1G70710	0.714	1.03e-28	2.46	Endo-β-1,4-glucanase precursor (EC 3.2.1.4).
15	AK121316	Os03g0760800	LOC_Os03g55290	AT2G39540	0.711	2.11e-28	2.45	Gibberellin regulated protein family protein.

16	AK106508	Os05g0108600	LOC_Os05g01810	AT1G20850	0.693	1.55e-26	2.39	Cysteine proteinase.
17	AK110572	Os10g0412700	LOC_Os10g27280	AT5G40020	0.688	4.53e-26	2.37	Thaumatin, pathogenesis-related family protein.
18	AK105204	Os07g0287400	LOC_Os07g18750	AT5G48485	0.688	5.08e-26	2.37	Plant lipid transfer/seed storage/trypsin-alpha amylase inhibitor domain containing protein.
19	AK070376	Os01g0769200	LOC_Os01g56320	AT4G20430	0.673	1.31e-24	2.32	Proteinase inhibitor I9,
								subtilisin propeptide domain containing protein.
20	AK061173	Os01g0814100	LOC_Os01g59870	AT2G27130	0.670	2.53e-24	2.31	Plant lipid transfer/seed storage/trypsin-alpha amylase inhibitor domain containing protein.
21	AK070268	Os03g0607200	LOC_Os03g41060	AT1G10588	0.668	3.56e-24	2.30	Gibberellin regulated protein family protein.
22	AK102139	Os04g0350100	LOC_Os04g28250	AT2G31980	0.663	1.13e-23	2.28	Proteinase inhibitor I25, cystatin family protein.
23	AK069220	Os03g0119300	LOC_Os03g02750	AT1G04110	0.662	1.46e-23	2.28	Proteinase inhibitor I9, subtilisin propeptide domain containing protein.
24	AK102835	Os06g0700000	LOC_Os06g48650	AT4G30020	0.658	2.97e-23	2.27	Proteinase inhibitor I9, subtilisin propeptide domain containing protein.
25	AK063308	Os01g0631500	LOC_Os01g44090	AT1G29380	0.654	6.96e-23	2.25	β-1,3-glucanase-like protein.
26	AK106887	Os01g0312800	LOC_Os01g21070	AT4G02290	0.654	6.96e-23	2.25	Endo-1,4-β-glucanase precursor (EC 3.2.1.4).
27	AK064705	Os09g0508200	LOC_Os09g32988	AT5G13140	0.640	8.98e-22	2.21	Pollen Ole e 1 allergen and extensin domain containing protein.
28	Os04g0465300	Os04g0465300	LOC_Os04g39110	AT5G14920	0.640	9.62e-22	2.20	Gibberellin regulated protein family protein.
29	AK102737	Os01g0651800	LOC_Os01g46290	AT4G18550	0.630	6.57e-21	2.17	Lipase, class 3 family protein.
30	AK121159	Os11g0640300	LOC_Os11g42070	AT3G14470	0.608	3.03e-19	2.09	Disease resistance protein family protein.

B

No.	Target Spot	Oligomer ID	MSU Gene	TAIR Locus	*r*	*P*	Z-score	Description by BLAST Analysis
1	Os05g0399400	Os05g0399400	LOC_Os05g33140	AT3G12500	0.679	3.43e-25	3.04	Chitinase (EC 3.2.1.14).
2	Os05g0574000	Os05g0574000	LOC_Os05g49830	AT4G18550	0.673	1.29e-24	3.01	Lipase, class 3 family protein.
3	Os03g0808500	Os03g0808500	LOC_Os03g59380	AT5G59320	0.672	1.76e-24	3.00	Plant lipid transfer protein/Par allergen family protein.
4	AK108479	Os09g0481400	LOC_Os09g30360	AT4G34050	0.654	7.04e-23	2.93	Caffeoyl-CoA O-methyltransferase (EC 2.1.1.104) (Trans-caffeoyl-CoA 3- O-methyltransferase) (CCoAMT) (CCoAOMT).
5	Os07g0169700	Os07g0169700	LOC_Os07g07420	AT5G51810	0.645	3.51e-22	2.89	Gibberellin n b20-oxidase (Fragment).
6	AK100306	Os07g0616800	LOC_Os07g42490	AT3G43190	0.642	6.70e-22	2.87	Sucrose synthase 3 (EC 2.4.1.13) (Sucrose-UDP glucosyltransferase 3).
7	AK071196	Os05g0399700	LOC_Os05g33150	AT3G12500	0.630	6.17e-21	2.82	Chitinase (EC 3.2.1.14).
8	Os05g0432200	Os05g0432200	LOC_Os05g35690	AT4G09610	0.614	1.11e-19	2.75	Gibberellin-regulated protein 2 precursor.

A

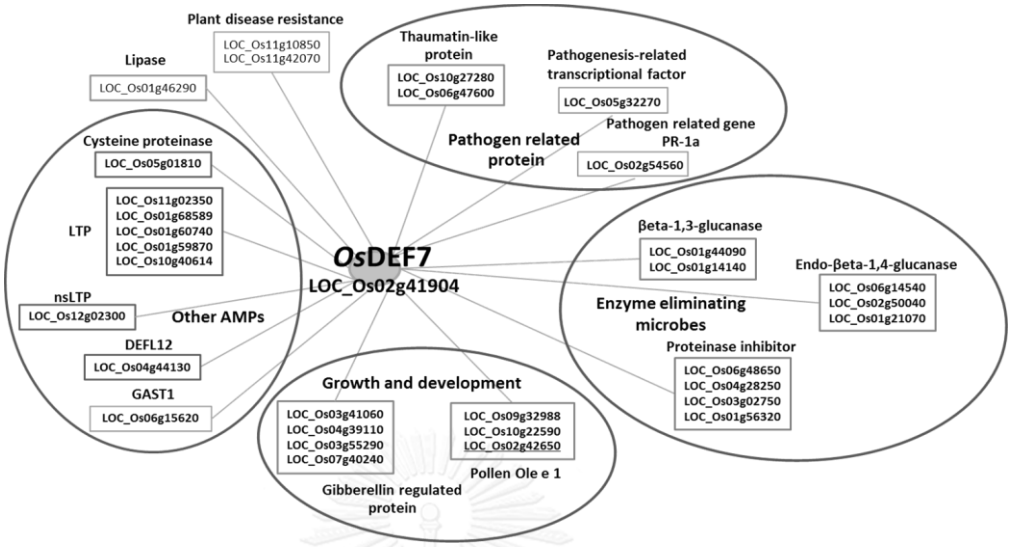

B

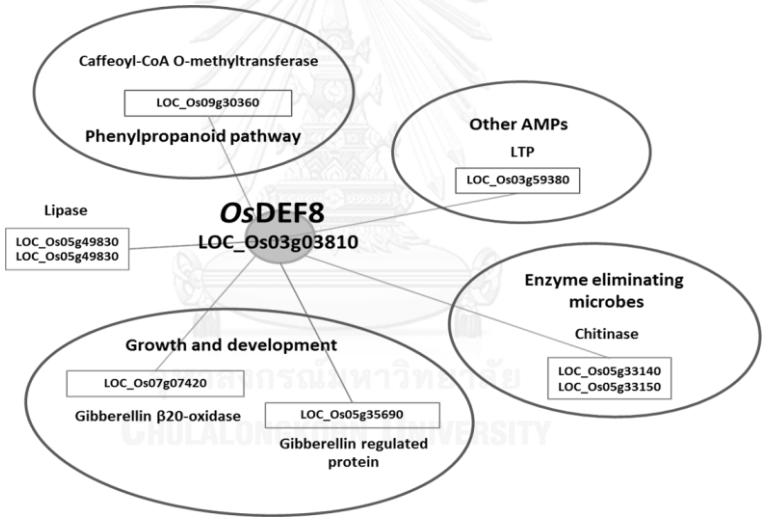

Fig. 4-1 Gene coexpression network analysis of *OsDEF7* (A) and *OsDEF8* (B).

The network analyzed by PlantArrayNet-Rice 300k. Coexpressed genes are circled in separated groups according to their predicted function with the r value 0.6. The locus numbers of each gene are also defined in the boxes. The closeness of their relationship does not be represented in the network.

Fig. 4-2 Organ-specific expression profiles of selected *OsDEFs*. The expression profile was retrieved from the Rice eFP browser in seedling, root, mature leaf, and young leaf, SAM, panicle development (P1–P6), and seed developmental stages (S1–S5). The heat map is drawn on the values retrieved from the browser. Pixel color intensity is proportional to the actual expression values which are calculated in log2 of expression values. The color bar reveals the changing magnitude of expression level from lower expression (yellow) to higher expression (red).

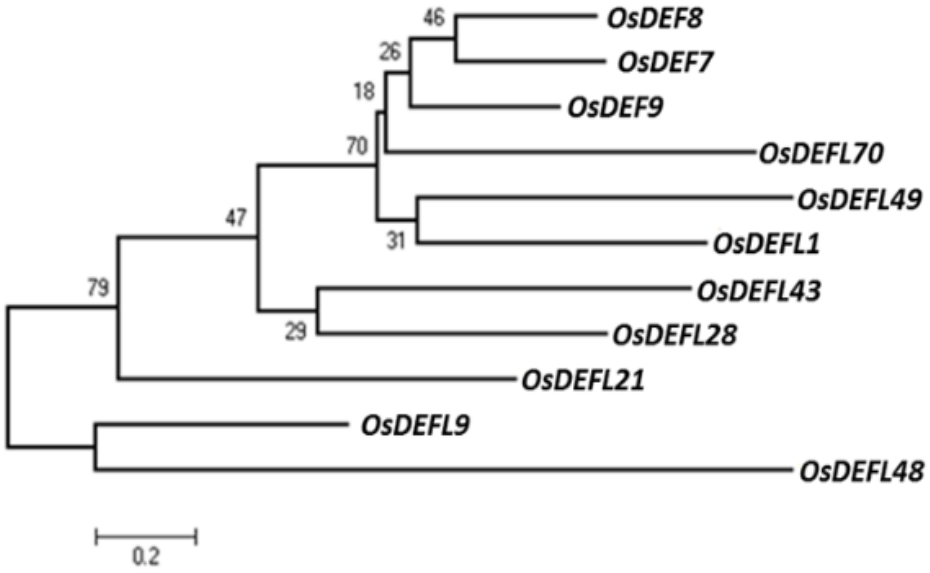

Fig. 4-3 Phylogenetic relationships of *Os*DEF7 and *Os*DEF8 within the *Os*DEF family. The trees were generated using neighbor-joining estimation analysis. The percentage of replicate trees in which the associated taxa clustered together in the bootstrap test (500 replicates). The scale bars indicate the evolutionary distances of 0.2 amino acid substitution per position.

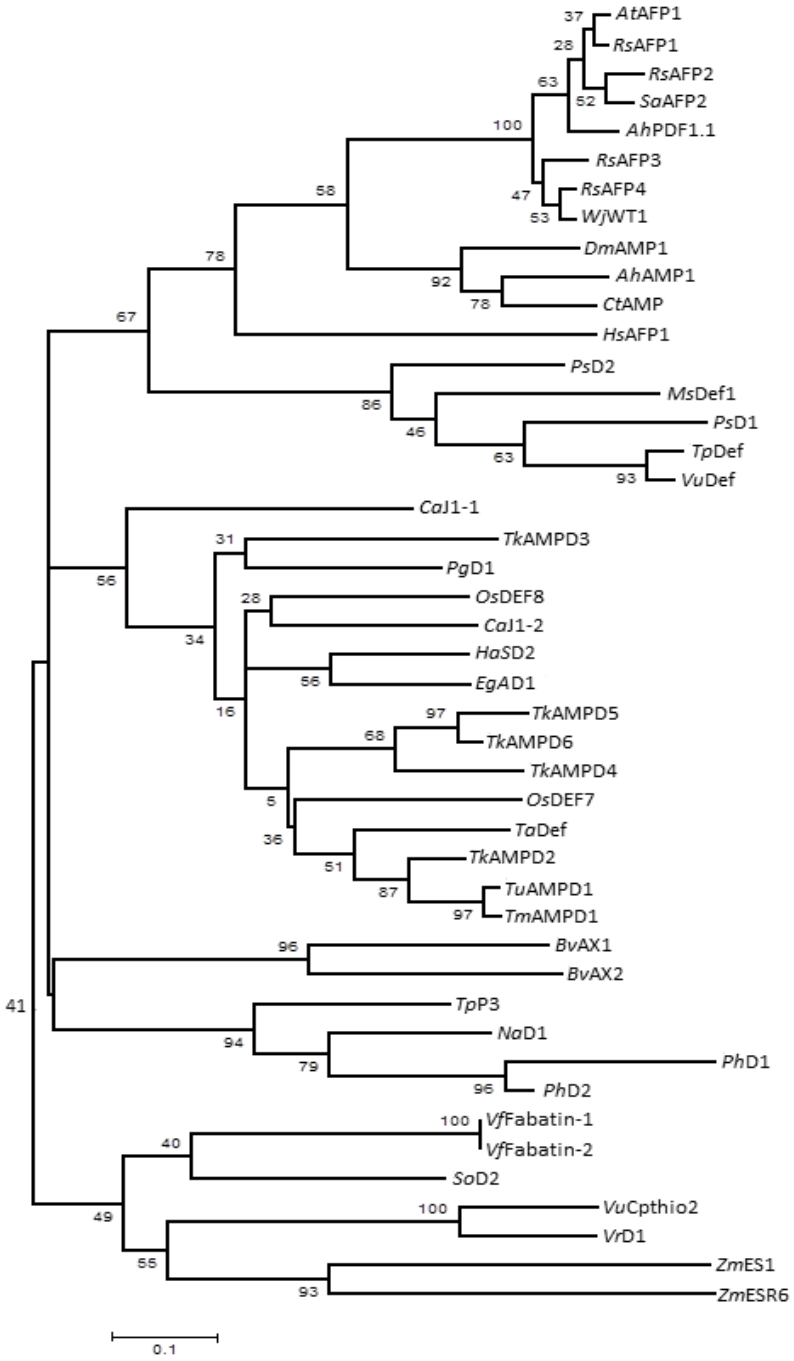

Fig. 4-4 Phylogenetic relationships of *Os*DEF7 and *Os*DEF8 with other plant DEFs. The trees were generated using neighbor-joining estimation analysis. The percentage of replicate trees in which the associated taxa clustered together in the bootstrap test (500 replicates). The scale bars indicate the evolutionary distances of 0.1 amino acid substitution per position.

The nucleotide sequences of *OsDEF7* and *OsDEF8* were 150 bp and 171 bp, respectively. The alignments revealed that they share 61% identity of nucleotide sequence, and have 55% identity of amino acid sequence. Additionally, both *OsDEF7* and *OsDEF8* were predicted as extracellular proteins showing the first 31 and 25 amino acids as signal peptides, respectively.

4.1.2 Expression of *OsDEFs* in *E. coli*

To confirm the antimicrobial activities of both *Os*DEFs identified from the coexpression network analysis, the expression vectors harboring *OsDEF7* and *OsDEF8* fused with glutathione s-transferase (GST) were constructed and expressed both recombinant peptides in *E. coli Rosetta-gami* (DE3). The predicted signal peptides were not included in the cloning. The calculated molecular weights of mature *Os*DEF7 and *Os*DEF8 were 5.6 and 6.0 kDa, respectively. While, the theoretical pI were 8.92 and 8.97, respectively. The fusion proteins, GST-*Os*DEF7 and GST-*Os*DEF8 were expressed as soluble proteins having molecular weights of ~35 kDa which is in agreement with the expected sizes (**Fig. 4-5**). After on-column cleavage of GST, the purified recombinant *Os*DEF7 and *Os*DEF8 were eluted as shown by single bands of approximately 11 and 12 kDa, respectively (**Fig. 4-5**). The observed proteins showed higher molecular weight than the predicted ones. The purified *Os*DEF7 and *Os*DEF8 were formed as the dimeric peptides. The production yields for both purified recombinant *Os*DEF7 and *Os*DEF8 were 0.63 and 0.96 mg L^{-1}, respectively.

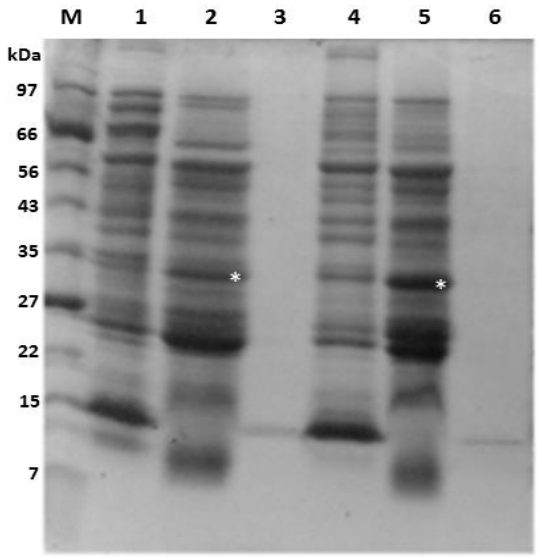

Fig. 4-5 SDS–PAGE analysis of GST-*Os*DEF7 and -*Os*DEF8 fusion protein expressed in *E. coli Rosetta-gami* (DE3). Lane 1 and 4 illustrate the soluble fraction of cell transformed with pGEX_*OsDEF7* and pGEX_*OsDEF8* at 0 hour without induction. Lane 2 and 5 indicate the soluble fraction of cell transformed under 0.1mM IPTG induction after 24 hours. Lane 3 and 6 show the recombinant *Os*DEF7 and *Os*DEF8 purified by GST affinity column. Low molecular weight marker is shown in the left lane (M). The asterisks show the GST-*Os*DEFs.

4.1.2.1 Antimicrobial activities of *OsDEFs*

The in vitro antimicrobial activities of both peptides were tested. The purified recombinant *Os*DEF7 and *Os*DEF8 showed inhibitory activity against three strains of plant pathogenic bacteria; *Xoo*, *Xoc* and *Erwinia carotovora*. The MIC value of recombinant *Os*DEF7 against both rice bacterial pathogens, *Xoo*, and *Xoc* were 3.90 µg mL^{-1} while the recombinant

*Os*DEF8 demonstrated the same MIC value as that of *Os*DEF7 for *Xoo*. Interestingly, much lower MIC value of 0.64 µg mL^{-1} for *Os*DEF8 against *Xoc* were obtained. Noticeably, both recombinant peptides exhibited the same MIC value of 63 µg mL^{-1} against *Erwinia carotovora* (**Table 4-3**).

To test the antifungal activity against *F. oxysporum* and *H. oryzae*, various concentrations of *Os*DEF7 and *Os*DEF8 ranging from 0.75 to 3 µg mL^{-1} were used. From the result, the hyphal growth inhibition of both fungal strains could be observed after three days of incubation. The inhibitory effects of these rice DEFs were increased when applying higher concentration (**Fig. 4-6**).

Table 4-3 MIC assays of *Os*DEF7 and *Os*DEF8. The antibacterial activity assay was conducted with different concentrations of *Os*DEFs in 96-well plate. The absorbance was measured at 600 nm and the MIC value was then calculated.

*Os*DEF	MIC (µg mL^{-1})		
	X. oryzae pv. *oryzae*	*X. oryzae* pv. *oryzicola*	*E. carotovora*
DEF7	3.90	3.90	63
DEF8	3.90	0.64	63

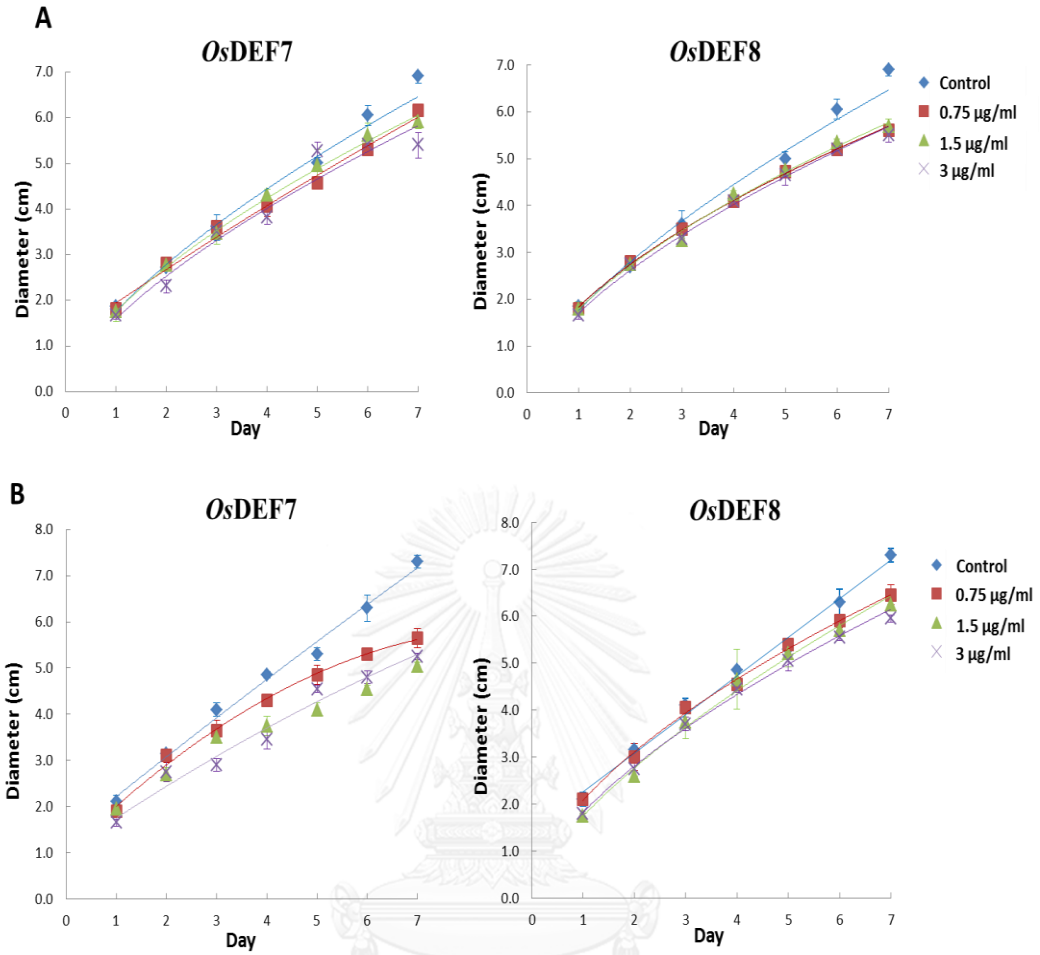

Fig. 4-6 The antifungal activities of *Os*DEF7 and *Os*DEF8 against *F. oxysporum* (A) and *H. oryzae* (B). The hyphae point technique was used (Bains and Bisht, 1995). The cells were grown in PDA supplemented with various concentraions of *Os*DEFs ranging from 0.75, 1.5 and 3 µg mL^{-1}, and incubated at 30°C for 8 days. Measurement of the diameter of the zone of inhibition (in centimeters) was carried out by disk diffusion assay, and the results are shown in the graphs.

4.1.2.2 Homology modeling of *Os*DEFs

Due to the difference found in the inhibitory activity between both *Os*DEFs against *Xoc*, the molecular structures of these DEFs were compared. The defensin *Na*D1 from *Nicotiana alata* (PDB: 1MR4) was selected as a model due to the highest similarity (55%). Subsequently, 400 hypothesized structures of both *Os*DEFs were generated by Discovery Studio software. Among these 3D structures, the most suitable structure with using less energy, 325.8 and 291.8 kJ, respectively, were chosen. Structurally, both peptides are composed of three anti-parallel β-sheets and one α-helix that are highly conserved among this group. Four intramolecular disulfide bridges formed by eight strictly conserved cysteine residues are contributed to the structure stabilization. The cysteine-linked pattern of Cys1-Cys8, Cys2-Cys5, Cys3-Cys6, Cys4-Cys7 is shown as Cys3-Cys49, Cys14-Cys34, Cys20-Cys43, Cys24-Cys45 in the generated structure. The difference in the loop-linked region between β2- and β3-sheets of *Os*DEF7 and *Os*DEF8 were observed. This loop is formed by the amino acids in between the Cys24 and Cys45 that formed a disulfide bond (**Fig. 4-7A, 7B**). This is because the difference in the number of amino acids. *Os*DEF7 contains 18 amino acids, while *Os*DEF8 has 16 residues (**Fig. 4-7C**). Therefore, the structural difference in this region could contribute to the different antimicrobial activity between these two rice DEFs.

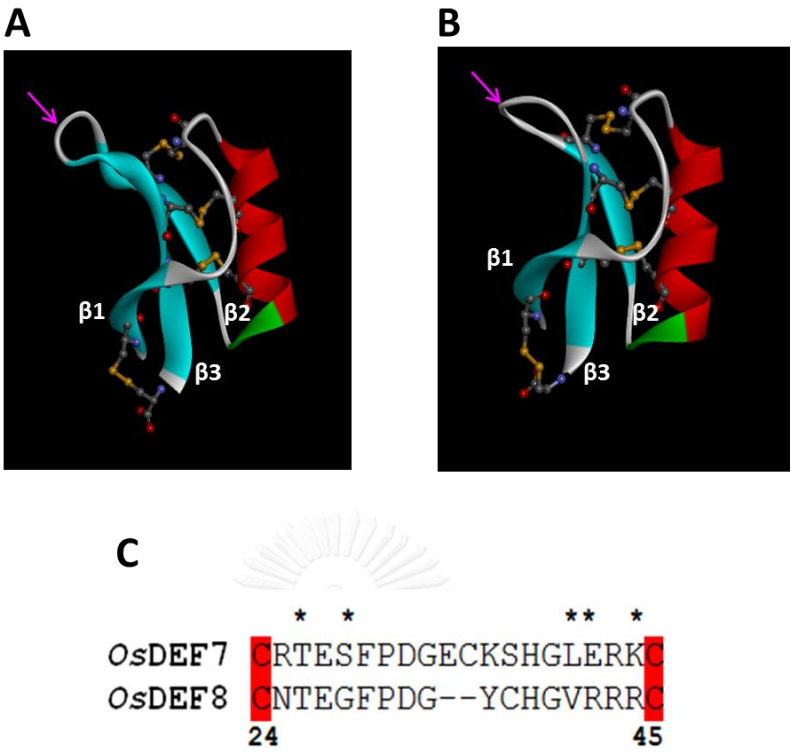

Fig. 4-7 The homology modeled structures of *Os*DEF7 and *Os*DEF8. The structures of *Os*DEF7 (A) and *Os*DEF8 (B) were predicted by Discovery Studio where β1, β2, β3 represent the order of β sheets. The arrow pointed the loops linked between β2 and β3 sheets. C; amino acid compositions in the disulfide linked between Cys24 and Cys45. The asterisks show the crucial amino acids for antimicrobial activity reported in De Samblanx et al., (1997).

4.1.3 Expression of *OsDEFs* in *Synechocystis*

The pPMQAK1_ *OsDEFs* were expressed under P*trc*1Ocore and P*trc*1O in the competent DH5αZ1 to estimate the possibility of expression in cyanobacteria. The result revealed that *OsDEFs* under both P*trc*1Ocore and P*trc*1O could not be expressed in DH5αZ1. Thus, the transcripts of *OsDEFs* were checked by RT-PCR. The results showed that the mRNAs of *Os*DEFs were transcribed with strep tag (**Fig. 4-8 A, 4-8B**). Moreover, BCD constructs were tried. *Os*DEFs could not be expressed (**Fig. 4-8C**). The N- terminus strep and flag tag were also tested to ensure the translation process of the tagged protein. Nevertheless, the expression of *Os*DEFs in *E. coli* from both constructs could not be solved by these methods. However, all *OsDEF* constructs namely; pPMQAK1 containing P*trc*1Ocore and P*trc*1O, and BCD constructs were transformed into *Synechocystis* to check the ability of expression.

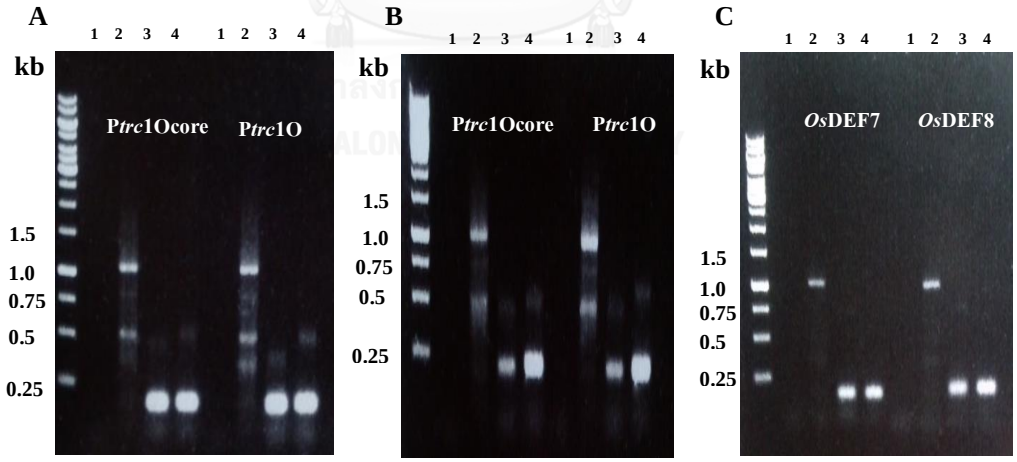

Fig. 4-8 RT-PCR of *OsDEFs* expressed in DH5αZ1. *OsDEF7* (A), *OsDEF8* (B) expressed under P*trc*1Ocore and P*trc*1O, and expressed by BCD constructs (C); 1: -RT_16s RNA primer, 2: +RT_16s RNA primer, 3: +RT_DEF primer, 4: +RT_DEF/ strep primer.

The expression vectors of *OsDEFs* were transformed and further expressed in *Synechocystis*. However, the results were similar to the expression in *E. coli* DH5αZ1 that they were completely transcribed without any protein translated. The transcripts of cyanobacteria expression were verified by RT-PCR (**Fig. 4-9**). Hence, the homologous recombination, pEERM3+ was used as recombination vector. The constructs of pEERM3+_*OsDEFs* in were transformed into *Synechocystis*. Accordingly, *Os*DEFs could not be expressed by genomic recombination. The mRNAs were also checked. The result showed that *OsDEFs* were expressed, but no protein (**Fig. 4-10**).

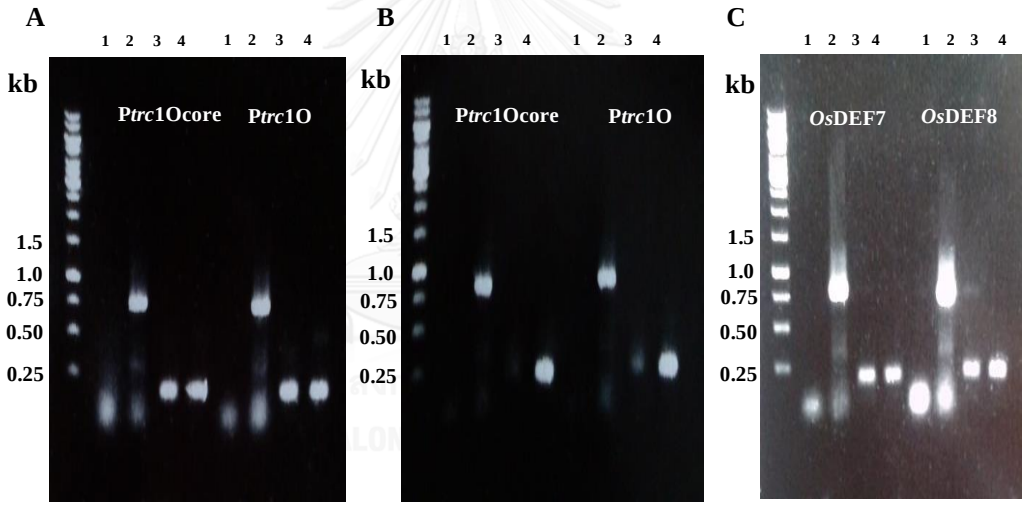

Fig. 4-9 RT-PCR of *OsDEFs* expressed in *Synechocystis*. *OsDEF7* (A), *OsDEF8* (B) expressed under P*trc*1Ocore and P*trc*1O, and expressed by BCD constructs (C); 1: -RT_16s RNA primer, 2: +RT_16s RNA primer, 3: +RT_DEF primer, 4: +RT_DEF/strep primer.

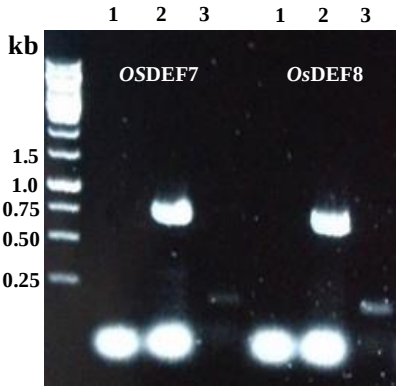

Fig. 4-10 RT-PCR of *OsDEFs* from homologous recombination in *Synechocystis*. 1: -RT_16s RNA primer, 2: +RT_16s RNA primer, 3: +RT_DEF primer.

To check whether *Os*DEF7 and *Os*DEF8 are not toxic to *Synechocystis*, the growth rate and chl *a* content comparing to the normal cell were observed. The result showed that the cell transformed with pEERM_*Os*DEF7 and *OsDEF8* could not affect the growth of *Synechocystis*, but they supported their growth since the rates were doubled to OD_{730} around 5 at the tenth – observation day. While the cell transformed with pEERM showed around 2 OD_{730} (**Fig 4-11**). Correlatively, both *Os*DEFs exhibited the improving in the amount of chl *a* in the cell. The cell engineered with homologous recombination vector revealed 1.1 µg per 10^8 cell. The cells expressing *Os*DEF7 and *Os*DEF8 showed 2.4 and 2.1 µg per 10^8 cell, respectively (**Fig. 4-12**).

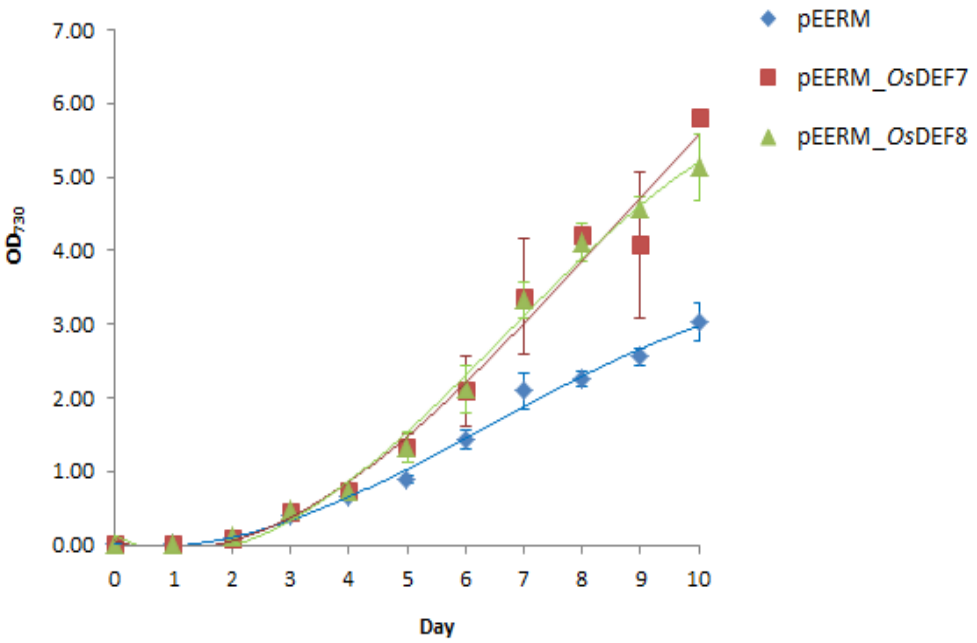

Fig. 4-11 Growth rate of engineered *Synechocystis* transformed by pEERM and pEERM_ *OsDEFs.* The recombinant cells were inoculated at an OD of 0.0025 and grown in BG-11 medium with 25 µg mL^{-1} kanamycin under 50 $\mu Em^{-2}s^{-1}$ white light, at 30°C and 120 rpm. The growth was measured as optical density at 730 nm. Three independent experiments were performed, mean +/- standard deviations.

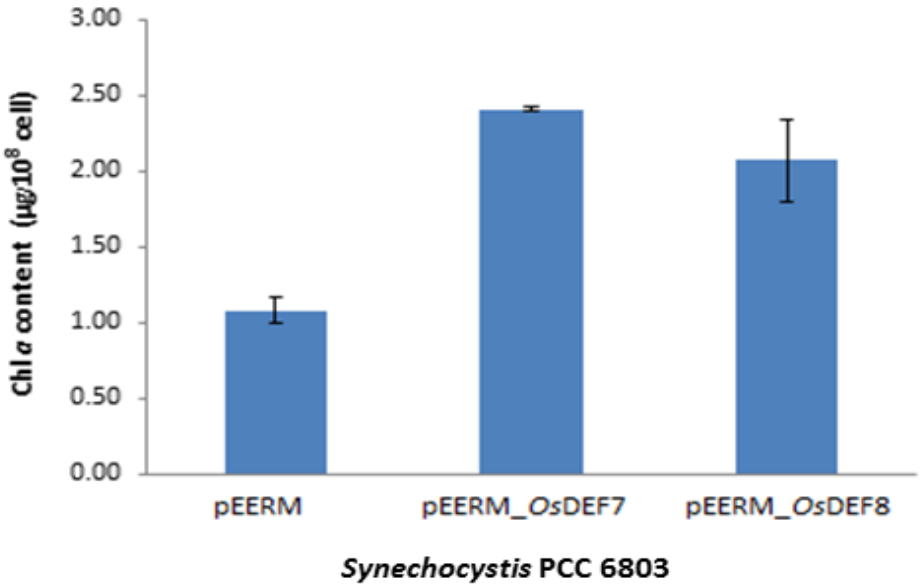

Fig. 4-12 Chlorophyll *a* content of engineered cells *Synechocystis* with pEERM and pEERM_ *OsDEFs*. The engineered cells were grown in BG-11 medium with 25 μg mL^{-1} kanamycin under 50 μ$Em^{-2}s^{-1}$ white light, 30°C and 120 rpm until OD_{730} reached 0.5 to 0.6 and the chl *a* contents were then measured. The results are representative of three independent experiments, mean +/- the standard deviations.

4.2 *trans*-resveratrol production

4.2.1 Gene analysis of genes involved in *trans*-resveratrol production

To ensure the possibility of *trans*-resveratrol producing in *Synechocystis*, the genes were selected from previous studies. The optimized sequences of the genes involved *trans*-resveratrol production were synthesized. The example result of the genes after optimization shown in Appendix B. The enzymes involved in *trans*-resveratrol production were predicted as cytosolic proteins, but C4H. The nucleotide sequences of and the molecular information of enzymes were shown in **Table 4-4.** The expression vectors of these genes were constructed to transform into *Synechocystis*.

Table 4-4 Bioinformatics information of genes involved in *trans*-resveratrol production

Gene	Gene name	Organism	Accession number	Cellular localization	Size (bp)	Mw (kDa)
PAL	*Zm*PAL	*Zea mays*	L77912	Cytoplasm	2112	75
C4H	*Vv*C4H	*Vitis vinifera*	AM468511.2	ER	1432	56
4CL	*Vv*4CL	*Vitis vinifera*	AM428701.2	Cytoplasm	1647	60
STS	*Vv*STS	*Vitis vinifera*	DQ366301	Cytoplasm	1179	43
TAL	*Rs*TAL	*Rhodobacter sphaeroides*	77464988	Cytoplasm	1572	55

4.2.2. Cloning and expression of genes encoding enzymes involved in *trans*-resveratrol production in *Synechocystis*

The fragments of individual genes involved in *trans*-resveratrol production such as *PAL*, *TAL*, *4CL*, and *STS* under both promoters; P*trc*1Ocore and P*trc*1O could be cloned into expression vector pPMQAK1. The expression vectors containing genes involved in *trans*-resveratrol were then transformed and expressed in DH5α*Z*1, and detected by Western blot analysis using antibody against strep tagged-proteins. Converse to the result of *Os*DEFs expression, some genes of enzymes in *trans*-resveratrol producing pathway could be expressed in *E. coli* under both promoters such as *TAL*, *4CL* and *STS*, but *PAL*. The result revealed that TAL, 4CL and STS indicated the molecular weight around 56, 60, and 43 kDa, respectively. The Western blot analysis from *E. coli* expression was shown in **Fig. 4-13**. As *PAL* could not be expressed under neither P*trc*1Ocore nor P*trc*1O, the transcripts of *PAL* were hence checked by RT-PCR (**Fig. 4-14A**). The results exhibited the similar result to the expression of *Os*DEFs, there were the mRNAs of the genes expressed in *E. coli*, but they could not be translated to the protein. To increase chance of translation, BCD constructs was preliminarily tried with *STS*, it accordingly showed no protein expressed with the appearance of mRNA (**Fig. 4-14B**). Nonetheless, the expression constructs with two different promoters and BCD constructs were further transformed into cyanobacteria.

From the cloning of the fused genes involved in *trans*-resveratrol production, the fragment of the fused genes could not be amplified the full length of the fused genes with the primer containing P*trc*1O promoter. The PCR

fragments after amplification were cloned and checked the sequences. The result showed that the primer could bind in the mid of the *4CL*. The Western blot analysis of the fused genes also confirmed the sized of the protein that it had slightly higher molecular weight than that of TAL. The results of Western blot analysis of the genes expression under the same promoter (P*trc*1O) was showed in **Fig. 4-15.** Accordingly, the fragment of the fused genes could not be amplified by the primer containing P*trc*1Ocore promoter by many PCR conditions adjusted and DNA polymerase used, *Taq*, Phusion and PrimeSTAR, and PrimeSTAR GXL. Therefore, the nested-PCR was applied for amplifying both fragments. This could little improve the yield of PCR products. However, the digested fragments could not be ligated into pPMQAK1 with tried conditions; 1:3, 1:5, 1:7, 1:10. This would be because of too long PCR product of the fused genes of *TAL*, *4CL*, and *STS* which around 5 kb. Hence, *trans*-resveratrol production in *Synechocystis* focused on the possibility of production from the individual gene expressing enzymes in the cell.

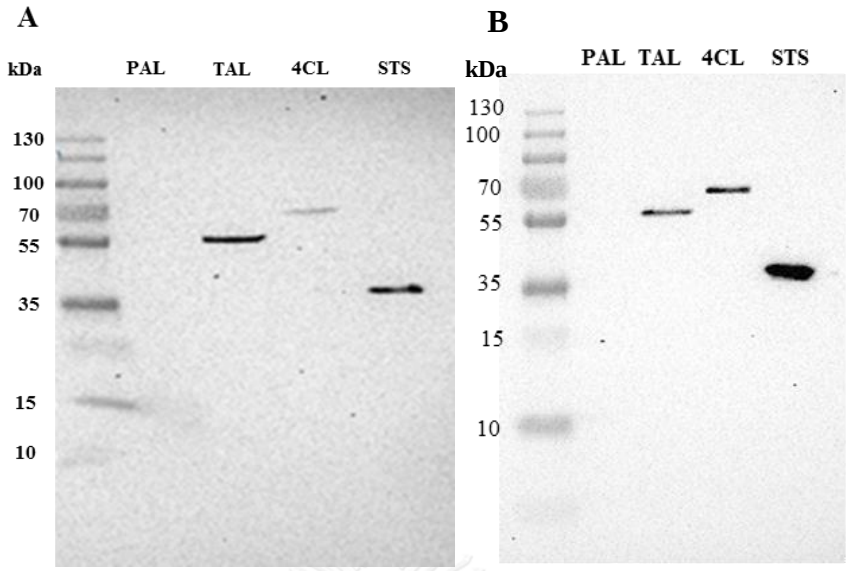

Fig. 4-13 Western blot analysis of the engineered cells expressing enzymes involved in *trans*-resveratrol pathway under the control of either P*trc*1Ocore (A) or P*trc*1O (B) in DH5αZ1. Lane PAL, TAL, 4CL, and STS: crude extracts from engineered *E. coli* cells expressing respective enzymes.

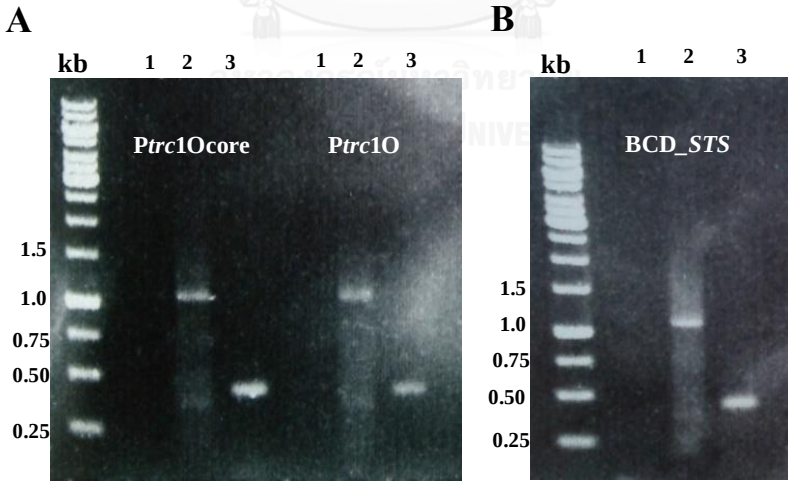

Fig. 4-14 RT-PCR of *PAL* expressed under P*trc*1Ocore and P*trc*1O (A), and *STS* expressed by BCD constructs (B) in DH5αZ1; 1: -RT_16s RNA primer, 2: +RT_16s RNA primer, 3: +RT_specific gene primer.

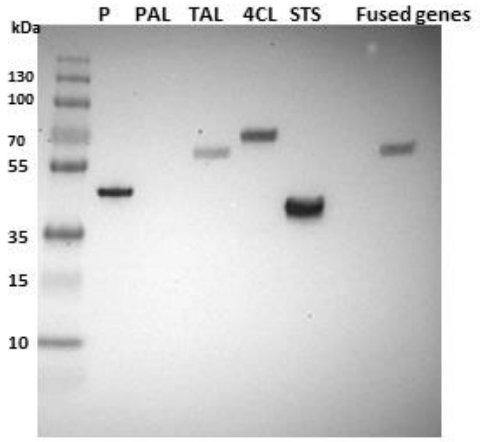

Fig. 4-15 Western blot analysis of the engineered cells expressing the enzymes involved in the *trans*-resveratrol pathway under the control of P*trc*1O in DH5*α*Z1. Lane P: Positive protein of strep tag, Lane PAL, TAL, 4CL, and STS: crude extracts from engineered *E. coli* cells expressing respective enzymes, Lane Fused genes: crude extracts from engineered *E. coli* expressing fused of TAL, 4CL and STS.

From the gene expressions in *Synechocystis*, total cell extract of wild-type *Synechocystis* and the transformants were fractionated by SDS-PAGE. It revealed that both wild type and mutant strains showed many protein bands which they were similar (**Fig. 4-16A**). These were confirmed by Western blot analysis. Likewise *E. coli* expression, the correlated protein bands to TAL, 4CL, STS were presented under both promoters (**Fig. 4-16B**), but not in that of the wild type. The PAL expressed from P*trc*1Ocore and P*trc*1O, and BCD_*STS* could not found in *Synechocystis* (**Fig. 4-17**). Their transcripts were verified by RT-PCR. The result showed the appearance of mRNAs of *PAL* under both promoters, as well as that of *STS* from BCD construct (**Fig. 4-18**). These proved

that PAL could not be expressed in *Synechocystis* under both promoter studied. Therefore, the short pathway of *trans*- resveratrol production starting from TAL followed by 4CL and STS was focused.

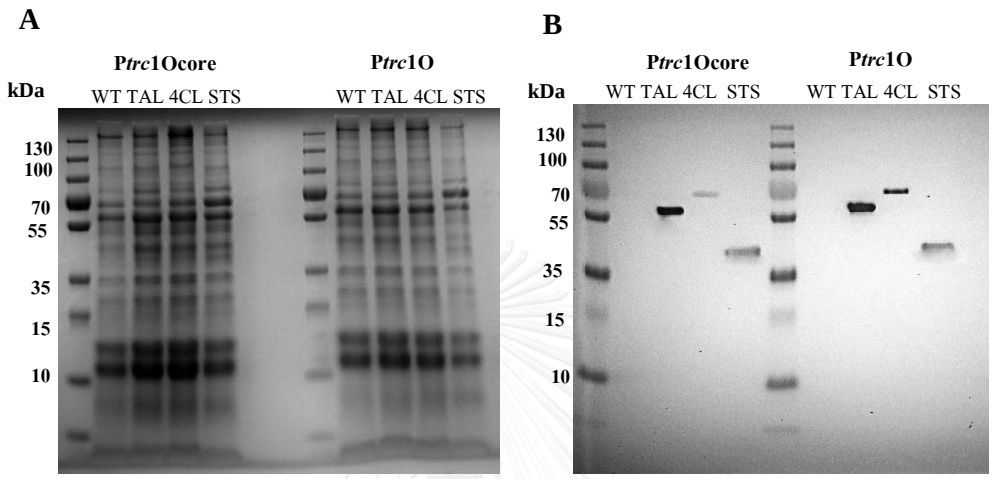

Fig. 4-16 Expression analysis of the enzymes involved in *trans*-resveratrol production in *Synechocystis* under two different promoters. (A) SDS-PAGE and stained with Coomassie blue (A) and Western blot analysis probed with antibodies against strep-tagged proteins (B) of the engineered cells expressing the enzymes in the resveratrol pathway under the control of either P*trc*1Ocore or P*trc*1O. Lane WT: crude extracts from wild-type *Synechocystis* containing pPMQAK1. TAL, 4CL, and STS: crude extracts from engineered *Synechocystis* cells expressing respective enzymes.

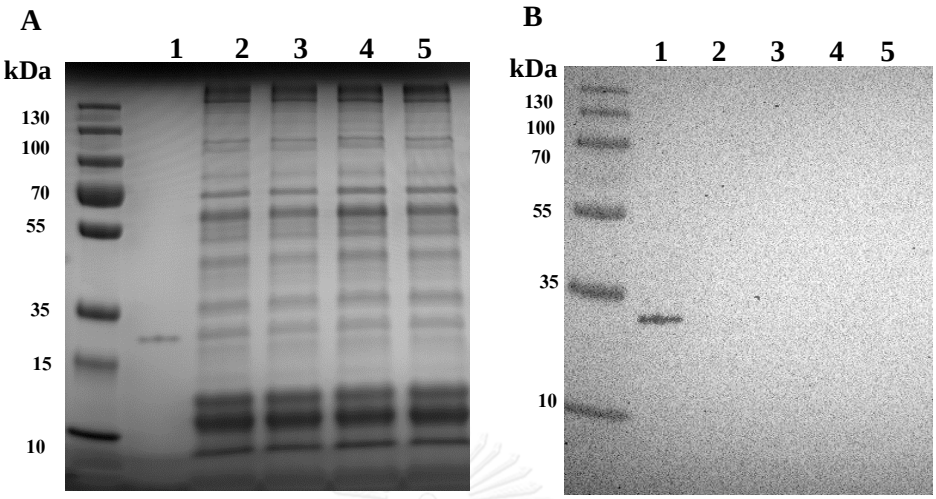

Fig. 4-17 Expression analysis of *PAL* in *Synechocystis* under two different promoters and *STS* expressed by BCD constructs. A: SDS-PAGE of the transformant pPMQAK1_*PAL* and BCD_*STS*. Lanes: 1= positive control of strep tag. 2= crude extracts from wild-type *Synechocystis* transformed with empty pPMQAK1. 3 and 4= crude extracts from *Synechocystis* expressing PAL under P*trc*1Ocore and P*trc*1O. 5= crude extracts from *Synechocystis* with BCD_STS. B: Western blot analysis of A.

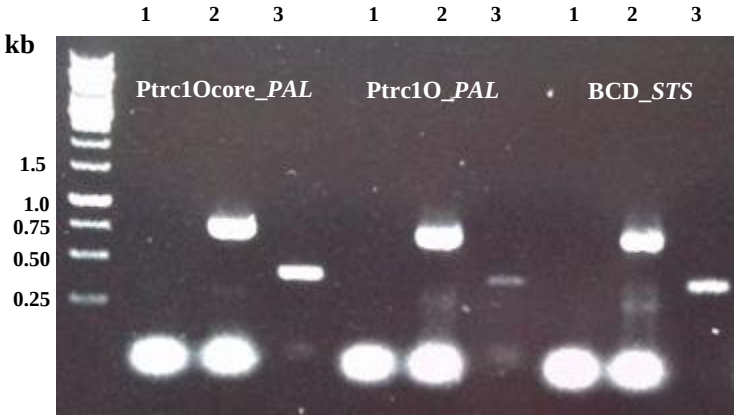

Fig. 4-18 RT-PCR analysis of *PAL* expressed under P*trc*1Ocore and P*trc*1O and BCD_*STS* in *Synechocystis*; 1: -RT_16s RNA primer, 2: +RT_16s RNA primer, 3: +RT_specific gene primer.

4.2.3. The expression level of enzymes involved in *trans*-resveratrol production from *Synechocystis*

The expression level of enzymes involved in *trans*-resveratrol production under P*trc*1Ocore and P*trc*1O were determined from engineered *Synechocystis*. The supernatants from the total cell extract were purified by strep-tactin column. After purification, the proteins were separated by SDS-PAGE to check the purity of purification. The single band of enzymes was obtained from TAL and 4CL expressing in *Synechocystis* (**Fig. 4-19**). While STS could not be observed in the SDS-PAGE. However, the supernatants from cell expressing STS before and after purification were checked by Western blot analysis. The result found that there were STS in the supernatant before purification, and they did not appear after purification. This proved that the expressed STS was

already purified in the column, but in less amount which could not be seen on the SDS-PAGE. Additionally, the expression as the inclusion bodies was also checked from all cells expressing enzymes involving *trans*-resveratrol production. The expression of TAL and 4CL was totally the soluble protein. STS could find in both soluble and inclusion bodies which this was further optimized for *trans*-resveratrol production.

From expression of TAL, 4CL and STS under P*trc*1Ocore, TAL showed highest expression level which yielded 17.9±0.4 μg per 10^8 cells. While, 4CL and STS revealed similar expression of 6.3±0.6 and 7.0±0.9 μg per 10^8 cells, respectively which they were two times less than TAL. Accordingly, the expression of these genes under P*trc*1O had the same pattern of expression level that TAL was the highest level of expressed protein, followed by 4CL and STS. The obtained protein contents under P*trc*1O were 20.0±1.3, 9.9±0.8, and 8.0±0.5 μg per 10^8 cells, respectively, respectively (**Fig. 4-20**).

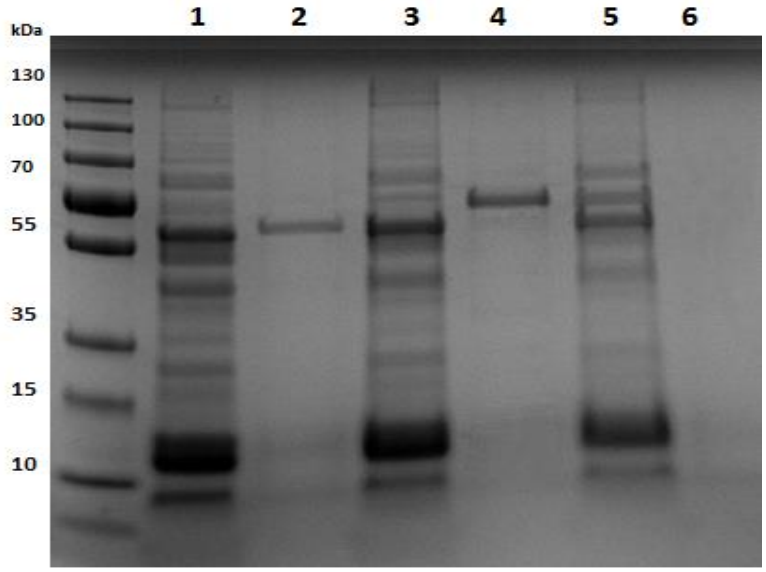

Fig. 4-19 Protein purification of recombinant enzymes involved in the *trans*-resveratrol biosynthetic pathway from *Synechocystis* PCC 6803 using P*trc*1O promoter. The recombinant enzymes were purified using strep-tactin column. The purified enzymes of the *trans*-resveratrol pathway were separated by SDS-PAGE and stained with Coomassie blue. Lane 1,3,5: supernatants from *Synechocystis* containing TAL, 4CL, and STS, Lane 2,4,6: purified respective enzymes.

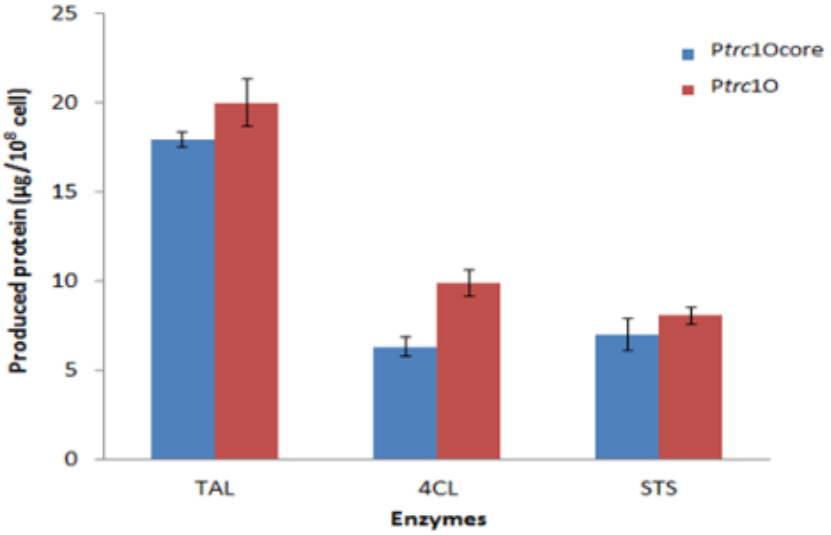

Fig. 4-20 Production yield of purified recombinant enzymes in engineered *Synechocystis* PCC 6803. The recombinant enzymes were purified using strep-tactin column.

4.2.4 The effects of enzymes involved *trans*-resveratrol production on *Synechocystis*

4.2.4.1 The effects on the growth rate

The effect of enzymes involved *trans*-resveratrol production expressed from P*trc*1Ocore and P*trc*1O on the growth, there was a little difference in growth between both cyanobacterial promoters where strains expressed enzymes under P*trc*1Ocore had a slower growth but in the end reached the same OD to P*trc*1O. While the strain with empty vector (pPMQAK1) revealed the slowest growth rate throughout the period of two weeks. The difference between WT and all mutant strains (TAL, 4CL, STS) under P*trc*1Ocore, however, was not significant. Also, the three mutant

strains expressed under P*trc*1O showed the same growth pattern, and they slightly improved in growth after 10 day culturing. None of the mutants from both promoters were significantly different from WT over the observation period of 14 days (**Fig. 4-21**). This could be suggested that expressions of TAL, 4CL, STS have no impact on normal growth of *Synechocystis*.

A

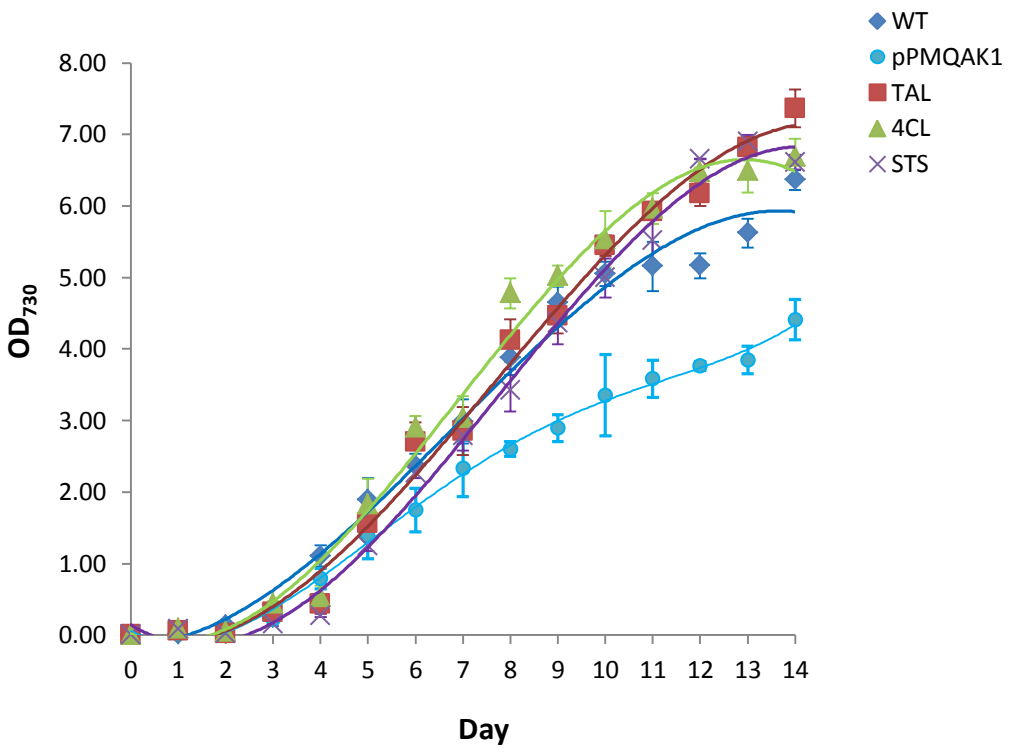

B

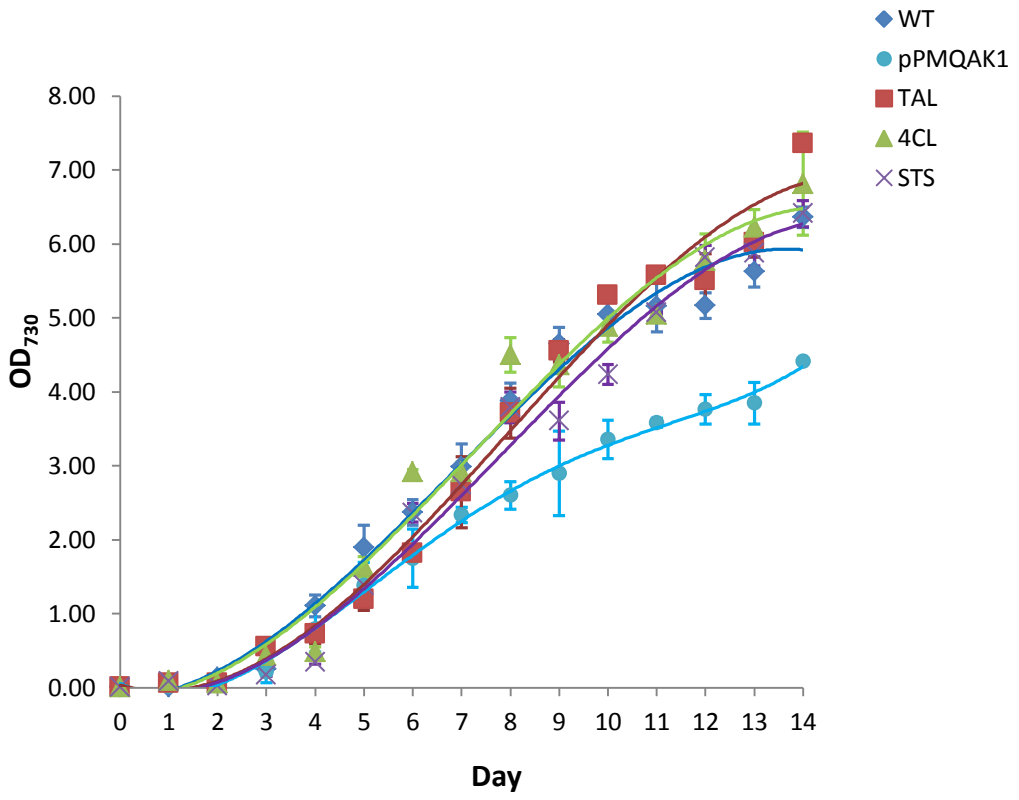

Fig. 4-21 Growth rate of engineered cells of *Synechocystis* PCC 6803 expressing the enzymes of the *trans*-resveratrol biosynthetic pathway under two promoters P*trc*1Ocore (A) and P*trc*1O (B). WT and engineered *Synechocystis* cell cultures were inoculated at an OD of 0.0025 and grown in BG-11 medium with 25 µg mL^{-1} kanamycin under 50 $\mu Em^{-2}s^{-1}$ white light, at 30°C and 120 rpm. Growth was measured as optical density at 730 nm. Three independent experiments were performed, mean +/- standard deviations.

4.2.4.2 The effects on the chl *a* content

To determine whether the recombinant enzyme expressions resulted in changes in the chl *a* content in the cells, the chl *a* content of wild-type cells, cells with empty vector, and engineered cells expressing the respective enzymes were investigated. There was no differences in the chl *a* content when comparing the wild-type cells and cells with empty vectors, both showing about 1.2 μg chl *a* per 10^8 cell. The cells expressing enzymes of the *trans*-resveratrol biosynthetic pathway, using either P*trc*1Ocore or P*trc*1O, revealed similar pattern of the chl *a* content. The cells expressing TAL showed no significant difference in the chl *a* levels comparing to wild-type cells, but cell expressing STS revealed slightly less chl *a* content. Interestingly, cells expressing 4CL, from both promoters, showed the highest chl *a* content of 1.6 μg chl *a* per 10^8 cell (**Fig. 4-22**).

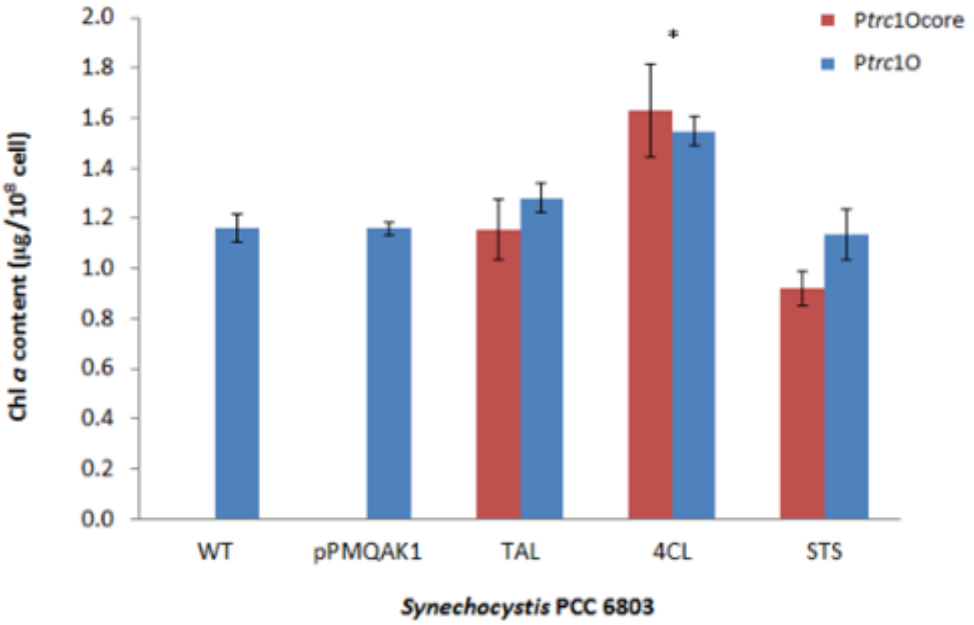

Fig. 4-22 Chlorophyll *a* content of engineered *Synechocystis* PCC 6803 expressing the enzymes of the *trans*-resveratrol biosynthetic pathway. WT and engineered cells of *Synechocystis* were grown in BG-11 medium with 25 µg mL^{-1} kanamycin under 50 µ$Em^{-2}s^{-1}$ white light, 30 ^{o}C and 120 rpm until OD_{730} reached 0.5 to 0.6. The results are representative of three independent experiments, mean +/- the standard deviations. The asterisk represents statistical significant difference ($p < 0.05$) by t-test.

4.2.5 Estimation of the *trans*-resveratrol production in *Synechocystis*

4.2.5.1 Metabolites detection from the *Synechocystis* expressed enzymes involved in *trans*-resveratrol production

The engineered *Synechocystis* expressed enzymes in the pathway of *trans*-resveratrol production were detected the productions of the compounds involving in the pathway. The result showed that the cells expressing TAL presented the production of *p*-coumaric acid in the cell (**Fig. 4-23**). The peaks of candidate *p*-coumaric acid showed the retention time at 14.3 min and exhibited the molecular weight at 163.02 m/z. These were confirmed with the *p*-coumaric acid standard which those peaks were similar to the standard. The produced *p*-coumaric acid was quantitated by standard curve of *p*-coumaric acid. From this, the engineered *Synechocystis* expressing TAL could produce *p*-coumaric acid in differences concentrations from both promoters. The cells expressing TAL under P*trc*1O could produce three times higher than that from P*trc*1Ocore, accounting for 18.4±1.5 and 5.0±0.7 µg per 10^8 cell, respectively (**Fig. 4-24**). While engineered *Synechocystis* expressing 4CL and STS revealed no production of the compounds from *trans*-resveratrol pathway which were similar to the non-engineered cell and the cell transformed with pPMQAK1.

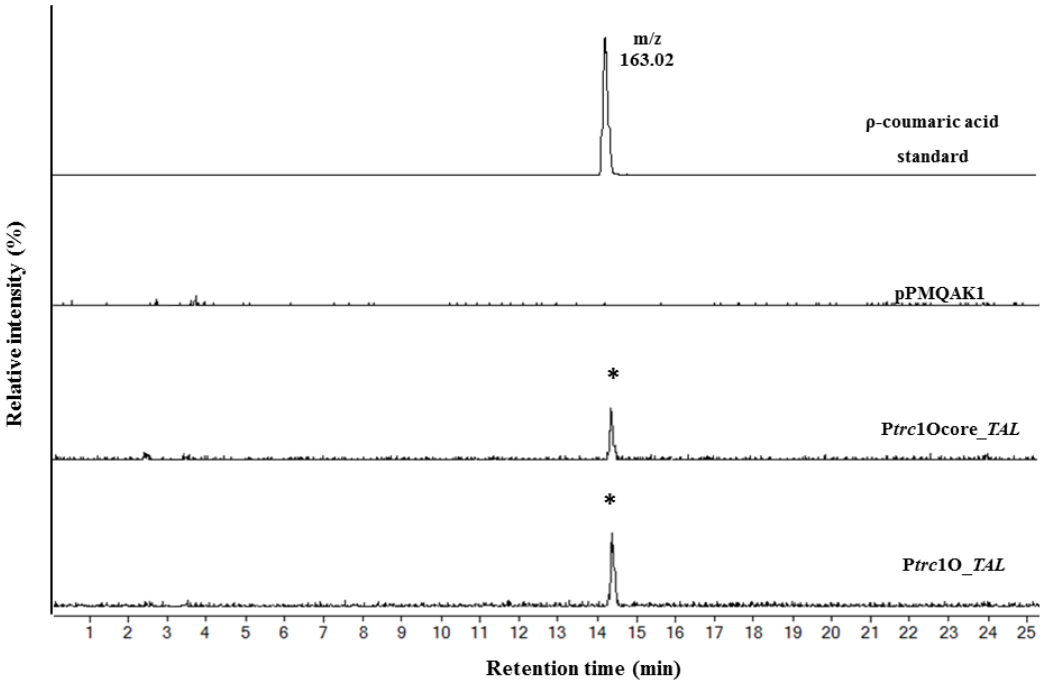

Fig. 4-23 LC-MS analysis of *Synechocystis* PCC 6803 expressing TAL under controlled of P*trc*1Ocore and P*trc*1O. The engineered cells of *Synechocystis* were grown in BG-11 medium with 25 µg mL^{-1} kanamycin under 50 $\mu Em^{-2}s^{-1}$ white light, 30°C and 120 rpm until OD_{730} reached 0.5 to 0.6. The cells were collected for LC-MS analysis. Molecular weight of *p*-coumaric acid standard = 163.02. The asterisks show the produced compounds from the cell extract.

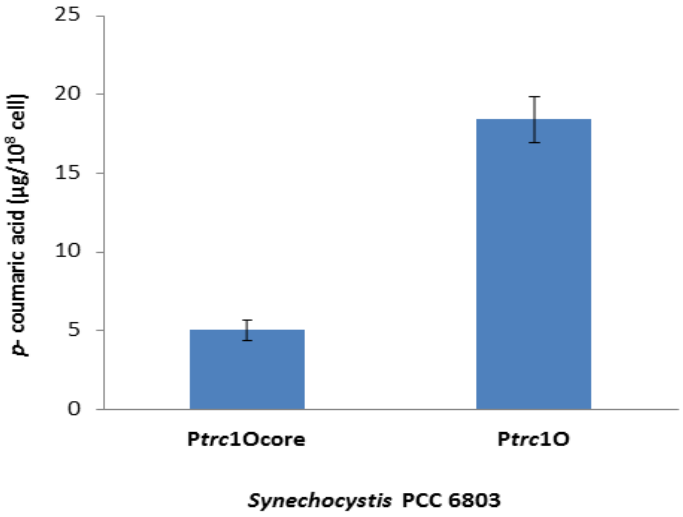

Fig. 4-24 Production of *p*-coumaric acid in *Synechocystis* PCC 6803 expressing TAL under controlled of P*trc*1Ocore and P*trc*1O. The engineered cells of *Synechocystis* were grown in BG-11 medium with 25 µg mL^{-1} kanamycin under 50 µ$Em^{-2}s^{-1}$ white light, 30°C and 120 rpm until OD_{730} reached 0.5 to 0.6. The cells were collected for LC-MS analysis. The results are representative of three independent experiments, mean +/- the standard deviations.

4.2.5.2 Optimization conditions of *trans*-resveratrol production

To optimize the production of *trans*-resveratrol, the cell expressing STS was focused as there was some protein expressed in the inclusion body (**Fig. 4-25**). In bacterial expression, the expressing STS was improved by growing the cell in lower temperature. In this study, the growth condition of *Synechocystis* was adjusted by performing the experiment in the growth chamber with the controlling light and temperature. The cell expressing STS were grown at 30°C under 30 µ$Em^{-2}s^{-1}$ light until the OD_{730} around

0.5-0.6. The growth temperature was then reduced to 25°C and continued culturing for 24 h. From the study, this condition could improve the STS expression. The expression revealed much higher than the previous growth condition, accounted for 119.3±13.0 and 87.5±4.7 µg protein per 10^8 cell from expressing under P*trc*1O and P*trc*1Ocore, respectively (**Fig. 4-26**). While the previous conditions showed the expression of STS from both promoters only around 6 µg protein per 10^8 cell.

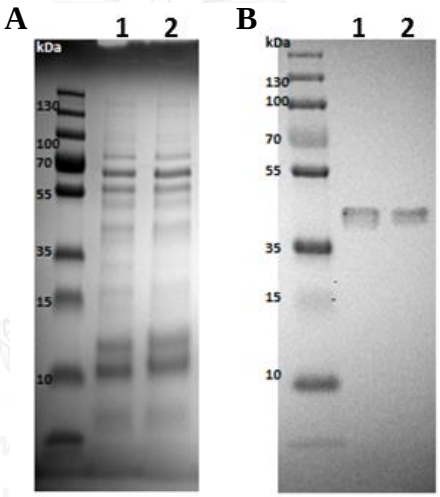

Fig. 4-25 Expression analysis of expressed STS in *Synechocystis* PCC 6803 using two different promoters. A: SDS-PAGE stained with Coomassie blue, and B: Western blot analysis probed with antibodies against strep-tagged proteins. Lane 1 and 2: pellet of the *Synechocystis* expressing STS under the control of either P*trc*1Ocore or P*trc*1O, respectively.

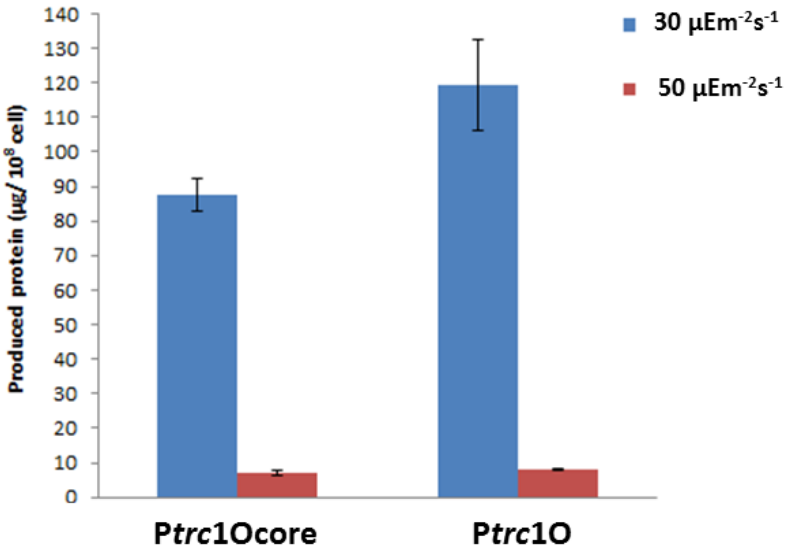

Fig. 4-26 Production yield of expressed STS in *Synechocystis* PCC 6803 using two different promoters. The engineered cells of *Synechocystis* were grown in BG-11 medium with 25 µg mL^{-1} kanamycin under 30 and 50 $\mu Em^{-2}s^{-1}$ white light, 30°C and 120 rpm until OD_{730} reached 0.5 to 0.6. The cells were collected extracted for purification by strep-tactin column. The results are representative of three independent experiments, mean +/- the standard deviations.

To produce *trans*-resveratrol in other organisms, the substrate of the pathway was added into the medium (Donnez et al., 2009; Wang et al., 2011). Likewise, *p*-coumaroyl CoA was supplemented in BG-11 to produce *trans*-resveratrol in *Synechocystis*. The cells expressing STS under both promoters grown under different growth conditions as described in 3.11.4.2 were treated with *p*-coumaroyl CoA. The concentrations were varied from 0-100 nM. Moreover, the effects of treating these substrate concentrations

into the medium on the growth rate of the cell were observed. The result found that the cells expressing STS under both promoters grown under 50 $\mu Em^{-2}s^{-1}$ showed similar pattern that the concentrations of *p*-coumaroyl CoA slightly affected the growth rate of the treated cells, as they showed lower in growth than wild type. Obviously, the engineered cells treated with *p*-coumaroyl CoA grown under lower light (30 $\mu Em^{-2}s^{-1}$) exhibited two-times less in their growth rate than that under high light (50 $\mu Em^{-2}s^{-1}$) under both promoters, and they showed closely growth rate in all substrate treated cells (**Fig. 4-27**). Moreover, the chl *a* content of the cells expressing STS under P*trc*1Ocore in both growth conditions were not significant different in all substrate treated. They exhibited the chl *a* content ranged from 1.5-3.2 µg per 10^8 cell. While the cells expressing STS under P*trc*1O showed the similar pattern of chl *a* content that the cell grown under low light were doubled in chl *a* content than that grown under high light in all additional *p*-coumaroyl CoA concentrations. That were around 1.9-2.6 µg per 10^8 cell in low light, and 0.9-1.4 µg per 10^8 cell in high light (**Fig. 4-28**). Although growing the cells at low light and low temperature (25°C) gave more STS produced in the cell than those grown at higher light and higher temperature (30°C). The *trans*-resveratrol and its derivatives could not be produced in the cells expressing STS under both promoters from all treated concentrations of *p*-coumaroyl CoA.

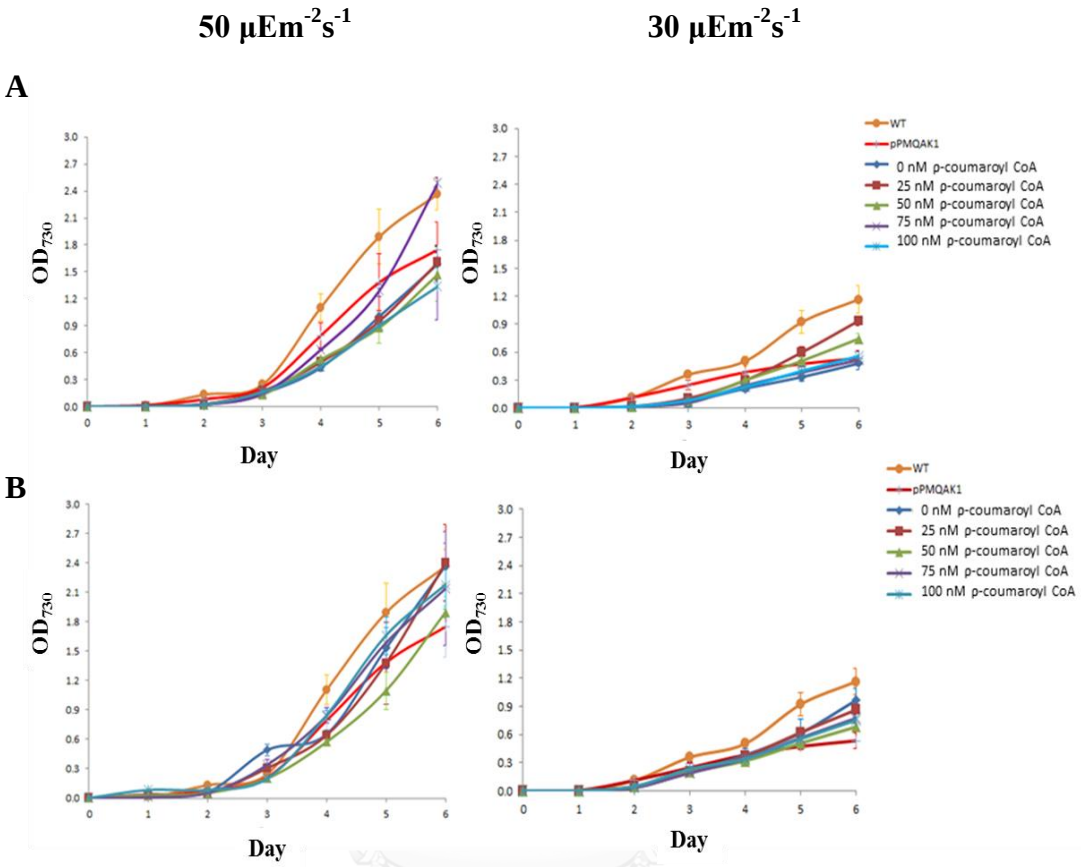

Fig. 4-27 Growth rate of *Synechocystis* PCC 6803 expressing STS under two promoters P*trc*1Ocore (A) and P*trc*1O (B) in different growth conditions. WT and engineered *Synechocystis* cell cultures were inoculated at an OD of 0.0025 and grown in BG-11 medium with 25 µg mL^{-1} kanamycin under 30 and 50 $\mu Em^{-2}s^{-1}$ white light, at 30°C and 120 rpm. Growth was measured as optical density at 730 nm. Three independent experiments were performed, mean +/- standard deviations.

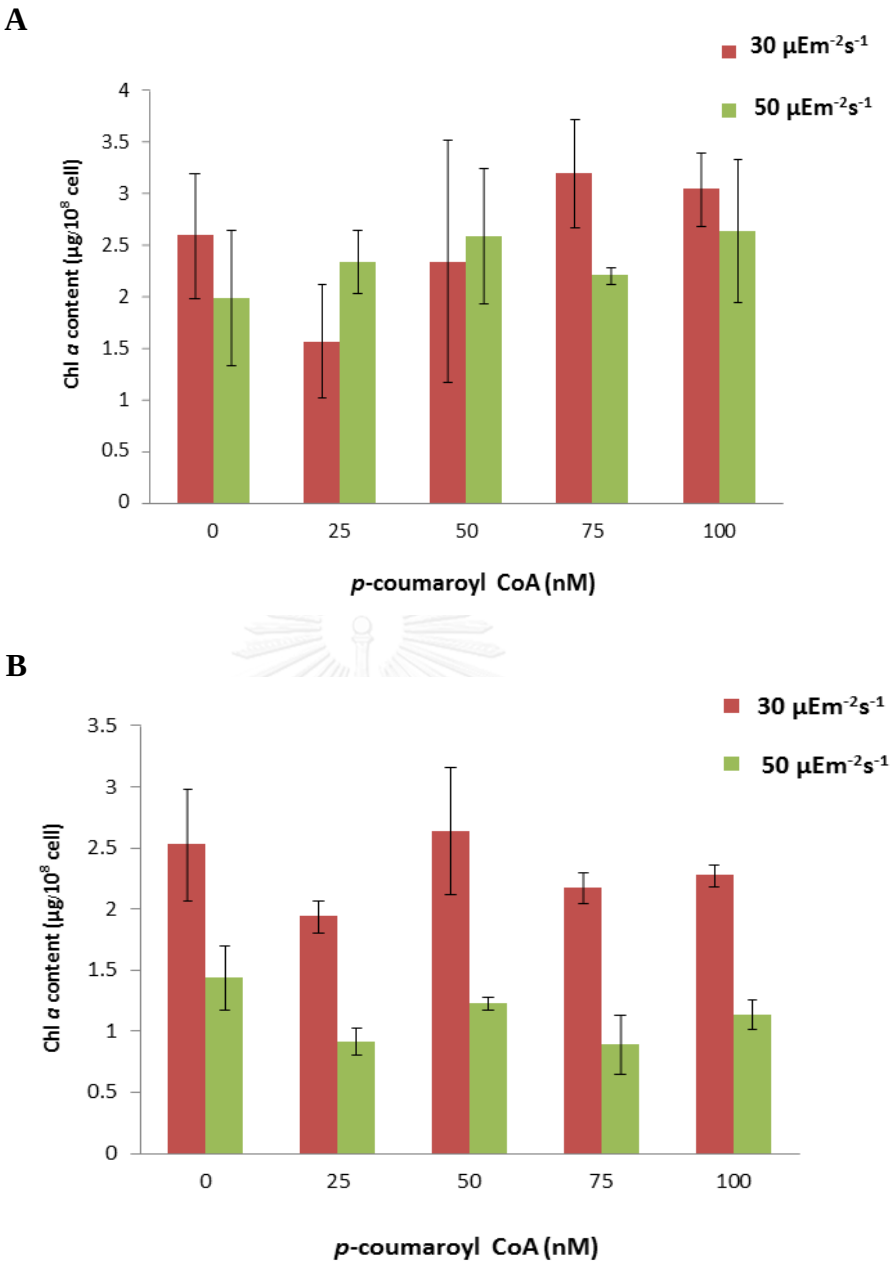

Fig. 4-28 Chlorophyll *a* content of *Synechocystis* PCC 6803 expressing STS under P*trc*1Ocore (A) and P*trc*1O (B). WT and engineered cells of *Synechocystis* were grown in BG-11 medium with 25 µg mL^{-1} kanamycin under 30 and 50 µ$Em^{-2}s^{-1}$ white light, 30°C and 120 rpm until OD_{730} reached 0.5 to 0.6. The results are representative of three independent experiments, mean +/- the standard deviations.

4.2.5.3 In vitro production of *trans*-resveratrol

To test the possibility of *trans*-resveratrol production from all involving enzymes, the cell expressing TAL, 4CL and STS were mixed and extracted for testing in vitro experiment. The results revealed that there was no *trans*-resveratrol and its derivatives produced from the mixture in all conditions studied. Nevertheless, *p*-coumaric acid could be detected in the mixtures (**Fig. 4-29**). The tyrosine-free mixture and tyrosine-added mixtures showed *p*-coumaric acid produced ranging from 0.35 to 1.42 mg L^{-1} after incubating for 7 hours. While the production doubled when incubating for 14 hours which were ranged from 0.72 to 2.73 mg L^{-1} (**Fig. 4-30**). To check the activity of STS, the crude cell extract of STS expressed under P*trc*1O was treated with 100 nM *p*-coumaroyl CoA. However, *trans*–resveratrol could not be detected in the mixture.

Interestingly, all mixtures analyzed by LC-MS analysis revealed the distinguished peak at 8.03 min (**Fig. 4-31A**). This unknown showed the molecular weight of 164.0587. They were further analyzed by Auto MS/MS with the collision-induced dissociation **(**CID**)** at 10. This compound showed the fragmentation pattern as 164.05, 147.03, 124.00, 103.04, 91.04, and 72.00 (**Fig. 4-31B**). Nevertheless, this compound could not conclude the structure from this fragmentation.

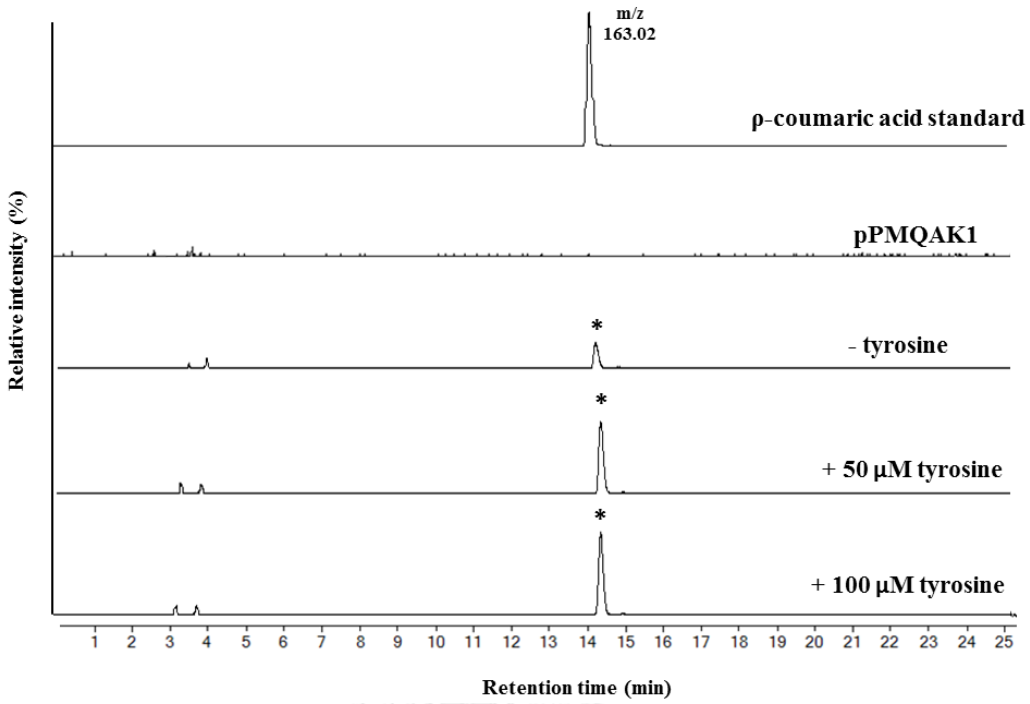

Fig. 4-29 LC-MS analysis of in vitro production of *p*-coumaric acid. The engineered cells of *Synechocystis* expressing TAL, 4CL, and STS under P*trc1*O were grown in BG-11 medium with 25 µg mL^{-1} kanamycin under 50 µ$Em^{-2}s^{-1}$ white light, 30°C and 120 rpm until OD_{730} reached 0.5 to 0.6. The cells were extracted and the mixed crude cell extracts were treated with 0, 50 and 100 µM tyrosine. The reactions were incubated at 30°C for 7 hours. The products were extracted for LC-MS analysis. The results are representative of three independent experiments, mean +/- the standard deviations. Molecular weight of *p*-coumaric acid standard = 163.02. The asterisks show the produced compounds from the mixed crude cell extracts.

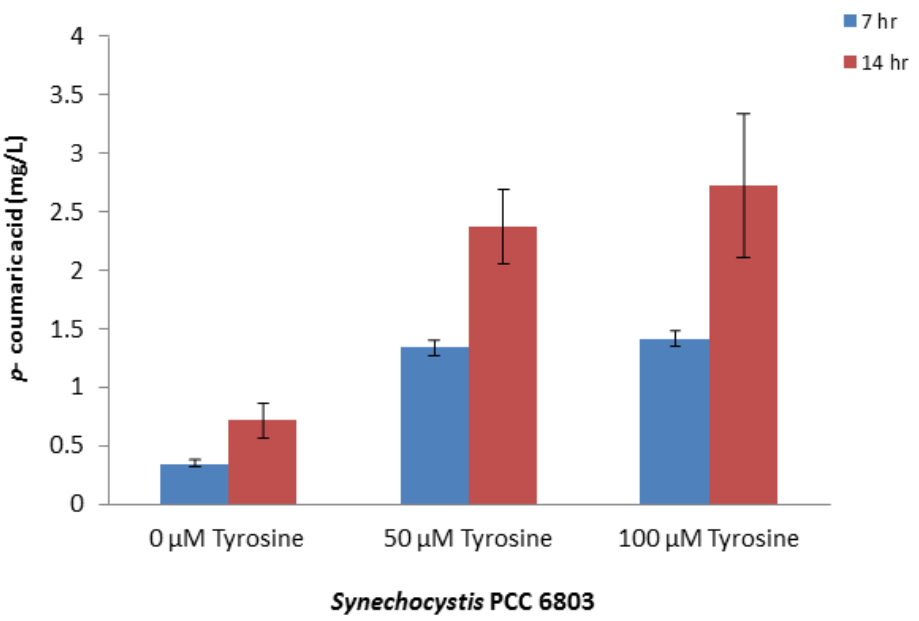

Fig. 4-30 In vitro production of *p*-coumaric acid. The mixed crude cell extracts were treated with different concentration of tyrosine; 0, 50 and 100 µM and incubated at 30^{o}C for 7 and 14 hours. The products were extracted for LC-MS analysis. The results are representative of three independent experiments, mean +/- the standard deviations.

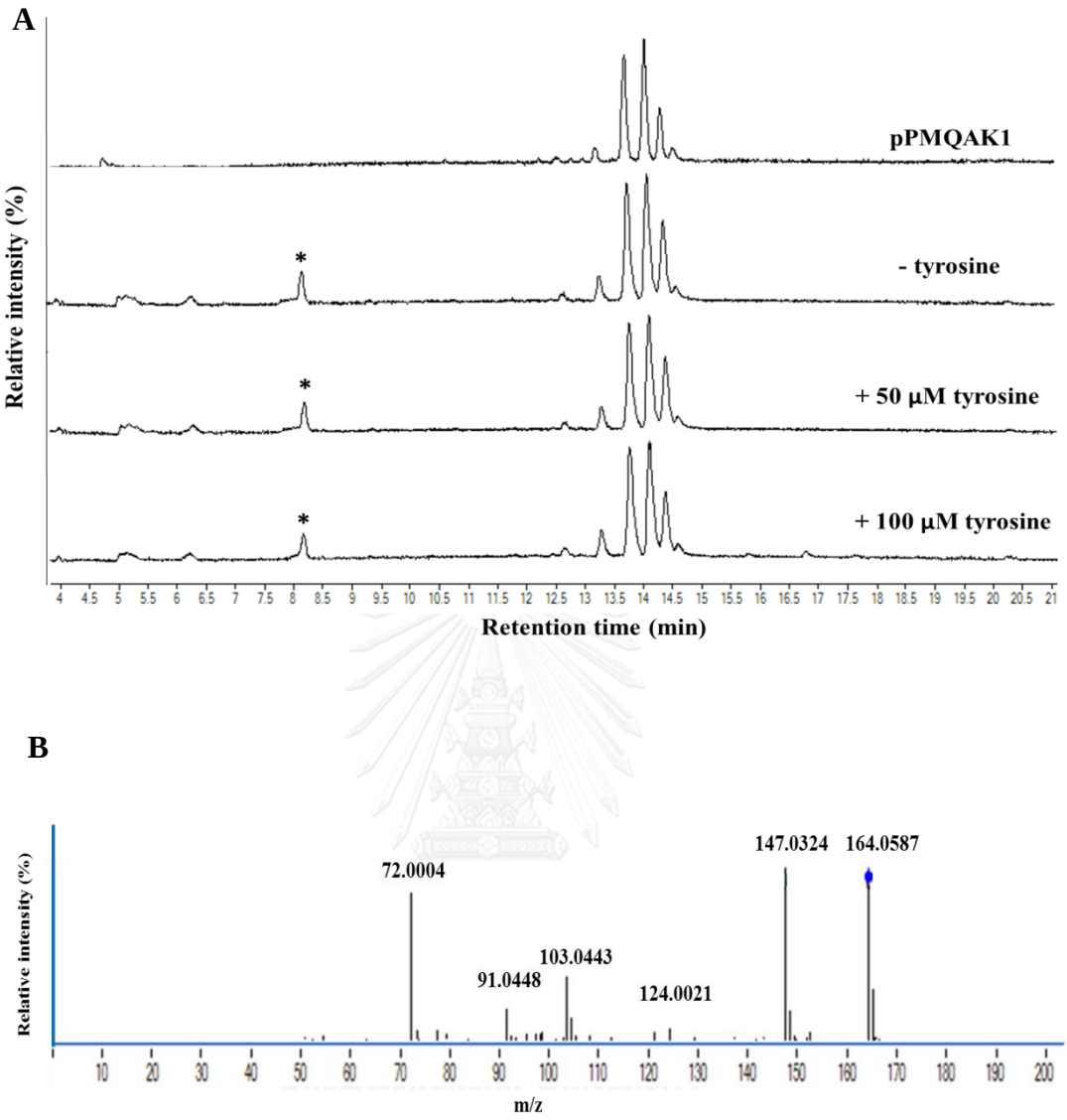

Fig. 4-31 LC-MS analysis of unknown compound from the in vitro reaction.

A: the chromatogram of the in vitro production. The asterisks show the produced compounds from the mixture. B: fragmentation of unknown compound analyzed by auto MS/MS with CID = 10, blue closed dot shows the molecular weight of the unknown compound = 163.02.

CHAPTER V

DISCUSSION

5.1 AMPs production

5.1.1 In silico analyses of AMPs

Plant AMPs have been identified and reported for functions (Hammami et al., 2009[a]). They divided into several families. CRPs are particularly well represented among plants and they have been focused because of their stable structures (Silverstein et al., 2007). Among these CRPs, defensin family has been largely studied, around 16.8 % of the identified AMP related in Genbank/ NCBI/ Entrez databases (from Clara Pestana-Calsa et al., 2010). Furthermore, there are many reports on its primarily effective biological activity. Rice was exemplified in this work as it is a commercial crops suffering from infected pathogens. Though it has been less studied in rice AMPs, CRPs were identified in the whole-genome of *O. sativa* (Silverstein et al., 2007). Some of these genes are the member AMPs. From these information, the in silico and coexpression network analyses were used to guide the promising candidate *OsDEFs* for improving rice cultivation or other applications. The online microarray databases have been effectively used for analyzing the distribution of correlated genes according to degree of stringency and predicting genes coexpressed with others (Fu and Xue, 2010; Lee et al., 2009). These have been proved that the gene coexpression analysis is a powerful method for gene characterization. In the genome of *O. saltiva*, there are 57 genes encoding of *DEF* and *DEFL*. They

all showed 15% amino acid similarity which those are the pattern of cysteine represented the defensin family (**Fig. A-2**, Appendix A). From coexpression network analysis, only one-third of the *OsDEFs* could be analyzed from databases since the nucleotide probes are not available in the microarray plate. Only 22 *OsDEFs* are available either Plantarraynet or RiceArrayNet and 11 genes of these *OsDEFs* showed correlation with plant protective process. Since, the limitation of the accessible databases, the unidentified 35 *OsDEFs* have thus never been studied and the questions remained to be answered for those other *OsDEFs* if they are expressed. Therefore, many candidate *OsDEFs* would be missed.

Eleven *OsDEFs* showed coexpressed with the groups of the plant pathogen responsive-proteins, disease resistance protein and/or resistance protein candidates (**Fig. 4-1**). These results justified that 11 *OsDEFs* would play an important role in the defense mechanism. Moreover, there was a study suggesting that plant DEFs would involve in growth and development protein, as they could protect the female gametophytes during fertilization process (Cordts et al., 2001). In this study, *OsDEFs* were linked with small CRPs supporting growth such as Stig1 family protein, plant hormone, and RALF (**Fig. A-1**). RALF and RALFL have been reported as the essential proteins for root development promoting the growth of plants (Pearce et al., 2001).

Among the pathogen responsive- genes coexpressed with *OsDEF7* and *OsDEF8*, many of those genes have been reported for their involvement in pathogen resistances. *Pi-ta* has been confirmed as rice blast resistance genes (Bryan et al., 2000). TLPs were reported as an antibacterial and antifungal

activity (Gorjanović et al., 2007; Krebitz et al., 2003). Chitinases (EC 3.2.1.14) and β-1,3-glucanases (EC 3.2.1.39) are enzyme eliminating microbes which have been classified as PR proteins (Schaefer et al., 2005). They have been called antifungal hydrolases since they inhibit fungal growth in model experiments (Sela-Buurlage et al., 1993). The transgenic plants exhibiting increased chitinase activity could be resistant to rice sheath blight pathogen (Lin et al., 1995; Nandakumar et al., 2007). Proteinase inhibitors including cysteine and serine proteinases inhibitors, found in plant seeds and storage organs, are also involved in pathogen response (Silverstein et al., 2007). *O. sativa* proteinase inhibitor could mediate or mimic the plant defense in rice leaves to cope with the blast pathogen (Agrawal et al., 2002). Therefore, the co-expression of *OsDEF7* and *OsDEF8* with those genes strongly indicated the involvement of both DEFs in pathogen responses. Moreover, several *OsDEFs* including *OsDEF7* and *OsDEF8* coexpressed with small CRPs reported to support growth and development such as gibberellin regulated proteins. These proteins play an essential role in many aspects of plant growth and development, such as seed germination, stem elongation, flower and fruit development, including the physiological processes of rice (Takasaki et al., 2008). These findings could suggest a role of these rice DEFs including growth and development (**Fig. A-3**). There was a previous study on multiple functions of tomato DEF2 which are related to defense and development (Stotz et al., 2009).

Apart from coexpression network analysis, expression levels in the specific tissue could assume the function of gene as they would be expressed

more in the tissue that susceptible to pathogen infection. *OsDEF7* and *OsDEF8* showed significant high level of expression throughout tissue. This could be inferred that they would exist to against pathogens. Moreover, *OsDEFs* and rice *AMPs* have been checked the expression levels (**Fig. A-4**, Appendix A). Many rice *AMPs* revealed higher expression in rice tissue namely, *THION*, *LTP*, *HEV* and snakin family (*GASR*). Especially, *GASR* showed apperearently high expression level throughout the organs (**Fig. A-4**, Appendix A). Possibly, members in these families would involve in plant defense mechanisms which the candidates could also be selected by in silico and coexpression network analyses (Krissana, 2014) (**Fig. A-3, A-4** in Appendix A). With coexpression network analysis together with the gene expression data, *Os*DEF7 and *Os*DEF8 could be identified. Therefore, these approaches are a powerful method to identify novel gene functions.

5.1.2 Production of *OsDEFs* in *E. coli*

The purified *Os*DEFs formed the dimeric peptides. Several AMPs were reported to express as polymeric forms instead of being expressed as a monomeric one (Li et al. 2011). In certain case, expressing as a multi peptide gave much higher expression yield of expression than monomers (Zhou et al., 2009[a]; Zhou et al., 2009[b]). *Na*D1 from the flower of *N. alata* was reportedly formed the cross-linked dimers as indicated on SDS-PAGE. It is formed by the association of the β1-strands from the two monomers. This creates an extended β-sheet leading to the formation of a more compact and symmetrical dimer which is stabilized by three hydrogen bonds such as Lys4–Lys4, Ser35–Cys47,

and a strong H- bond, salt bridge, between Cys47–Arg40 (**Fig. A-5**). *Os*DEF8 showed the amino acid of Cys47 and Arg40 in the sequence (**Fig. A-5D**).Therefore, it could also form the salt bridge of Cys47 -Arg40 to stabilized its dimer structure. In the NAD1 dimeric structure, Lys4–Lys4 is considered as the strong bond to maintain the dimer. The point mutation of Lys4 thus presented the monomer which it had low activity against the growth of *F. oxysporum*. Moreover, this dimerization is significantly correlated with its activity against pathogens (Lay et al., 2012). Our results suggest the in vitro activities of *Os*DEF7 and *Os*DEF8 against several plant pathogens including *Xoo, Xoc,* and *F. oxysporum* that are rice pathogens.

5.1.2.1 Antimicrobial activities and homology structures of *Os*DEFs

Comparing the MIC values of these two rice DEFs ranging from 0.64 to 63 µg mL^{-1} to that of AMP from *Oudneya africana* seeds at 313 µg mL^{-1} against gram-negative bacteria; *Pseudomonas aeruginosa* and *Dickeya dadantii* (Hammami et al., 2009[b]), these two recombinant rice AMPs are much more efficient. Although the tested bacteria were different, they all were gram-negative bacteria. This finding proves that rice possesses AMPs that could functionally inhibit its own pathogens. However, the expression level could be limited and most AMPs are not expressed in a leaf where is the most targeted infection site. Recently, a study has shown that the application of recombinant AMP on tomato leaves could confer fungal resistance providing the further uses of recombinant AMPs as a plant fungicide (Wu et al., 2011). The obtained production yield

of these two recombinant *Os*DEFs in *E. coli* was quite adequate for further applications. The host differences for heterologous expression and purification methods should be considered for higher production yield and purification process. Additionally, the approaches to develop the production of AMPs in *E. coli* were reviewed in Li et al. (2011).

Interestingly, the recombinant *Os*DEF8 exhibited lower MIC value for *Xoc* when compared to *Xoo*. This could be suggested that *Os*DEF8 has a higher binding affinity to the membranes of *Xoc* than that of *Os*DEF7. Although both pathovars share high similarity in genomic sequences, it has been shown that their gene expression patterns were different upon infection (Seo et al., 2008). This observation might indicate the difference in membrane composition between *Xoc* and *Xoo* resulting in the different MIC values obtained from *Os*DEF8. There were some differences in antimicrobial activity between *Os*DEF7 and *Os*DEF8. Their structural differences were investigated (**Fig. 4-7**). It has been reported that the type of amino acids constructing the loop linked between β2-β3 sheets is involved in the antimicrobial activity (De Samblanx et al., 1997). Several differences in amino acid sequence and length in this region were found. Although the length of amino acids forming the loop that contribute to AMP activity has not been reported. Since the loop structural difference between both *Os*DEFs is the only region identified in the modeled structures, this proposed that the loop region is contributed to different activity between *Os*DEF7 and *Os*DEF8.

As the fungicide, both *Os*DEFs was structurally similar to NaD1 from *N. alata* which was reported the mechanism as antifungal activity against several filamentous fungi, including *F. oxysporum*. It interacts with the fungal cell wall, permeability of the plasma membrane (van der Weerden et al., 2008; van der Weerden et al., 2010). Additionally, the phylogenic tree showed that *Os*DEF7 linked with *Ta*Def from *Triticum aestivum* which has been reported for the activity against gram-negative bacteria, *Pseudomonas solanacearum* and *Xanthomonas campestris* (De Caleya et al., 1972). *Os*DEF8 also linked to *Ca*J1-2 which has been reported as antifungal against *F. oxysporum* (Meyer et al., 1996) (**Fig.4-4**). These could be suggested that both *Os*DEFs could exhibit antifungal activity.

5.1.3 Production of *Os*DEFs in *Synechocystis*

*Os*DEF7 and *Os*DEF8 could not be found and the protein degradation could not observe in the cells. Therefore, the gene expression in the cell of *Synechocystis* was detected. The transcripts of both *Os*DEFs were completely transcribed without any protein translated. This would be because of either toxicity of *Os*DEFs or the differences codon usage between *O. sativa* and *Synechocystis*. As the *Os*DEFs are small peptides. This would be sensible to the *Synechocystis* to reduce their harm. Previously, the yield of plant gene expressed in *Synechocystis* could improve by codon optimization (Lindberg et al., 2010). They expressed kudzu (*Pueraria montana*) isoprene synthase (*IspS*) (Genbank: AY316691) in *Synechocystis.* This study was exemplified for

comparing the differences of codon usage between plant and cyanobacteria. The nucleotide sequences of native gene were compared to the optimized ones that they were optimized by Java Codon Adaptation (JCAT) (http://www.jcat.de) with CAI = 1.0. The codon optimized *IspS* showed 73% similarity with the native kudzu *IspS*. With this relatively high percent similarity of native kudzu *IspS* to the optimized sequence for *Synechocystis*, this study strongly suggested that the codon optimization is required for expression. Native *Os*DEF7 and *Os*DEF8 revealed 68 and 78% similarity to their sequences optimized for *Synechocystis*, respectively. This indicated that the % similarity of both *Os*DEFs were not far different from that of kudzu *IspS*. Likewise, the optimization of *Os*DEFs could improve the expression in *Synechocystis*. Moreover, there has been proved that the expression of the small molecule of CRPs could proceed in *Synechocystis*. For example, the metallothionein-I from human containing 20 Cys with low molecular weight of 6 to 7 kDa successfully expressed in *Synechocystis* (Chen et al., 1999).

In this study, chl *a* content increased when the cells transformed by the recombination vector (pEERM3+) containing *Os*DEFs. This vector contains the strong promotor, prnbP for cyanobacteria expression. By cloning into this vector, the gene target will be inserted into the genome of cyanobacteria in a complex photochemical enzyme of the photosystem II. Their mRNAs showed the insertion into cyanobacteria genome, but no expression. The oxygenic photosynthetic organisms contain monovinyl chlorophyll (Porra, 1997). To produce chl *a*, the 8-vinyl reductase is required for converting divinyl chlorophyll to monovinyl chlorophyll. It is also involved in bacteriochlorophyll

biosynthesis such as *R. sphaeroides.* This enzyme was identified in marine cyanobacteria of the genera *Prochlorococcus* and *Synechococcus* (Nagata et al., 2005). From searching this gene in the genome of *Synechocystis* PCC 6803, it was found around 48% similar to 8-vinyl reductase from *R.sphaeroides*. Therefore, transforming *Os*DEFs into the genome of *Synechocystis,* PCC 6803 would affect its chl *a* biosynthesis which would also support the growth of the cells.

5.2 *Trans*-resveratrol production in *Synechocystis*

5.2.1 Expression of genes involved in *trans*-resveratrol biosynthetic pathway

The information of biological parts has been collected and has been shared by the Registry (http://partsregistry.org). This provides the resource of genetic parts to facilitate the research community for engineering the synthetic biology projects (Kyndt et al., 2002). The applicability and versatility of the Biobrick collections constructed from the registry has been reported (Lijavetzky et al., 2008).

P*trc*1Ocore and P*trc*1O are both hybrids of the *E.coli trp* promoter and the *lacUV5* promoter (see information in **Fig. B-3**, Appendix B). P*trc*1Ocore is a derivative of P*trc*1O truncated with a symmetric *lacO* (*lacOsym*) in the core region of the -35 and -10 elements (Camsund et al., 2014). P*trc*1O contains *lacO1* located 6-bp downstream of -10 box which is proximal to the core promoter (Huang et al. 2010; Oehler et al., 1994). As *lacOsym* of P*trc*1Ocore contains an improved *lacO* operator of P*trc*1O, it may have greater affinity

resulting in higher expression than P*trc*1O. The numbers of nucleotide between the boxes also affect the strength of the promoter in vivo (Camsund et al. 2014; Brosius et al., 1985). The specific activity of P*trc*1O was detected in *Synechocystis* in relation to P*rnp*B (the promoter of housekeeping gene, rnaseP). It showed high expression in with and without induction by IPTG. Furthermore, P*trc*1O assembled with a ribosome-binding site (BBa_B0034), and a double terminator (BBa_B0015) was effectively tested the function of different fluorescent proteins in *Synechocystis* (Huang et al., 2010).

To ensure the possibility of *trans*-resveratrol producing in *Synechocystis*, the genes that have already been studied or confirmed for the ability of producing *trans*-resveratrol were selected. *ZmPAL* has been reported to be the bifunctional *PAL*s, as its ability to use both tyrosine and phenylalanine as the substrate (Neish, 1961). Basically, *RsTAL* is a unique bacterial enzyme that produces a chromophore of a photosensory protein (Nishiyama et al., 2010; Rösler et al., 1997). Reportedly, introducing of this gene into *A. thaliana* could enhance the metabolic flux to the phenylpropanoid pathway (Halls and Yu, 2008). As the grape has been the richest source of *trans*-resveratrol, *C4H*, *4CL* and *STS1* from *V. vinifera* were selected. Moreover, these genes were optimized for the codon usage in *Synechocystis* PCC 6803. A CAI of 1.0 is considered to be perfect in the desired expression organisms, and a CAI of > 0.8 is regarded as good, in terms of high gene expression level. In this work, CAI was upgraded from around 0.60 in native gene to more than 0.85 to increase the efficiency of translation. Among four biosynthetic enzymes (PAL, C4H, 4CL, and STS) required for the *trans*-resveratrol production. C4H is the only enzyme that is

localized at the ER membrane (Achnine et al., 2004) while the others are localized in the cytosol. Therefore, engineering this pathway in microorganisms prefers the alternative shorter pathway starting from bacterial cytosol-localized TAL to bypass the plant ER-localized C4H which would make it difficult to express in microorganisms including the cyanobacterium *Synechocystis* PCC 6803 (**Fig. 2-1**). To estimate the binary function of PAL in *Synechococystis*, *ZmPAL* was introduced into the cell. In this study, the transcripts of the four genes *PAL*, *TAL*, *4CL*, and *STS*, encoding the enzymes of the *trans*-resvertarol biosynthetic pathway, were thus examined in the unicellular cyanobacterium *Synechococystis* using two different promoters, P*trc*1Ocore and P*trc*1O. However, C4H did not include in this study because its cloning to the expression vectors had not been successful. The broad-host-range shuttle vector, pPMQAK1 for heterologous expression in *Synechocystis* has formerly been reported for its slightly high replicative ability (comparing to the average copy number of *Synechocystis* chromosome) in cyanobacteria (Huang et al., 2010).

These recombinant plasmids were afterward transformed into *Synechocystis* by triparental mating. With triparental mating, *E.coli* HB101 cells containing conjugal plasmid pRL443 could simplify the transformation to cyanobacteria. After conjugation, HB101 contain both the helper plasmid and the recombinant plasmid. The helper plasmid has methylase to methylate *Ava*I, II and III target sites (called M. AvaI, II, III), protecting pPMQAK1 from the native *Ava*I, II and III restriction enzymes of some cyanobacteria strains. This strategy could ease both homologous and heterologous expression (Karakaya and Mann, 2008; Huang et al., 2010).

ZmPAL could not be expressed under both promoters which would possibly be the result of less stability of mRNA. While *TAL*, *4CL*, and *STS* could be expressed and there was no significant difference in the expression levels of those introduced gene expressed from pPMQAK1 under both promoters. As, P*trc*1Ocore and P*trc*1O are both very strong LacI-repressed promoters inefficiently repressed by heterologously expressed LacI in *Synechocystis* which contain lower numbers of LacI per cell compared to in *E.coli* (Camsund et al., 2014). Therefore, the genes encoding enzymes of the *trans*-resveratrol pathway should be expressed with full capacities of the two respective promoters. The expressions of these recombinant proteins did not affect the growth of the cyanobacterial cells. TAL showed highest expression yield comparing to 4CL and STS. This may suggest that *TAL* would be easier to bind with RNA polymerase (RNAP) and/or its mRNA would be simpler for the translation process in *Synechocystis* than that of the other genes. Nevertheless, the ability of gene expression in *Synechocystis* depends on many factors such as the RNAP complex, the interactions between RNAP, promoter and LacI, as well as the amount of LacI per cell. Interestingly, the expression of 4CL in the *trans*-resveratrol pathway resulted enhanced level of chl *a* in *Synechosystis*. This enzyme essentially catalyzes the formation of CoA thioesters of *p*-coumaric acid. Since *p*-coumaric acid cannot be formed in *Synechosystis* without the heterologous expression of TAL or PAL/C4H. 4CL might be able to use an endogenous metabolite that is structurally similar to *p*-coumaric acid as a substrate. The resulting product would either participate in or affect the chl *a* formation resulting in the increased chl *a* content. In fact, Xue et al., 2014)

reported that the native laccase in *Synechocystis* recognized and degraded *p*-coumaric acid, obtained in the *Synechocystis* heterologously expressing TAL, into its decarboxylated compound, 4-vinylphenol (Xue et al., 2014). This strongly indicated the presence of endogenous *p*-coumaric acid-like substrate in the *Synechocystis* cells. Additionally, this could be inferred that the expressed 4CL is functionally active in *Synechocystis.*

5.2.2 Optimization of *trans*-resveratrol production in *Synechocystis*

The complete *trans*-resveratrol biosynthetic pathway was engineered in *E. coli* and *S. cerevisiae* and it successfully produced by feeding the medium with the substrate of the pathway. It has been also found that *E. coli* can produce higher amount of *trans*-resveratrol than that produced in yeast when the genes from same sources were introduced into the two different host cells (**Table 2-2**) (Beekwilder et al., 2006, Donnez et al., 2009). This suggested the possibility to produce the *trans*-resveratrol in *Synechocystis.*

The *p*-coumaric acid could be produced in the *Synechocystis* expressing TAL under both promoters. This proved that *Synechocystis* could utilize their tyrosine produced in the cell from the shikimate pathway as the substrate for the pathway of secondary metabolites, phenylpropanoid pathway. Importantly, TAL expressed under P*trc*1O showed much higher production of *p*-coumaric acid than that under P*trc*1Ocore that correlated to the expression yield of expressed TAL. Therefore, P*trc*1O would be a good promoter for producing *p*-coumaric acid in *Synechocystis*. Due to the cells expressing TAL could produce *p*-coumaric acid in the cells, its activity was be affirmed.

Previously, 4-vinylphenol (decarboxylated *p*-coumaric acid) has occurred in the production of *p*-coumaric acid in *Synechocystis*. *p*-Coumaric acid is converted to decarboxylated compound resulting in lower the yield of *p*-coumaric acid (Xue et al., 2014). In this study, 4-vinylphenol was not found in *Synechocystis* expressing TAL. Possibly, the small amount *p*-coumaric acid produced from both promoter accounting around 5-18 µg per 10^8 cell was not enough to sensible the cell to converted this compound to its decarboxylated form.

Since *p*-coumaric acid is known to be toxic to cell growth and fermentation capability (Watts et al., 2006). To avoid this, the hybrid gene of *4CL* and *STS* from various plants has widely been engineered in *E. coli* (Watts et al., 2006; Conrado et al., 1899), and in yeast (Becker et al., 2003; Zhang et al., 2006; Shin et al., 2011). Moreover, the concentrations of *p*-coumaric acid and the reaction time have to be optimized. Therefore, the production of *trans*-resveratrol from cells expressing 4CL treated with *p*-coumaric acid would not be practical. Nonethesless, the activity of expressed 4CL could be assumed from the increment of chl *a* content after expressing in *Synechocystis*.

From this study, the soluble enzymes of the *trans*-resveratrol pathway (TAL, 4CL, STS) could separately be expressed in *Synechocystis* cells, but STS also expressed as the inclusion bodies. This could be solved by the similar strategy used in protein expression in bacteria. The cells of *Synechocystis* expressing STS could produce more soluble protein in the cell at low temperature, as the inclusion bodies are lessened under the lower temperature condition (Trevors et al., 2012).

To evaluate the production of *trans*-resveratrol with other production sources, the cell expressing STS were treated with the substrate, *p*-coumaroyl CoA in the medium. With these conditions, the growth rate did not affected by substrate treating, but they were affected by light intensity which was low light showing less growth. Regarding to the chl *a* content, all cells expressing STS from P*trc*1Ocore showed similar chl *a* content in all condition studied. This would be possibly that the STS expressed under this promoter would lead to up-regulate some proteins involved in chl *a* biosynthesis supporting its production. While expressing under P*trc*1O might affect the functions of the enzyme in chl *a* biosynthesis, light-dependent protochlorophyllide oxidoreductase. Hence, the cells expressing STS from P*trc*1O tend to accumulate less chl *a* when they grow in the high light condition. Unfortunately, *trans*-resveratrol could not be detected in the cells expressing STS under both promoters. This could possibly be inferred that 1) *Synechocystis* has no transporter for uptaking *p*-coumaroyl CoA and/or 2) they have the transporter, but either the *p*-coumaroyl CoA transferred or availability of malonyl CoA were not enough to produce *trans*-resveratrol or 3) STS was possibly not function in *Synechocystis.* However, the transporters of *p*-coumaroyl CoA or any compound in flavonoid biosynthesis pathway have not been studied. In *A. thaliana*, transparent testa12 has been reported to involve in the transportation of phenolic compound (Marinova et al., 2007). Therefore, this gene was checked in the genome of *Synechocystis,* but there was no significant similarity found. Additionally, *p*-coumaroyl CoA could not be detected in the cells because of very less amount or none of *p*-coumaroyl CoA transferred. Thus, the transportation of *p*-coumaroyl CoA into the cells of

Synechocystis has been in question, and the production of *trans*-resveratrol by feeding the cells expressing STS would need many more studies.

Moreover, the in vitro production experiment indicated that TAL could functionally convert tyrosine to *p*-coumaric acid. The produced *p*-coumaric acid was not different between adding 50 µM and 100 µM tyrosine. While the longer incubation time leads to produce more products. This suggested that the TAL is saturated with 50 µM tyrosine, so extended the incubation time would better improve the reaction yield. Nevertheless, the *trans*-resveratrol could not be detected. This could be because of many factors such as the produced *p*-coumaric acid by TAL was not adequate to flow into the pathway. The in vitro study in *E. coli* could yield *trans*-resveratrol when 0.25 mM *p*-coumaric acid was fed into the crude cells extracted from BL 21 expressing *A. thaliana* 4CL (Lim et al., 2011). The in vivo production of *trans*-resvertrol in yeast reported the optimal *p*-coumaric acid concentration was 16 mg L^{-1} medium incubated for 80 cultivation hours (Shin et al., 2011). In addition, the reaction performed with the addition of 100 µM tyrosine for 14 incubation hours would still produce less *p*-coumaric acid than that added in the yeast experiment that was not enough for 4CL to produce *p*-coumaroyl CoA. Interestingly, the unidentified compound showing Mw of 164.0587 was detected when performing in vitro reaction but its structure could not be defined by MS/MS spectrum, although its m/z is similar to that of *p*-coumaric acid.

Further improvement of metabolic capabilities of *Synechocystis*, transforming all three vectors of pPMQAK1_*TAL*, pPMQAK1_*4CL*, and

pPMQAK1_*STS* into *Synechocystis* would improve the production of *trans*-resveratrol. The transformation of expression vector containing all three genes involved in the pathway into *Synechocystis* may produce *trans*-resveratrol. Nonetheless, the final size of the expression vector needs to be considered to obtain a successful transformation. The shuffling of genes involved in the *trans*-resveratrol pathway in different expression constructions revealed various production yield of *trans*-resveratrol in *E. coli* (Lim et al., 2011). However, the differences in heterologous gene sources, codon optimization, and the expression procedures could be the crucial factors for gene expression and protein production. Apart from gene expression, the intracellular malonyl CoA, another resveratrol precursor, is also a crucial factor for *trans*-resveratrol. This is provided from malonyl CoA biosynthesis by irreversible carboxylation of acetyl CoA**.** It is utilized for fatty acid biosynthesis. Liu et al. (2011) reported the engineered *Synechocystis* as source for fatty acid production. This finding suggested that the native malonyl CoA produced in *Synechocystis* is available for fatty acid biosynthesis. However, the flux of malonyl CoA produced in the cell entering the engineered resveratrol biosynthetic pathway needs to be reassessed. Furthermore, improving the intracellular malonyl CoA pool of *E. coli* resulted in a final improved yield of *trans*-resveratrol (Lim et al., 2011). Taken together, *Synechocystis*, that is evolutionarily closer to the *E. coli* in term of biochemical characteristics, is still potentially a promising host for *trans*-resveratrol production under the optimized conditions.

CHAPTER VI

CONCLUSION

6.1 AMP production

The in silico analyses were utilized to screen rice AMPs from the database and to estimate the expression level. The coexpression network analysis was taken to evaluate the functions of rice AMPs by coexpressing with the genes involved in plant protective mechanisms. By these analyses, the two candidate rice AMPs (*Os*DEF7 and *Os*DEF8) could be selected from 57 *Os*DEFs to confirm the activity by expressing in *E. coli*. From this study, *Os*DEF7 and *Os*DEF8 could be produced and in vitro functionally inhibited plant pathogens; namely bacteria such as *X. oryzae* pv. *oryzae, X. oryzae* pv. *oryzicola*, and *Erwinia carotovora*, and fungi such as *F. oxysporum* and *H. oryzae.* This evidently indicated that the candidate rice DEFs could be selected and further expressed to study the feasible inhibitory functions to against the pathogens. The heterologous expression of *Os*DEFs in *Synechocystis* by either from the expression vectors pPMQKA1 containing P*trc*1Ocore and P*trc*1O or homologous recombination expression with pEERM, did not succeed to produce these peptides, although the gene expressions of both genes were observed. This expression did not affect the growth and chl *a* content of *Synechocystis.* The improved production of *Os*DEFs in *Synechocystis* PCC6803 by codon optimization is suggested.

6.2 *Trans*-resveratrol production

Three enzymes, TAL, 4CL, and STS, involved in the *trans*-resveratrol production could successfully be expressed and purified in *Synechocystis* as soluble proteins. The production yields of these enzymes were similar when comparing between expressions using two different promoters, yielding in the range of 6.3 to 20.0 μg per 10^8 cells. The heterologous expression of these three enzymes individually did not affect the growth of *Synechocystis.* Interestingly, cyanobacterial cells expressing 4CL showed a slightly increased chl *a* content. Moreover, the cell expressing STS could produce more soluble proteins culturing under lower temperature and light intensity. The metabolite detection of the cells expressing enzymes involved in *trans*-resveratrol production showed the production of *p*-coumaric acid from *Synechocystis* expressing TAL under both promoters. To produce *trans*-resveratrol in *Synechocystis* PCC 6803, the classical methods performed in other microorganisms was applied. The cells expressing STS were treated with various concentrations of *p*-coumaroyl CoA in different growth conditions. The growth rate and chl *a* content did not affected by feeding the substrate, but temperature and light intensity. However, *trans*-resveratrol could not be produced under these conditions. In vitro reactions of mixed crude cells expressing each of respective enzymes treated with various concentration of tyrosine were performed. Correlatively, *p*-coumaric acid was produced from the mixture, and its yield was increased with the longer incubation time. They could, however, not produce *trans*-resveratrol, but the unknown compound was found.

6.3 *Synechocystis* as an alternative expression host

From this study, although the productions of plant AMPs and *trans*- resveratrol did not succeed in *Synechocystis*, the essential points could be suggested to improve the production in *Synechocystis* as follows:

1. Codon optimization is recommended for protein production in *Synechocystis.*
2. The selection of appropriate promoters expression vector, and expression method can improve gene expression level in *Synechocystis*.
3. Growth conditions of engineered *Synechocystis* can be varied to optimize protein production.
4. General biochemical information in *Synechocystis* such as the availability of precursors, metabolic flux, transporters, and detoxifying mechanisms should be considered and is in need for further development.

REFERENCES

Achnine L, Blancaflor EB, Rasmussen S, Dixon RA. Colocalization of L-phenylalanine ammonia-lyase and cinnamate 4-hydroxylase for metabolic channeling in phenylpropanoid biosynthesis. Plant Cell. 2004;16:3098-109.

Agrawal GK, Rakwal R, Jwa NS, Agrawal VP. Effects of signaling molecules, protein phosphatase inhibitors and blast pathogen (*Magnaporthe grisea*) on the mRNA level of a rice (*Oryza sativa* L.) phospholipid hydroperoxide glutathione peroxidase (*OsPHGPX*) gene in seedling leaves. Gene. 2002;283:227-36.

Anekonda TS. Resveratrol—A boon for treating Alzheimer's disease? Brain Res Rev. 2006;52:316-26.

Basaran P, Rodríguez-Cerezo E. Plant Molecular Farming: Opportunities and challenges. Crit Rev Biotechnol. 2008;28:153-72.

Baur JA, Sinclair DA. Therapeutic potential of resveratrol: the *in vivo* evidence. Nat Rev Drug Discov. 2006;5:493-506.

Becker JV, Armstrong GO, Merwe MJ, Lambrechts MG, Vivier MA, et al. Metabolic engineering of *Saccharomyces cerevisiae* for the synthesis of the wine-related antioxidant resveratrol. FEMS Yeast Res. 2003;4:79-85.

Beekwilder J, Wolswinkel R, Jonker H, Hall R, de Vos CH, et al. Production of resveratrol in recombinant microorganisms. Appl Environ Microbiol. 2006;72:5670-2.

Berrocal-Lobo M, Segura A, Moreno M, López G, García-Olmedo F, et al. Snakin-2, an antimicrobial peptide from potato whose gene is locally induced by

wounding and responds to pathogen infection. J Plant Physiol. 2002;128: 951-61.

Bertelli A, Giovannini L, Stradi R, Bertelli A, Tillement J. Plasma, urine and tissue levels of *trans*-and *cis*-resveratrol (3, 4', 5-trihydroxystilbene) after short-term or prolonged administration of red wine to rats. Int J Tissue React. 1995;18:67-71.

Bertelli AAE. Wine, research and cardiovascular disease: Instructions for use. Atherosclerosis. 2007;195:242-7.

Bolintineanu DS, Kaznessis YN. Computational studies of protegrin antimicrobial peptides: a review. Peptides. 2011;32:188-201.

Bradamante S, Barenghi L, Villa A. Cardiovascular Protective effects of resveratrol. Cardiovasc Drug Rev. 2004;22:169-88.

Bradford MM. A rapid and sensitive method for the quantitation of microgram quantities of protein utilizing the principle of protein-dye binding. Anal Biochem. 1976;72:248-54.

Bryan GT, Wu K-S, Farrall L, Jia Y, Hershey HP, et al. A single amino acid difference distinguishes resistant and susceptible alleles of the rice blast resistance gene *Pi-ta*. Plant Cell. 2000;12:2033-45.

Caaveiro JMM, Molina A, González-Mañas JM, Rodríguez-Palenzuela P, García-Olmedo F, et al. Differential effects of five types of antipathogenic plant peptides on model membranes. FEBS Lett. 1997;410:338-42.

Cammue BP, De Bolle MF, Terras FR, Proost P, Van Damme J, et al. Isolation and characterization of a novel class of plant antimicrobial peptides form *Mirabilis jalapa* L. seeds. J Biol Chem. 1992;267:2228-33.

Camsund D, Heidorn T, Lindblad P. Design and analysis of LacI-repressed promoters and DNA-looping in a cyanobacterium. J Biol Eng. 2014;8:4.

Carmona MJ, Molina A, Fernández JA, López-Fando JJ, García-Olmedo F. Expression of the α-thionin gene from barley in tobacco confers enhanced resistance to bacterial pathogens. Plant J. 1993;3:457-62.

Charvolin D, Douliez JP, Marion D, Cohen-Addad C, Pebay-Peyroula E. The crystal structure of a wheat nonspecific lipid transfer protein (ns-LTP1) complexed with two molecules of phospholipid at 2.1 A resolution. FEBS J. 1999;264: 562-8.

Chen Z, Ren L, Shao Q, Shi D, Ru B. Expression of mammalian metallothionein-I gene in cyanobacteria to enhance heavy metal resistance. Marine Poll Bull. 1999;39:155-8.

Cho J, Lee DG. The antimicrobial peptide arenicin-1 promotes generation of reactive oxygen species and induction of apoptosis. Biochim Biophys Acta. 2011;1810:1246-51.

Chouabe C, Eyraud V, Da Silva P, Rahioui I, Royer C, et al. New mode of action for a knottin protein bioinsecticide: Pea Albumin 1 subunit b (PA1b) is the first peptidic inhibitor of V-ATPase. J Biol Chem. 2011;286:36291-6.

Clara Pestana-Calsa M, LAC Ribeiro I, Calsa J. Bioinformatics-coupled molecular approaches for unravelling potential antimicrobial peptides coding genes in Brazilian native and crop plant species. Curr Protein Pept Sci. 2010;11:199-209.

Cordts S, Bantin J, Wittich PE, Kranz E, Lörz H, et al. *ZmES* genes encode peptides with structural homology to defensins and are specifically expressed in the female gametophyte of maize. Plant J. 2001;25:103-14.

Craik DJ. Discovery and applications of the plant cyclotides. Toxicon. 2010;56:1092-102.

Dathe M, Wieprecht T. Structural features of helical antimicrobial peptides: their potential to modulate activity on model membranes and biological cells. Biochim Biophys Acta. 1999;1462:71-87.

De-Paula VS, Razzera G, Medeiros L, Miyamoto CA, Almeida MS, et al. Evolutionary relationship between defensins in the Poaceae family strengthened by the characterization of new sugarcane defensins. Plant Mol Biol. 2008;68:321-35.

De Bolle MC, Osborn R, Goderis I, Noe L, Acland D, et al. Antimicrobial peptides from*Mirabilis jalapa* and *Amaranthus caudatus*: expression, processing, localization and biological activity in transgenic tobacco. Plant Mol Biol. 1996;31:993-1008.

De Caleya RF, Gonzalez-Pascual B, García-Olmedo F, Carbonero P. Susceptibility of phytopathogenic bacteria to wheat purothionins *in vitro*. Appl Microbiol. 1972;23:998-1000.

De Samblanx GW, Goderis IJ, Thevissen K, Raemaekers R, Fant F, et al. Mutational analysis of a plant defensin from radish (*Raphanus sativus* L.) reveals two adjacent sites important for antifungal activity. J Biol Chem. 1997;272:1171-9.

Devaux PF. Static and dynamic lipid asymmetry in cell membranes. Biochemistry. 1991;30:1163-73.

Dixon RA, Paiva NL. Stress-induced phenylpropanoid metabolism. Plant Cell. 1995;7:1085-97.

Dolis D, Moreau C, Zachowski A, Devaux PF. Aminophospholipid translocase and proteins involved in transmembrane phospholipid traffic. Biophys Chem. 1997;68:221-31.

Dong W, Li N, Gao D, Zhen H, Zhang X, et al. Resveratrol attenuates ischemic brain damage in the delayed phase after stroke and induces messenger RNA and protein express for angiogenic factors. J Vasc Surg. 2008;48:709-14.

Donnez D, Jeandet P, Clement C, Courot E. Bioproduction of resveratrol and stilbene derivatives by plant cells and microorganisms. Trends Biotechnol. 2009;27:706-3.

Eaton-Rye JJ: The construction of gene knockouts in the cyanobacterium *Synechocystis* sp. PCC 6803. In: Photosynthesis Research Protocols. Springer; 2004: 309-24.

Elhai J, Wolk CP. Conjugal transfer of DNA to cyanobacteria. Methods in enzymology. 1988;167:747.

Fahrendorf T, Dixon RA. Stress responses in alfalfa (*Medicago sativa* L.) XVIII: molecular cloning and expression of the elicitor-inducible cinnamic acid 4-hydroxylase cytochrome P450. Arch Biochem Biophys. 1993;305:509-15.

Fernández-Mar MI, Mateos R, García-Parrilla MC, Puertas B, Cantos-Villar E. Bioactive compounds in wine: resveratrol, hydroxytyrosol and melatonin: A review. Food Chem. 2012;130:797-813.

Ferrer JL, Austin MB, Stewart Jr C, Noel JP. Structure and function of enzymes involved in the biosynthesis of phenylpropanoids. Plant Physiol Biochem. 2008;46:356-70.

Fu F-F, Xue H-W. Coexpression analysis identifies rice starch regulator1, a rice AP2/EREBP family transcription factor, as a novel rice starch biosynthesis regulator. Plant Physiol. 2010;154:927-38.

Gao G-H, Liu W, Dai J-X, Wang J-F, Hu Z, et al. Solution structure of PAFP-S: a new knottin-type antifungal peptide from the seeds of *Phytolacca americana*. Biochemistry. 2001;40:10973-8.

Garvin S, Öllinger K, Dabrosin C. Resveratrol induces apoptosis and inhibits angiogenesis in human breast cancer xenografts *in vivo*. Cancer Letter. 2006;231:113-22.

Gasteiger E, Gattiker A, Hoogland C, Ivanyi I, Appel RD, et al. ExPASy: the proteomics server for in-depth protein knowledge and analysis. Nucleic Acids Research. 2003;31:3784-8.

Goodstein DM, Shu S, Howson R, Neupane R, Hayes RD, et al. Phytozome: a comparative platform for green plant genomics. Nucleic Acids Res. 2012;40:D1178-86.

Gorjanović S, Beljanski MV, Gavrović-Jankulović M, Gojgić-Cvijović G, Bejosano F. Antimicrobial activity of malting barley grain thaumatin-like protein isoforms, S and R. J Inst Brew. 2007;113:206-12.

Guillon S, Trémouillaux-Guiller J, Pati PK, Rideau M, Gantet P. Harnessing the potential of hairy roots: dawn of a new era. Trends Biotechnol. 2006;24:403-9.

Halls C, Yu O. Potential for metabolic engineering of resveratrol biosynthesis. Trends Biotechnol. 2008;26:77-81.

[a]Hammami R, Ben Hamida J, Vergoten G, Fliss I. PhytAMP: a database dedicated to antimicrobial plant peptides. Nucleic Acids Res. 2009;37:D963-8.

[b]Hammami R, Hamida JB, Vergoten G, Lacroix JM, Slomianny MC, et al. A new antimicrobial peptide isolated from *Oudneya africana* seeds. Microbiol Immunol. 2009;53:658-66.

Hancock REW, Sahl H-G. Antimicrobial and host-defense peptides as new anti-infective therapeutic strategies. Nat Biotech. 2006;24:1551-7.

Haught C, Davis GD, Subramanian R, Jackson KW, Harrison RG. Recombinant production and purification of novel antisense antimicrobial peptide in *Escherichia coli*. Biotechnol Bioeng. 1998;57:55-61.

Heidorn T, Camsund D, Huang H.H, Lindberg P, Oliveira P, et al. Synthetic biology in cyanobacteria: Engineering and analyzing novel functions. Methods Enzymol. 2011;497 :539-79.

Holaskova E, Galuszka P, Frebort I, Oz MT. Antimicrobial peptide production and plant-based expression systems for medical and agricultural biotechnology. Biotechnol Adv. 2015;33:1005-23.

Holvoet P. Oxidized LDL and coronary heart disease. Acta cardiol. 2004;59:479-84.

Horton P, Park KJ, Obayashi T, Fujita N, Harada H, et al. WoLF PSORT: protein localization predictor. Nucleic Acids Res. 2007;35:W585-7.

Hoskin DW, Ramamoorthy A. Studies on anticancer activities of antimicrobial peptides. Biochim Biophys Acta. 2008;1778:357-75.

Huang HH, Camsund D, Lindblad P, Heidorn T. Design and characterization of molecular tools for a synthetic biology approach towards developing cyanobacterial biotechnology. Nucleic Acids Res. 2010;38:2577-93.

Ingham Aaron B, Moore Robert J. Recombinant production of antimicrobial peptides in heterologous microbial systems. Biotechnol Appl Biochem. 2007;47:1-9.

Itoh J-I, Nonomura K-I, Ikeda K, Yamaki S, Inukai Y, et al. Rice plant development: from zygote to spikelet. Plant Cell Physiol. 2005;46:23-47.

Jain M, Nijhawan A, Arora R, Agarwal P, Ray S, et al. F-box proteins in rice. genome-wide analysis, classification, temporal and spatial gene expression during panicle and seed development, and regulation by light and abiotic stress. Plant Physiol. 2007;143:1467-83.

Jung H, Hwang I, Sung W, Kang H, Kang B, et al. Fungicidal effect of resveratrol on human infectious fungi. Arch Pharm Res. 2005;28:557-60.

Jung HJ, Seu YB, Lee DG. Candicidal action of resveratrol isolated from grapes on human pathogenic yeast *C. albicans*. J Microbiol Biotechnol. 2007;17:1324-9.

Kader J-C. Lipid-transfer proteins in plants. Annual Review of Plant Physiology and Plant Molecular Biology. 1996;47:627-54.

Kamimori H, Hall K, Craik DJ, Aguilar M-I. Studies on the membrane interactions of the cyclotides kalata B1 and kalata B6 on model membrane systems by surface plasmon resonance. Anal Biochem. 2005;337:149-53.

Karakaya H, Mann NH. Mutagenesis of the *tal* gene-encoding transaldolase in the cyanobacterium, *Anabaena* sp PCC7120. Turk J Biol. 2008;32:135-141.

Kedzierski L, Curtis J, Kaminska M, Jodynis-Liebert J, Murias M. In vitro antileishmanial activity of resveratrol and its hydroxylated analogues against *Leishmania major* promastigotes and amastigotes. Parasitol Res. 2007;102:91-7.

Kiselev K, Dubrovina A, Veselova M, Bulgakov V, Fedoreyev S, et al. The *rolB* gene-induced overproduction of resveratrol in *Vitis amurensis* transformed cells. J Biotechnol. 2007;128:681-92.

Koehbach J, Attah AF, Berger A, Hellinger R, Kutchan TM, et al. Cyclotide discovery in gentianales revisited—identification and characterization of cyclic cystine-knot peptides and their phylogenetic distribution in rubiaceae plants. J Pept Sci. 2013;100:438-52.

Kouakou TH, Téguo PW, Valls J, Kouadio YJ, Decendit A, et al. First evidence of *trans*-resveratrol production in cell suspension cultures of cotton (*Gossypium hirsutum* L.). Plant Cell Tissue Organ Cult. 2006;86:405-9.

Krebitz M, Wagner B, Ferreira F, Peterbauer C, Campillo N, et al. Plant-based heterologous expression of Mal d 2, a thaumatin-like protein and allergen of apple (*Malus domestica*), and its characterization as an antifungal protein. J Mol Biol. 2003;329:721-30.

Krissana Boonpa. Cloning, heterologous expression and antimicrobial activity of thionin and snakin from rice *Oryza sativa* L. subsp. *japonica*. Master thesis, Department of biotechnology, Faculty of science, Chulalongkorn university, 2014.

Kukrić ZZ, Topalić-Trivunović LN. Antibacterial activity of *cis*-and *trans*-resveratrol isolated from *Polygonum cuspidatum* rhizome. Acta Periodica Technologica. 2006;131-6.

Kulkarni MM, McMaster WR, Kamysz E, Kamysz W, Engman DM, et al. The major surface-metalloprotease of the parasitic protozoan, Leishmania, protects against antimicrobial peptide-induced apoptotic killing. Mol Microbiol. 2006;62:1484-97.

Kundu JK, Surh Y-J. Cancer chemopreventive and therapeutic potential of resveratrol: mechanistic perspectives. Cancer Lett. 2008;269:243-61.

Kyndt JA, Meyer TE, Cusanovich MA, Van Beeumen JJ. Characterization of a bacterial tyrosine ammonia lyase, a biosynthetic enzyme for the photoactive yellow protein. FEBS Lett. 2002;512:240-4.

Lay FT, Mills GD, Poon IKH, Cowieson NP, Kirby N, et al. Dimerization of plant defensin NaD1 enhances its antifungal activity. J Biol Chem. 2012;287: 19961-72.

Lee J-K, Gopal R, Seo CH, Cheong H, Park Y. Isolation and purification of a novel deca-antifungal peptide from potato (*Solanum tuberosum* L. cv. Jopung) against *Candida albicans*. Int J of Mol Sci. 2012;13:4021-32.

Lee JH, Kim JH, Hwang SW, Lee WJ, Yoon HK, et al. High-level expression of antimicrobial peptide mediated by a fusion partner reinforcing formation of inclusion bodies. Biochem Biophys Res Commun. 2000;277:575-80.

Lee TH, Kim YK, Pham TT, Song SI, Kim JK, et al. RiceArrayNet: a database for correlating gene expression from transcriptome profiling, and its application to the analysis of coexpressed genes in rice. Plant Physiol. 2009;151:16-33.

Lerche MH, Kragelund BB, Bech LM, Poulsen FM. Barley lipid-transfer protein complexed with palmitoyl CoA: the structure reveals a hydrophobic binding site that can expand to fit both large and small lipid-like ligands. Structure. 1997;5:291-306.

Li W, Li S, Zhong J, Zhu Z, Liu J, et al. A novel antimicrobial peptide from skin secretions of the earthworm, *Pheretima guillelmi* (Michaelsen). Peptides. 2011;32:1146-50.

Li X, Leong SS. A chromatography-focused bioprocess that eliminates soluble aggregation for bioactive production of a new antimicrobial peptide candidate. J Chromatogr A. 2011;1218:3654-9.

Li Y, Chen Z. RAPD: a database of recombinantly-produced antimicrobial peptides. FEMS Microbiol Lett. 2008;289:126-9.

Li Y. Recombinant production of antimicrobial peptides in *Escherichia coli*: a review. Protein Expr Purif. 2011;80:260-7.

Lijavetzky D, Almagro L, Belchi-Navarro S, Martínez-Zapater JM, Bru R, et al. Synergistic effect of methyljasmonate and cyclodextrin on stilbene biosynthesis pathway gene expression and resveratrol production in Monastrell grapevine cell cultures. BMC Res Notes. 2008;1:132.

Lim CG, Fowler ZL, Hueller T, Schaffer S, Koffas MAG. High-yield resveratrol production in engineered *Escherichia coli*. Appl Environ Microbiol. 2011;77:3451-60.

Lin W, Anuratha CS, Datta K, Potrykus I, Muthukrishnan S, et al. Genetic engineering of rice for resistance to sheath blight. Nat Biotech. 1995;13:686-91.

Lindberg P, Park S, Melis A. Engineering a platform for photosynthetic isoprene production in cyanobacteria, using *Synechocystis* as the model organism. Metab Eng. 2010;12:70-9.

Liu X, Sheng J, Curtiss R, 3rd. Fatty acid production in genetically modified cyanobacteria. Proc Natl Acad Sci U S A. 2011;108:6899-904.

Lu Y, Ma Y, Wang X, Liang J, Zhang C, et al. The first antimicrobial peptide from sea amphibian. Mol Immunol. 2008;45:678-81.

Mandal SM, Dey S, Mandal M, Sarkar S, Maria-Neto S, et al. Identification and structural insights of three novel antimicrobial peptides isolated from green coconut water. Peptides. 2009;30:633-7.

Marinova K, Pourcel L, Weder B, Schwarz M, Barron D, et al. The *Arabidopsis* MATE transporter TT12 acts as a vacuolar flavonoid/H+-antiporter active in proanthocyanidin-accumulating cells of the seed coat. Plant Cell. 2007;19: 2023-38.

Maroti G, Kereszt A, Kondorosi E, Mergaert P. Natural roles of antimicrobial peptides in microbes, plants and animals. Res Microbiol. 2011;162:363-74.

Matsuzaki K. Why and how are peptide–lipid interactions utilized for self-defense? Magainins and tachyplesins as archetypes. Biochim Biophys Acta. 1999;1462:1-10.

Mendez-Samperio P. Role of antimicrobial peptides in host defense against mycobacterial infections. Peptides. 2008;29:1836-41.

Meyer B, Houlne G, Pozueta-Romero J, Schantz M-L, Schantz R. Fruit-specific expression of a defensin-type gene family in bell pepper (upregulation during ripening and upon wounding). Plant Physiol. 1996;112:615-22.

Montesinos E. Antimicrobial peptides and plant disease control. FEMS Microbiol Lett. 2007;270:1-11.

Moual H, Thomassin J, Brannon J. Antimicrobial peptidesas an alternative approach to treat bacterial infections. J Clin Cell Immunol S. 2013;13:2.

Mousavi A, Hotta Y. Glycine-rich proteins. Appl Biochem Biotechnol. 2005;120:169-74.

Mutalik VK, Guimaraes JC, Cambray G, Lam C, Christoffersen MJ, et al. Precise and reliable gene expression via standard transcription and translation initiation elements. Nature Methods. 2013;10:354-60.

Nagata N, Tanaka R, Satoh S, Tanaka A. Identification of a vinyl reductase gene for chlorophyll synthesis in *Arabidopsis thaliana* and implications for the evolution of *Prochlorococcus* species. Plant Cell. 2005;17:233-40.

Nahirñak V, Almasia NI, Hopp HE, Vazquez-Rovere C. Snakin/GASA proteins: involvement in hormone crosstalk and redox homeostasis. Plant Signal Behav. 2012;7:1004-8.

Namdeo A. Plant cell elicitation for production of secondary metabolites: a review. Pharmacog Rev. 2007;1:69-79.

Nandakumar R, Babu S, Kalpana K, Raguchander T, Balasubramanian P, et al. Agrobacterium-mediated transformation of indica rice with chitinase gene for enhanced sheath blight resistance. Biologia Plant. 2007;51:142-8.

Nawrot R, Barylski J, Nowicki G, Broniarczyk J, Buchwald W, et al. Plant antimicrobial peptides. Folia Microbiol. 2014;59:181-96.

Neish AC. Formation of *m*- and *p*-coumaric acids by enzymatic deamination of the corresponding isomers of tyrosine. Phytochemistry. 1961;1:1-24.

Nishiyama Y, Yun CS, Matsuda F, Sasaki T, Saito K, et al. Expression of bacterial tyrosine ammonia-lyase creates a novel *p*-coumaric acid pathway in the biosynthesis of phenylpropanoids in *Arabidopsis*. Planta. 2010;232:209-18.

Odintsova TI, Vassilevski AA, Slavokhotova AA, Musolyamov AK, Finkina EI, et al. A novel antifungal hevein-type peptide from *Triticum kiharae* seeds with a unique 10-cysteine motif. FEBS J. 2009;276:4266-75.

Oehler S, Amouyal M, Kolkhof P, von Wilcken-Bergmann B, Müller-Hill B. Quality and position of the three lac operators of *E. coli* define efficiency of repression. EMBO J. 1994;13:3348.

Parachin NS, Mulder KC, Viana AAB, Dias SC, Franco OL. Expression systems for heterologous production of antimicrobial peptides. Peptides. 2012;38:446-56.

Parker JA, Arango M, Abderrahmane S, Lambert E, Tourette C, et al. Resveratrol rescues mutant polyglutamine cytotoxicity in nematode and mammalian neurons. Nat Genet. 2005;37:349-50.

Pattanaik B, Lindberg P. Terpenoids and their biosynthesis in cyanobacteria. Life (Basel). 2015;5:269-93.

Pearce G, Moura DS, Stratmann J, Ryan CA. RALF, a 5-kDa ubiquitous polypeptide in plants, arrests root growth and development. Proc Natl Acad Sci U S A. 2001;98:12843-7.

Petersen TN, Brunak S, von Heijne G, Nielsen H. SignalP 4.0: discriminating signal peptides from transmembrane regions. Nat Methods. 2011;8:785-6.

Piers KL, Brown MH, Hancock REW. Recombinant DNA procedures for producing small antimicrobial cationic peptides in bacteria. Gene. 1993;134:7-13.

Ponti D, MANGONI M, Mignogna G, Simmaco M, Barra D. An amphibian antimicrobial peptide variant expressed in *Nicotiana tabacum* confers resistance to phytopathogens. Biochem J. 2003;370:121-7.

Porra RJ. Recent progress in porphyrin and chlorophyll biosynthesis. Photochem Photobiol. 1997;65:492-516.

Potter GA, Patterson LH, Wanogho E, Perry PJ, Butler PC, et al. The cancer preventative agent resveratrol is converted to the anticancer agent piceatannol by the cytochrome P450 enzyme CYP1B1. Br J Cancer. 2002;86:774-8.

Rajanbabu V, Chen JY. Applications of antimicrobial peptides from fish and perspectives for the future. Peptides. 2011;32:415-20.

Ramessar K, Capell T, Christou P. Molecular pharming in cereal crops. Phytochem Rev. 2008;7:579-92.

Repka V. Elicitor-stimulated induction of defense mechanisms and defense gene activation in grapevine cell suspension cultures. Biologia Plant. 2001;44:555-65.

Rösler J, Krekel F, Amrhein N, Schmid J. Maize phenylalanine ammonia-lyase has tyrosine ammonia-lyase activity. Plant Physiol. 1997;113:175-9.

Rotem S, Mor A. Antimicrobial peptide mimics for improved therapeutic properties. Biochim Biophys Acta. 2009;1788:1582-92.

Sato T, Takabe K, Fujita M. Immunolocalization of phenylalanine ammonia-lyase and cinnamate-4-hydroxylase in differentiating xylem of poplar. C R Biol. 2004;327:827-36.

Sbaghi M, Jeandet P, Faivre B, Bessis R, Fournioux JC. Development of methods using phytoalexin (resveratrol) assessment as a selection criterion to screen grapevine in vitro cultures for resistance to grey mould (*Botrytis cinerea*). Euphytica. 1995;86:41-7.

Schaefer SC, Gasic K, Cammue B, Broekaert W, van Damme EJ, et al. Enhanced resistance to early blight in transgenic tomato lines expressing heterologous plant defense genes. Planta. 2005;222:858-66.

Schneider Y, Duranton B, Gossé F, Schleiffer R, Seiler N, et al. Resveratrol inhibits intestinal tumorigenesis and modulates host-defense-related gene expression in an animal model of human familial adenomatous polyposis. Nutr Cancer. 2001;39:102-7.

Segura A, Moreno M, Madueño F, Molina A, García-Olmedo F. Snakin-1, a peptide from potato that is active against plant pathogens. Mol Plant-Microbe Interact. 1999;12:16-23.

Sela-Buurlage MB, Ponstein AS, Bres-Vloemans SA, Melchers LS, van den Elzen PJ, et al. Only specific tobacco (*Nicotiana tabacum*) chitinases and [beta]-1, 3-glucanases exhibit antifungal activity. Plant Physiol. 1993;101:857-63.

Seo Y-S, Sriariyanun M, Wang L, Pfeiff J, Phetsom J, et al. A two-genome microarray for the rice pathogens *Xanthomonas oryzae* pv. oryzae and *X. oryzae* pv. oryzicola and its use in the discovery of a difference in their regulation of hrp genes. BMC Microbial. 2008;8:99.

Sharma S, Chopra K, Kulkarni SK. Effect of insulin and its combination with resveratrol or curcumin in attenuation of diabetic neuropathic pain: participation of nitric oxide and TNF-alpha. Phytother Res. 2007;21:278-83.

Shin SY, Han NS, Park YC, Kim MD, Seo JH. Production of resveratrol from *p*-coumaric acid in recombinant *Saccharomyces cerevisiae* expressing 4-coumarate:coenzyme A ligase and stilbene synthase genes. Enzyme Microb Technol. 2011;48:48-53.

Silverstein KA, Moskal WA, Jr., Wu HC, Underwood BA, Graham MA, et al. Small cysteine-rich peptides resembling antimicrobial peptides have been under-predicted in plants. Plant J. 2007;51:262-80.

Sinclair D. Sirtuins for healthy neurons. Nat Genet. 2005;37:339-40.

Song X, Wang J, Wu F, Li X, Teng M, et al. cDNA cloning, functional expression and antifungal activities of a dimeric plant defensin SPE10 from *Pachyrrhizus erosus* seeds. Plant Mol Biol. 2005;57:13-20.

Spelbrink RG, Dilmac N, Allen A, Smith TJ, Shah DM, et al. Differential antifungal and calcium channel-blocking activity among structurally related plant defensins. Plant Physiol. 2004;135:2055-67.

Sperstad SV, Haug T, Blencke HM, Styrvold OB, Li C, et al. Antimicrobial peptides from marine invertebrates: challenges and perspectives in marine antimicrobial peptide discovery. Biotechnol Adv. 2011;29:519-30.

Stanier R.Y, Kunisawa R, Mandel M, Cohen-Bazire G. Purification and properties of unicellular blue-green algae (order *Chroococcales*). Bacteriol. Rev. 1971;35: 171–205.

Stotz HU, Spence B, Wang Y. A defensin from tomato with dual function in defense and development. Plant Mol Biol. 2009;71:131-43.

Szkudelski T. The insulin-suppressive effect of resveratrol — An in vitro and in vivo phenomenon. Life Sciences. 2008;82:430-5.

Takasaki H, Mahmood T, Matsuoka M. Identification and characterization of a gibberellin-regulated protein, which is ASR5, in the basal region of rice leaf sheaths. Mol Genet Genomics. 2008;279:359-70.

Tamura K, Dudley J, Nei M, Kumar S. MEGA4: Molecular Evolutionary Genetics Analysis (MEGA) software version 4.0. Mol Biol Evol. 2007;24:1596-9.

Tassoni A, Fornalè S, Franceschetti M, Musiani F, Michael AJ, et al. Jasmonates and Na-orthovanadate promote resveratrol production in *Vitis vinifera* cv. Barbera cell cultures. New Phytol. 2005;166:895-905.

Tavares LS, Santos Mde O, Viccini LF, Moreira JS, Miller RN, et al. Biotechnological potential of antimicrobial peptides from flowers. Peptides. 2008;29:1842-51.

Teutsch HG, Hasenfratz MP, Lesot A, Stoltz C, Garnier JM, et al. Isolation and sequence of a cDNA encoding the Jerusalem artichoke cinnamate 4-hydroxylase, a major plant cytochrome P450 involved in the general phenylpropanoid pathway. Pro Natl Acad Sci U S A. 1993;90:4102-6.

Trevors JT, Bej AK, Mojib N, van Elsas JD, Van Overbeek L. Bacterial gene expression at low temperatures. Extremophiles. 2012;16:167-76.

van der Weerden NL, Lay FT, Anderson MA. The plant defensin, NaD1, enters the cytoplasm of *Fusarium oxysporum* hyphae. J Biol Chem. 2008;283:14445-52.

van der Weerden NL, Hancock RE, Anderson MA. Permeabilization of fungal hyphae by the plant defensin NaD1 occurs through a cell wall-dependent process. J Biol Chem. 2010;285:37513-20.

Veldhoen S, Laufer SD, Restle T. Recent developments in peptide-based nucleic acid delivery. Int J Mol Sciences. 2008;9:1276-320.

Vitrac X, Monti J-P, Vercauteren J, Deffieux G, Mérillon J-M. Direct liquid chromatographic analysis of resveratrol derivatives and flavanonols in wines with absorbance and fluorescence detection. Anal Chim Acta. 2002;458:103-10.

Walle T, Hsieh F, DeLegge MH, Oatis JE, Walle UK. High absorption but very low bioavailability of oral resveratrol in humans. Drug Metab Dispos. 2004;32:1377-82.

Wang CK, Colgrave ML, Ireland DC, Kaas Q, Craik DJ. Despite a conserved cystine knot motif, different cyclotides have different membrane binding modes. Biophys J. 2009;97:1471-81.

Wang Y, Halls C, Zhang J, Matsuno M, Zhang Y, et al. Stepwise increase of resveratrol biosynthesis in yeast *Saccharomyces cerevisiae* by metabolic engineering. Metab Eng. 2011;13:455-63.

Wang Y, Catana F, Yang Y, Roderick R, van Breemen RB. An LC-MS method for analyzing total resveratrol in grape juice, cranberry juice, and in wine. J Agric Food Chem. 2002;50:431-5.

Ware DH, Jaiswal P, Ni J, Yap IV, Pan X, et al. Gramene, a tool for grass genomics. Plant Physiol. 2002;130:1606-13.

Watts KT, Lee PC, Schmidt-Dannert C. Biosynthesis of plant-specific stilbene polyketides in metabolically engineered *Escherichia coli*. BMC Biotechnol. 2006;6:22.

Wenzel E, Soldo T, Erbersdobler H, Somoza V. Bioactivity and metabolism of *trans*-resveratrol orally administered to Wistar rats. Mol Nutr Food Res. 2005;49:482-94.

Whitehead TP, Robinson D, Allaway S, Syms J, Hale A. Effect of red wine ingestion on the antioxidant capacity of serum. Clin Chem. 1995;41:32-5.

Williams LD, Burdock GA, Edwards JA, Beck M, Bausch J. Safety studies conducted on high-purity *trans*-resveratrol in experimental animals. Food Chem Toxicol. 2009;47:2170-82.

Wu G, Li X, Fan X, Wu H, Wang S, et al. The activity of antimicrobial peptide S-thanatin is independent on multidrug-resistant spectrum of bacteria. Peptides. 2011;32:1139-45.

Xue Y, Zhang Y, Cheng D, Daddy S, He Q. Genetically engineering *Synechocystis* sp. pasteur culture collection 6803 for the sustainable production of the plant secondary metabolite *p*-coumaric acid. Proc Natl Acad Sci U S A. 2014;111:9449-54.

Xue Z, McCluskey M, Cantera K, Sariaslani FS, Huang L. Identification, characterization and functional expression of a tyrosine ammonia-lyase and its mutants from the photosynthetic bacterium *Rhodobacter sphaeroides*. J Ind Microbiol Biotechnol. 2007;34:599-604.

Zhang G, Wu H, Shi J, Ganz T, Ross CR, et al. Molecular cloning and tissue expression of porcine β-defensin-1. FEBS Lett. 1998;424:37-40.

Zhang H, Zhang W, Wang X, Zhou Y, Wang N, et al. Identification of a cysteine-rich antimicrobial peptide from salivary glands of the tick *Rhipicephalus haemaphysaloides*. Peptides. 2011;32:441-6.

Zhang Y, Li SZ, Li J, Pan X, Cahoon RE, et al. Using unnatural protein fusions to engineer resveratrol biosynthesis in yeast and mammalian cells. J Am Chem Soc. 2006;128:13030-1.

Zhao H, Lu J, Lü S, Zhou Y, Wei J, et al. Isolation and functional characterization of a cinnamate 4-hydroxylase promoter from *Populus tomentosa*. Plant Science. 2005;168:1157-62.

[a]Zhou L, Lin Q, Li B, Li N, Zhang S. Expression and purification the antimicrobial peptide CM4 in *Escherichia coli*. Biotechnol Lett. 2009;31:437-41.

[b]Zhou L, Zhao Z, Li B, Cai Y, Zhang S. TrxA mediating fusion expression of antimicrobial peptide CM4 from multiple joined genes in *Escherichia coli*. Protein Expr Purif. 2009;64:225-30.

APPENDIX

APPENDIX A

Additional data

Fig. A-1 Graphical presentation of gene coexpression network analysis of *Os*DEFs. The network shows how the *Os*DEFs analyzed by PlantArrayNet-Rice 300k are correlated with genes in other functions. There are 11 genes showing the correlation to gene involved in plant defense functions; *OsDEF1, OsDEF7, OsDEF8, OsDEF9, OsDEFL9, OsDEFL21, OsDEFL28, OsDEFL43, OsDEFL48, OsDEFL49* and *OsDEFL70*. These genes are retrieved under the parameters of r ≥0.6 and depth = 1. All networks are drawn with the same parameters. The network shows correlation with genes involve in many functions. A microarray spot representing a gene is denoted as a red-filled circle. The closeness of their relationship does not be represented the in the network.

OSDEF1

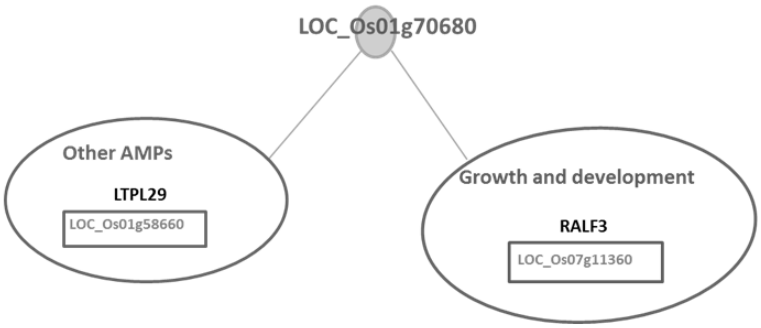

OSDEF9

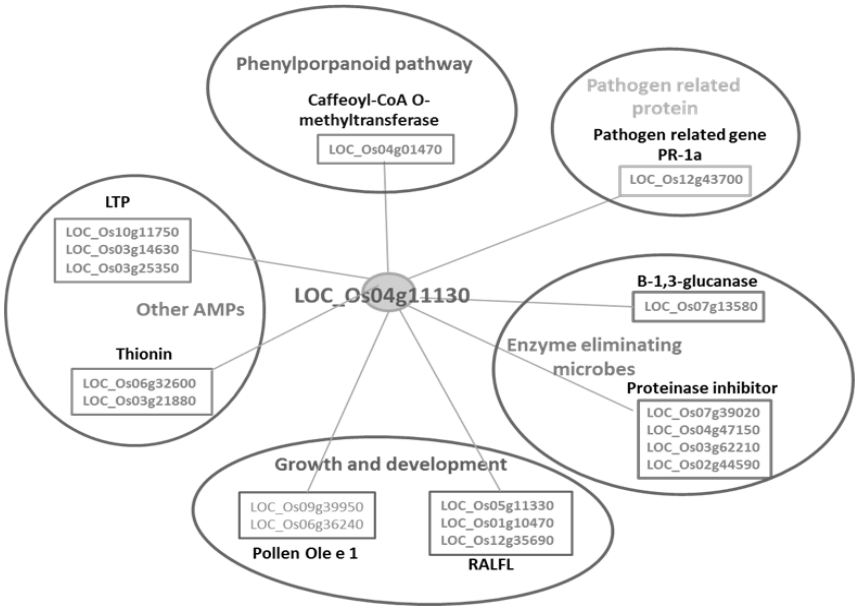

OSDEFL9

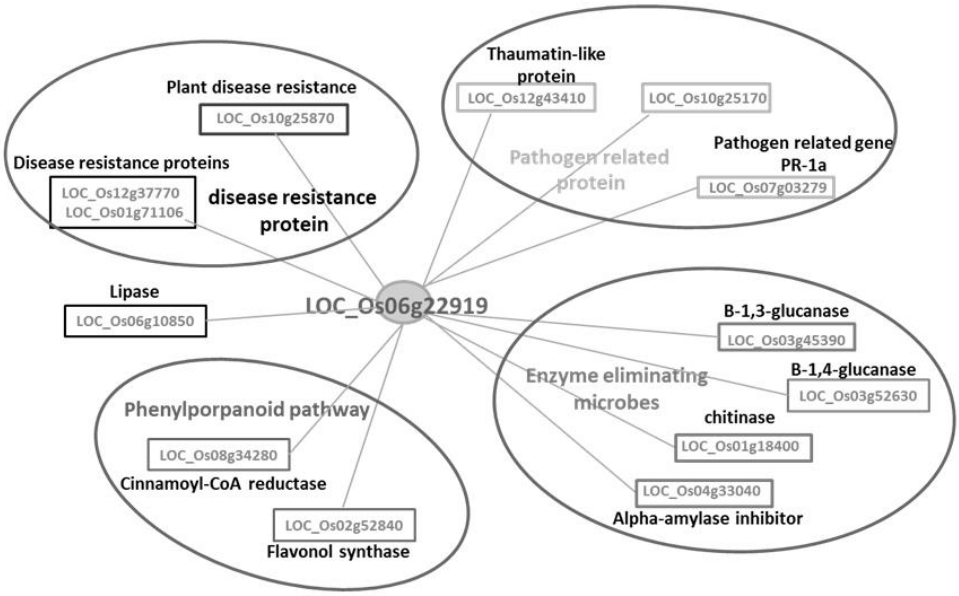

OSDEFL21

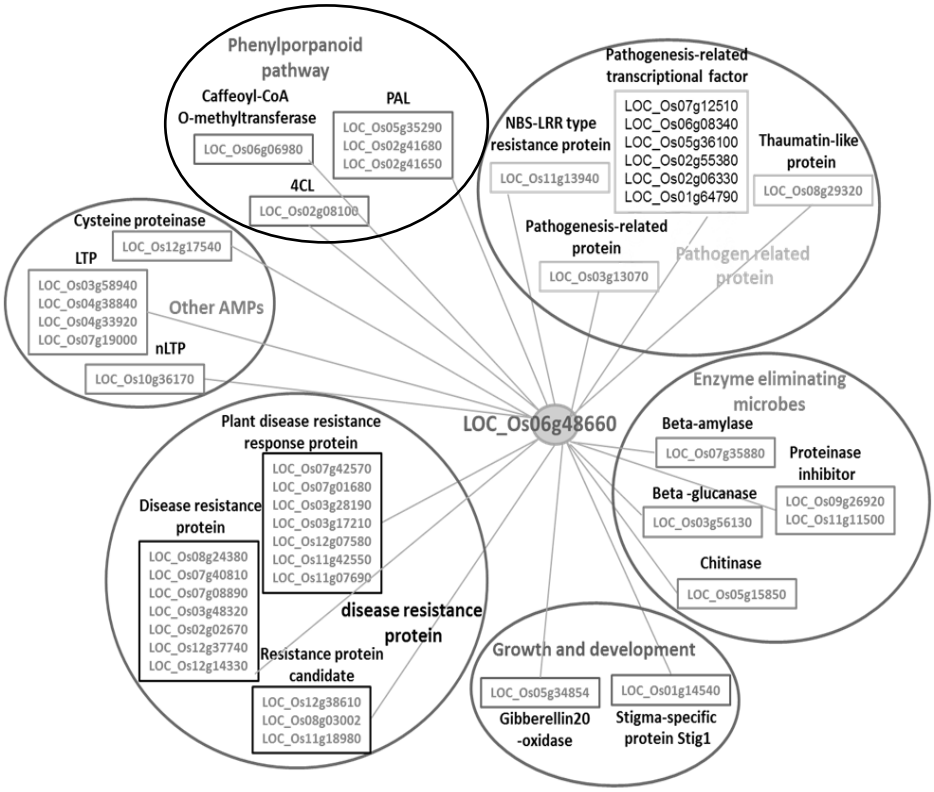

OSDEFL28

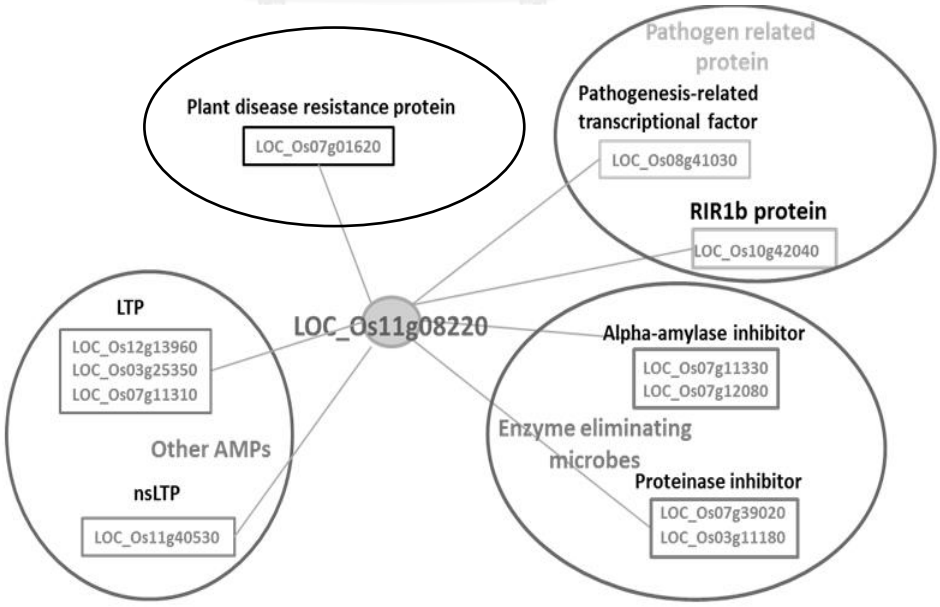

OSDEFL43

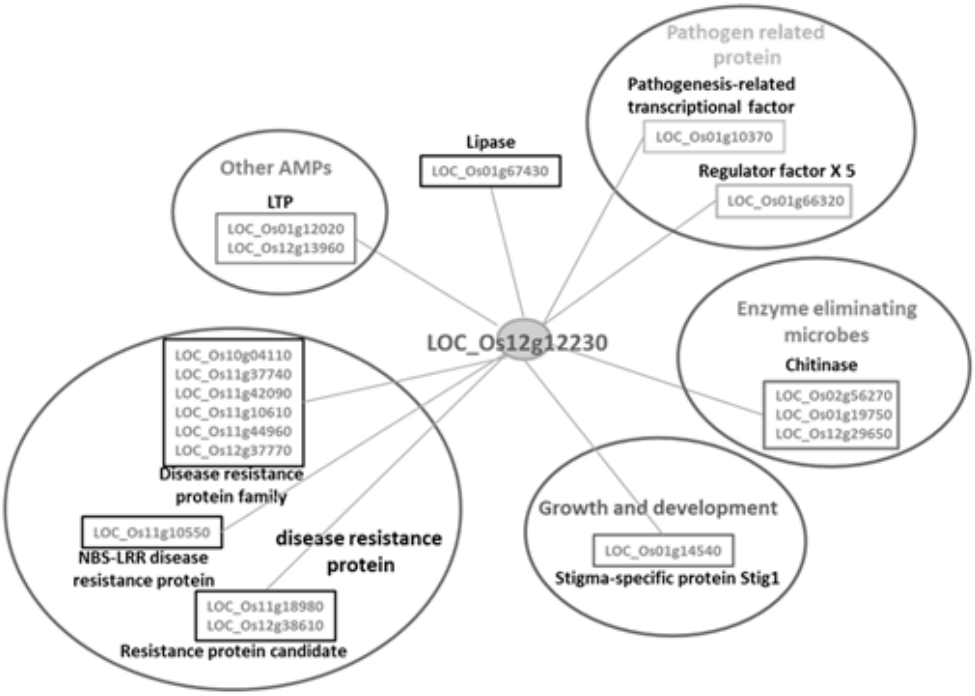

OSDEFL48

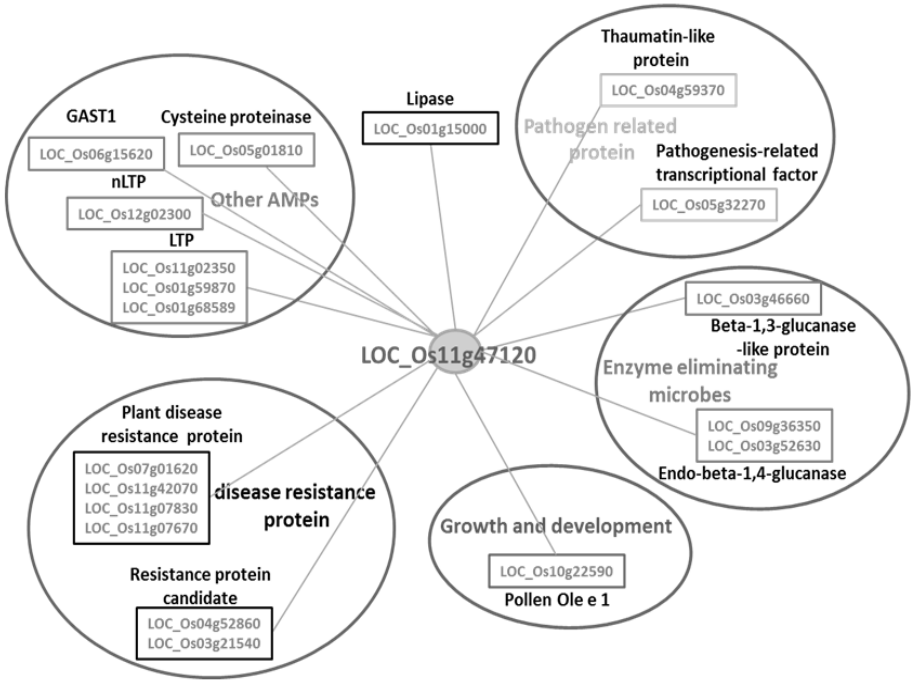

OSDEFL49

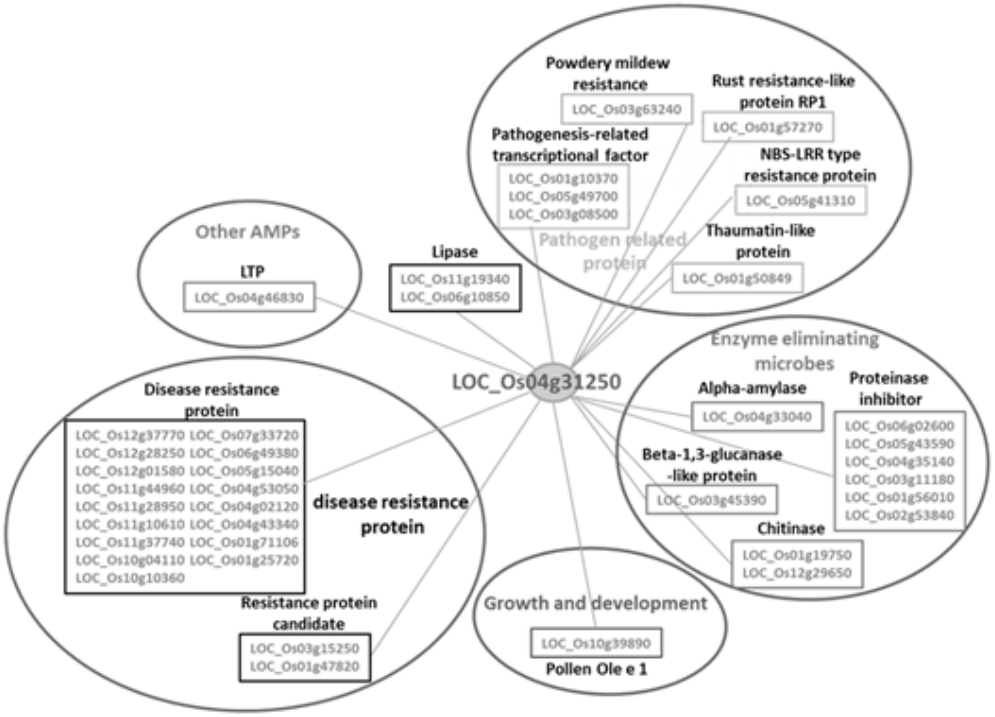

OSDEFL70

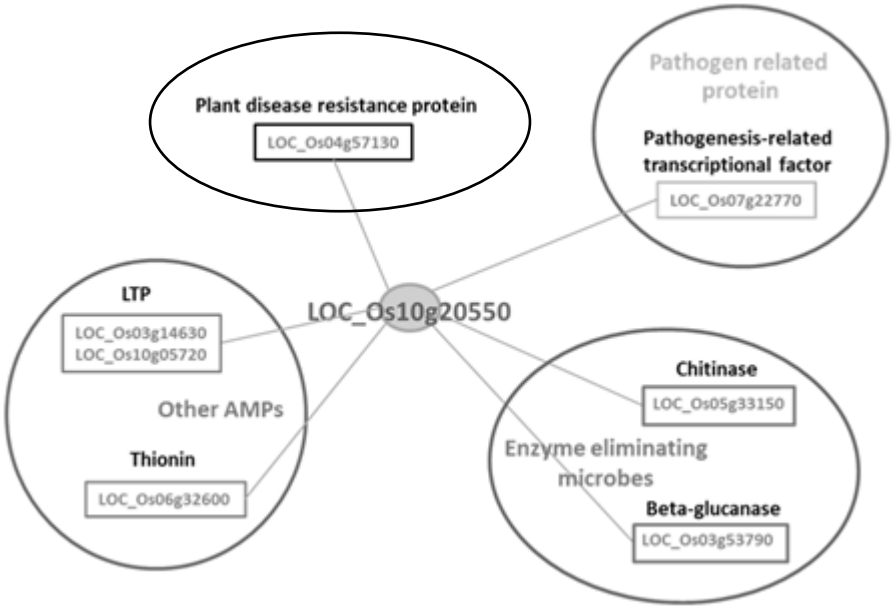

Fig. A-2 Protein sequences alignment of *OsDEFs*

Fig. A-3 The possible roles of rice *AMPs*

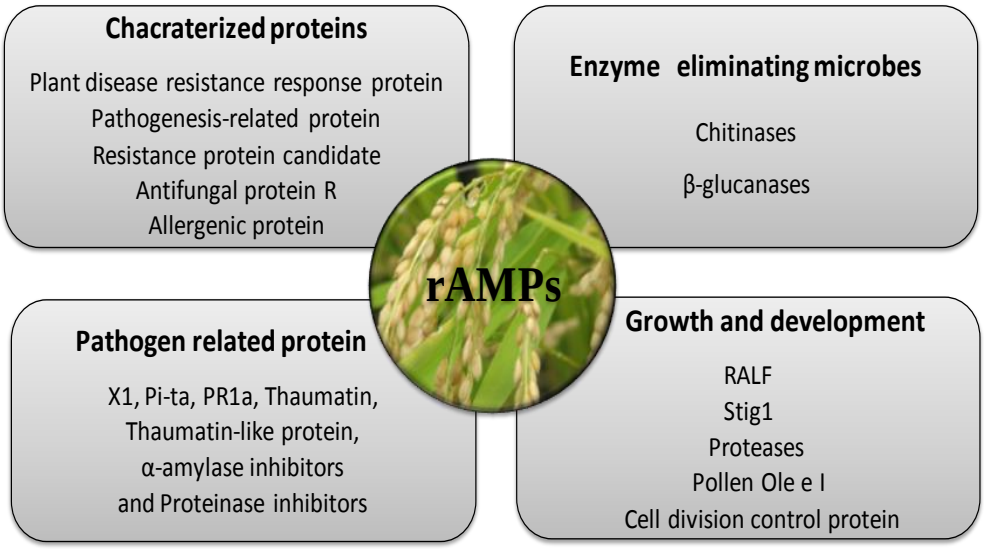

Fig. A-4 The expression levels of *Os*AMPs in different parts of rice. The expression profile represented expressing ranging from root to seeds is shown as log2 of expression values. The color bar at top reveals expression values.

Fig. A-5 Dimeric configurations of NaD1. A: Amino acid residues involved in the dimer interface for dimer shown as sticks, and the hydrogen bonds and salt bridges are shown in black as dotted lines. B: The electrostatic surface represent in NaD1 structure. C: Surface representation of dimeric NaD1is shown in gray; Lys4 residues are shown in magenta and cyan from each monomeric chain. Fig. A, B and C were taken from Lay et al., (2012). D: The amino acid sequence analysis comparing NAD1 with *Os*DEF7 and *Os*DEF8, the labeled blue show the crucial amino acids for dimer formation reported in Lay et al., (2012).

A **B** **C**

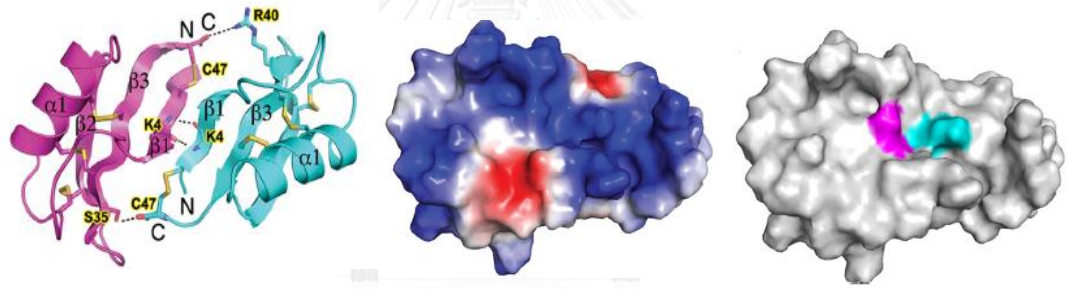

D

```
NAD1        -------ARECKTESNTFPGICITKPPCRKACISEKFTDG--HCSKILRRCLCTKPCVFD
OsDEF7      --------RHCLSQSHRFKGMCVSSNNCANVCRTESFPDGECKSHGLERKCFCKKVC---
OsDEF8      GPVMVAEARTCESQSHRFKGPCARKANCASVCNTEGFPDG--YCHGVRRRCMCTKPCP--
                   * * ::*: * * *  .  * ..* :* *.**   .  : *:*:*.* *
```

APPENDIX B

General information

Table B-1 Plant DEFs

Gene	**Organism**	**Accession number**	**Activity** (reviewed in van der Weerden et al, 2013)
*Ah*AMP1	*Aesculus hippocastanum*	AAB34970	Antifungal
*Bv*AX1	*Beta vulgaris*	P81493	Antifungal
*Bv*AX2	*Beta vulgaris*	P82010	Antifungal
*At*AFP	*Arabidopsis thaliana*	P30224	
*Vu*CPthio2	*Vigna unguiculata*	P84920	Antibacterial
*Vf*Fabatin1	*Vicia faba*	A58445	
*Vf*Fabatin2	*Vicia faba*	B58445	
*Ca*J1-1	*Capsicum annuum*	X95363	
*Ca*J1-2	*Capsicum annuum*	X95730	Antifungal
*Ms*Def1.1	*Medicago sativa*	AAV85437	
*Na*D1	*Nicotiana alata*	Q8GTM0	Antifungal
*Ph*D1	*Petunia hybrida*	Q8H6Q1	Antifungal
*Ph*D2	*Petunia hybrida*	Q8H6Q0	Antifungal
*Ps*D1	*Pisum sativum*	P81929	Antifungal
*Ps*D2	*Pisum sativum*	P81930	Antifungal
*Rs*AFP1	*Raphanus sativus*	P69241	Antifungal
*Rs*AFP2	*Raphanus sativus*	P30230	Antifungal
*Sa*AFP2a	*Sinapis alba*	P30232	
*Ha*SD2	*Helianthus annuus*	AF178634	Antifungal
*Tu*Tk-AMP-D1	*Triticum urartu*	EMS52097	
*Tk*AMPD2	*Triticum kiharae*	P84968	
*Tk*AMPD3	*Triticum kiharae*	P84970	
*Tk*AMPD4	*Triticum kiharae*	P84971	
*Tk*AMPD5	*Triticum kiharae*	P84966	
*At*Tk-AMP-D6	*Aegilops tauschii*	EMT11361	
*At*Tm-AMP-D1.2	*Aegilops tauschii*	EMT22728	
*Vr*D1	*Vigna radiata*	AAR08912	Antibacterial

*Ct*AMP	*Clitoria ternatea*	AAB34971	Antifungal
*Dm*AMP1	*Dahlia merckii*	AAB34972	Antifungal
*EG*AD1	*Elaeis guineensis*	AF322914	Antifungal
*Hs*AFP1	*Heuchera sanguinea*	AAB34974	Antifungal
*Pg*D1	*Picea glauca*	AY494051	Antifungal
*Ah*PDF1.1	*Arabidopsis halleri*	AAY27736	Zinc tolerance
*Rs*AFP3	*Raphanus sativus*	CAA65984	Antifungal
*Rs*AFP4	*Raphanus sativus*	O24331	Antifungal
*So*D2	*Spinacia oleracea*	P81571	Antifungal Antibacterial
*Ta*Def	*Triticum aestivum*	AB089942	Antibacterial
*Tp*Def	*Tephrosia platycarpa*	AAX86993	Antifungal
*Sl*TPP3	*Solanum lycospersicum*	AAA80496	Antifungal
*Vu*def	*Vigna unguiculata*	ACJ06538	Antifungal
*Wj*WT1	*Wasabi japonica*	BAB19054	Antifungal
*Zm*ES1	*Zea mays*	AAK08132	Protein synthesis inhibitor, Antibacterial
*Zm*ESR6	*Zea mays*	CAH61275	Antifungal, Antibacterial

Fig. B-1 GenScript OptimumGeneTM algorithm

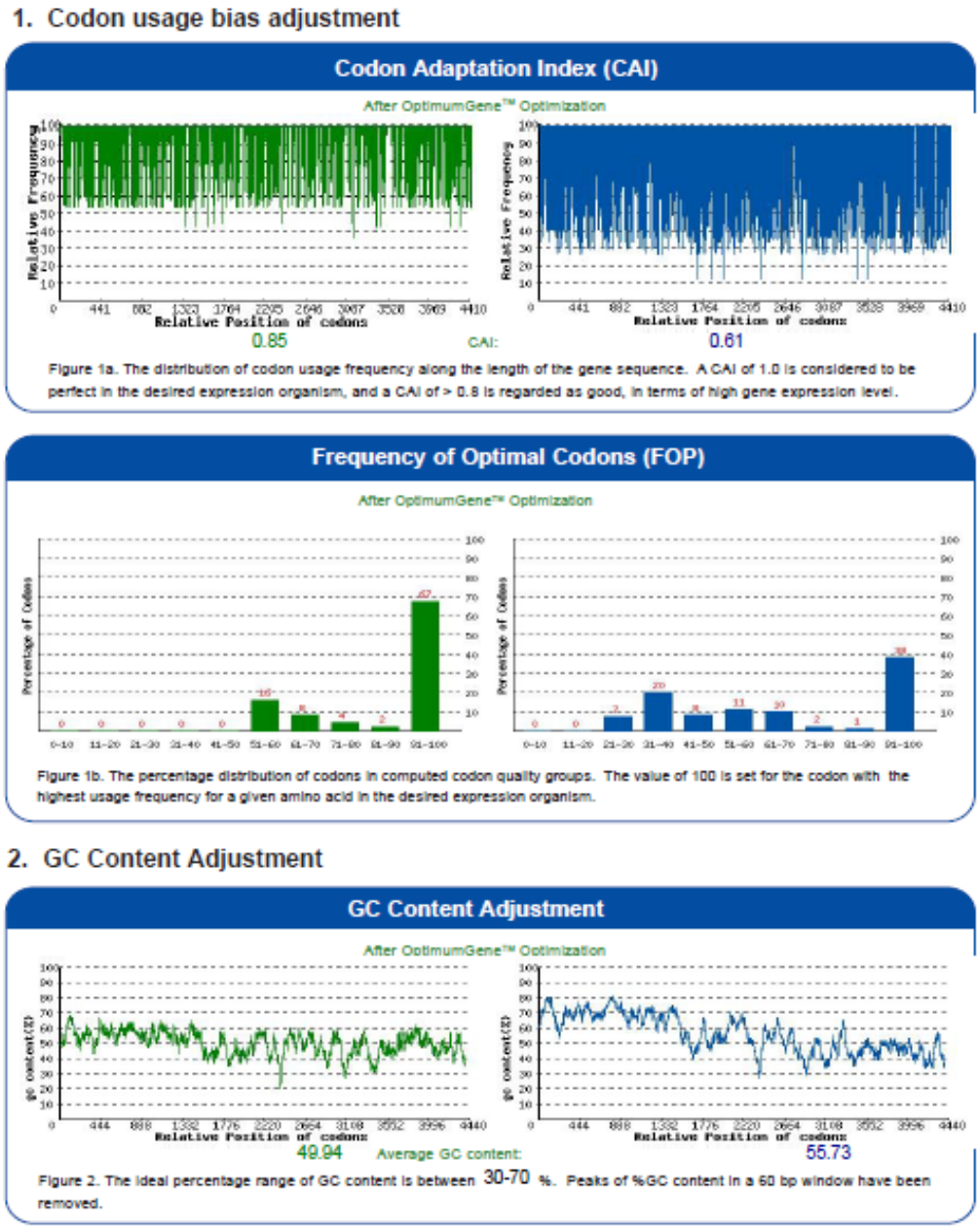

Fig. B-2 The partial nucleotide sequence of *Vv*STS optimized by GenScript OptimumGeneTM algorithm.

```
Optimized    11   ATGGCCTCTGTGGAAGAATTTCGCAACGCTCAACGTGCTAAAGGACCCGCTACTATTTTG
Original     11   ATGGCTTCAGTCGAGGAATTTAGAAACGCTCAACGTGCCAAGGGTCCGGCCACCATCCTA

Optimized    71   GCTATTGGGACTGCTACCCCCGACCACTGTGTGTATCAATCCGATTACGCCGACTACTAC
Original     71   GCCATTGGCACAGCTACCCCCGACCACTGTGTCTACCAGTCTGATTATGCTGATTACTAT

Optimized   131   TTTAAAGTTACCAAAAGTGAACATATGACTGCCTTGAAGAAAAAATTTAATCGCATTTGC
Original    131   TTCAAGGTCACTAAGAGCGAGCACATGACTGCGTTGAAGAAGAAGTTCAATCGCATATGT

Optimized   191   GATAAAAGTATGATTAAAAAACGTTACATTCATCTGACCGAAGAAATGTTGGAAGAACAC
Original    191   GACAAATCCATGATCAAGAAGCGTTACATTCATTTGACCGAAGAAATGCTTGAGGAGCAC

Optimized   251   CCCAATATTGGCGCTTACATGGCCCCCAGCTTAAACATTCGCCAAGAAATTATTACTGCT
Original    251   CCAAACATTGGTGCTTATATGGCTCCATCTCTTAACATACGCCAAGAGATTATCACTGCT

Optimized   311   GAAGTGCCCAAACTGGGCAAAGAAGCCGCTTTAAAAGCCCTGAAAGAATGGGGTCAGCCC
Original    311   GAGGTACCCAAGCTCGGTAAGGAAGCAGCATTGAAGGCTCTTAAAGAGTGGGGTCAGCCT
```

Fig. B-3 P*trc* promoters used (Camsund et al., 2014; Huang et al., 2010). P*trc*1Ocore is the P*trc*-derived promoters with *lacOsym* between the −35 box and −10 box. The *lacOsym* sequence varies in length from −1 bp (where 1 bp of *lacOsym* is part of the −35 box and −10 box, as underlined) to 19 bp. P*trc*1O is the P*trc*-promoters divided −35 and −10 element with 17-bp spacer and the 21-bp -*lac1O* operator located 6-bp downstream of the -10 box.

P*trc*1Ocore GAGCTGTTGACAATTGTGAGCGCTCACAATATAATGTGTGGAA

-35 box *lacOsym* -10 box

P*trc*1O TTGACAATTAATCATCCGGCTCGTATAATGTGTGGAATTGTGAGCGGATAACAATTTCACACA

-35 box 17-bp spacer -10 box *lac1O*

Fig. B-4 Vectors used; A: pJET cloning plasmid B: pGEX-6P-3, C: expression vectors pPMQAK1 (Huang et al., 2010).

A

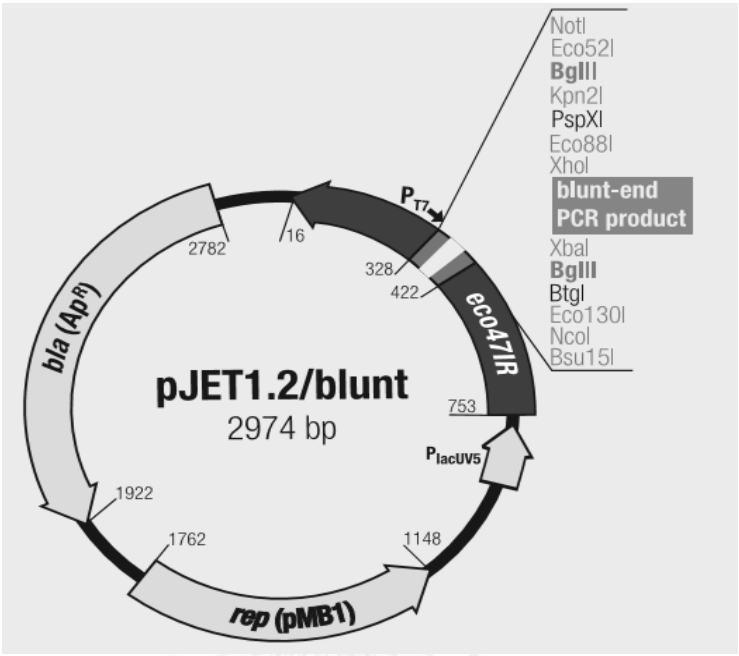

B

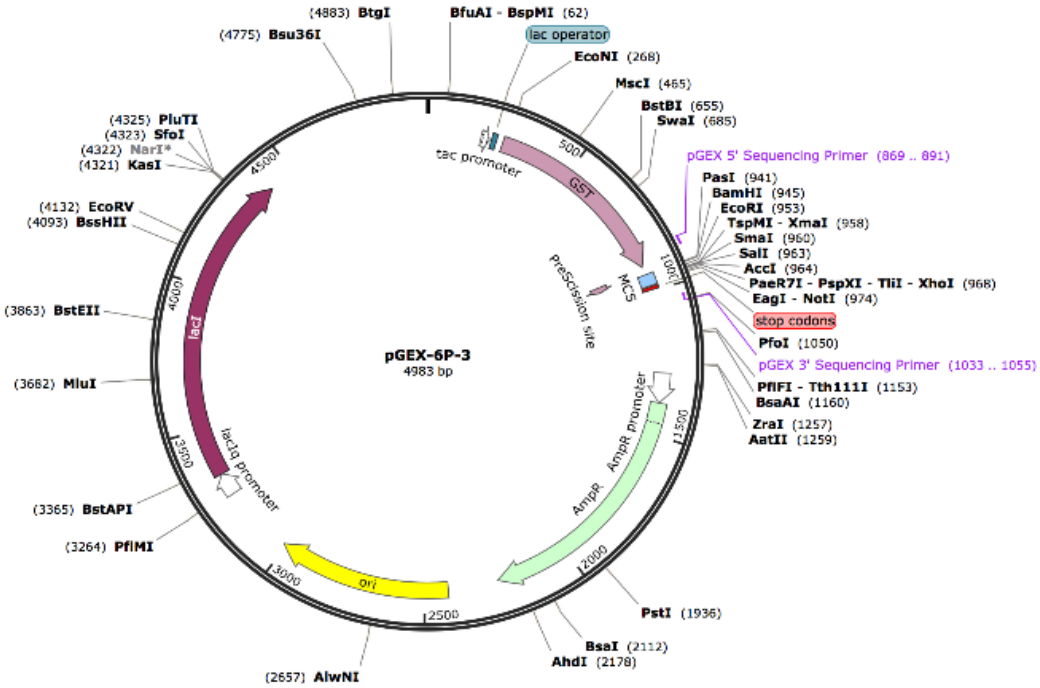

C

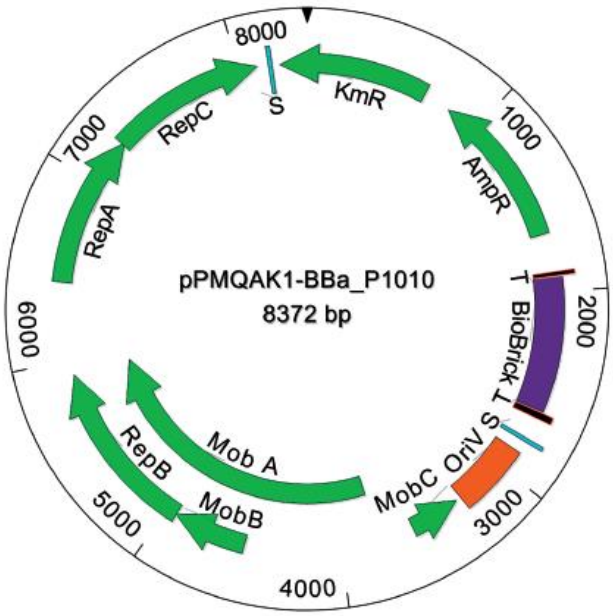

APPENDIX C

Primer lists

Table C-1 The list of oligonucleotide sequences used

Primer name	Primer Sequence (5´-3´)	T_m (°C)
DEF7_F	AAAGGATCCATGAGGCACTGCCTGTCGCAGAG	67.0
DEF7_R	AAAGTCGACCTAGCAGACCTTCTTGCAGAAG	63.0
DEF8_F	AAAGGATCCATGGGGCCGGTGATGGTGGCGGA	69.5
DEF8_R	AAAGTCGACTCAGGGGCAGGGCTTGGT	64.3
pGEX_SF	ACATGGACCCAATGTGCCTGGATG	59.1
DEF7_trcoreF	TTTGAATTCGAGCTGTTGACAATTGTGAGCGCTCACAATATAATGTGTG GAATAGTGGAGGTTACTAGATGAGGCACTGCCTGTCGCAGA	58.6
DEF7_trc1OF	TTTGAATTCTTGACAATTAATCATCCGGCTCGTATAATGTGTGGAATTGT GAGCGGATAACAATTTCACACATAGTGGAGGTTACTAGATGAGGCACT GCCTGTCGCAGA	58.6
DEF7_trcR	AACTGCAGAAAAAAAACCCCGCCCTGTCAGGGGCGGGGTTTTTTTTTTT ATTACTTCTCGAACTGAGGATGACTCCAACTTCCGCTACCGCAGACCTT CTTGCAGAAGCACTTG	59.3
DEF7_bcdF	TTTGAATTCGGGCCCAAGTTCACTTAAAAAGGAGATCAACAATGAAAG CAATTTTCGTACTGAAACATCTTAATCATGCTAAGGAGGTTTTCTAATG AGGCACTGCCTGTCGCAGA	58.6
DEF7_NstrepF	TTTGAATTCGAGCTGTTGACAATTGTGAGCGCTCACAATATAATGTGTG GAATAGTGGAGGTTACTAGATGTGGAGTCATCCTCAGTTCGAGAAGAG GCACTGCCTGTCGCAGAGCC	58.6
DEF7_NflagF	TTTGAATTCGAGCTGTTGACAATTGTGAGCGCTCACAATATAATGTGTG GAATAGTGGAGGTTACTAGATGGACTACAAAGACGATGACGACAAGAG GCACTGCCTGTCGCAGAGCC	58.6

DEF7_trcNR	AACTGCAGAAAAAAAACCCCGCCCTGTCAGGGGCGGGGTTTTTTTTTTT ATTAGCAGACCTTCTTGCAGAAGCACTTG	59.3
DEF7_p3F	TTTTCTAGAATGTGGAGTCATCCTCAGTTCGAGAAGAGGCACTGCCTGT CGCAGAGCC	58.6
DEF7_p3R	AACTGCAGTTATTAGCAGACCTTCTTGCAGAAGCACTTG	59.3
DEF8_trcoreF	TTTGAATTCGAGCTGTTGACAATTGTGAGCGCTCACAATATAATGTGTG GAATAGTGGAGGTTACTAGATGGGGCCGGTGATGGTGGC	60.0
DEF8_trc1OF	TTTGAATTCTTGACAATTAATCATCCGGCTCGTATAATGTGTGGAATTGT GAGCGGATAACAATTTCACACATAGTGGAGGTTACTAGATGGGGCCGG TGATGGTGGC	60.0
DEF8_trcR	AACTGCAGAAAAAAAACCCCGCCCTGTCAGGGGCGGGGTTTTTTTTTTT ATTACTTCTCGAACTGAGGATGACTCCAACTTCCGCTACCGGGGCAGGG CTTGGTGCACA	60.0
DEF8_bcdF	TTTGAATTCGGGCCCAAGTTCACTTAAAAAGGAGATCAACAATGAAAG CAATTTTCGTACTGAAACATCTTAATCATGCTAAGGAGGTTTTCTAATG GGGCCGGTGATGGTGGC	60.0
DEF8_NstrepF	TTTGAATTCGAGCTGTTGACAATTGTGAGCGCTCACAATATAATGTGTG GAATAGTGGAGGTTACTAGATGTGGAGTCATCCTCAGTTCGAGAAGGG GCCGGTGATGGTGGCGGA	60.0
DEF8_NflagF	TTTGAATTCGAGCTGTTGACAATTGTGAGCGCTCACAATATAATGTGTG GAATAGTGGAGGTTACTAGATGGACTACAAAGACGATGACGACAAGGG GCCGGTGATGGTGGCGGA	60.0
DEF8_trcNR	AACTGCAGAAAAAAAACCCCGCCCTGTCAGGGGCGGGGTTTTTTTTTTT ATTAGGGGCAGGGCTTGGTGCACA	60.0
DEF8_p3F	TTTTCTAGAATGTGGAGTCATCCTCAGTTCGAGAAGGGGCCGGTGATGG TGGCGGA	60.0
DEF8_p3R	AACTGCAGTTATTAGGGGCAGGGCTTGGTGCACA	60.0
ZmPALF	ATCTAGATCTATGGCTGGTAACGGTGC	59.7
ZmPALR	TAACTAGTGTACTATTTAATGTTAATGGGTAAGGG	58.6
PAL_trcoreF	TTTGAATTCGAGCTGTTGACAATTGTGAGCGCTCACAATATAATGTGTG GAATAGTGGAGGTTACTAGATGGCTGGTAACGGGGCTATTGT	57.1
PAL_trc1OF	TTTGAATTCTTGACAATTAATCATCCGGCTCGTATAATGTGTGGAATTGT GAGCGGATAACAATTTCACACATAGTGGAGGTTACTAGATGGCTGGTA	57.1

	ACGGGGCTATTGT	
PAL_trcR	AACTGCAGAAAAAAAACCCCGCCCTGTCAGGGGCGGGGTTTTTTTTTTT ATTACTTCTCGAACTGAGGATGACTCCAACTTCCGCTACCTTTAATGTTA ATGGGTAAGGGTTTCCCGT	57.3
PAL_rtR	GCGGGTCACTTCACTGGGTAAAGT	59.1
RsTALF	ATCTAGATCTATGCTGGCTATGAGCC	58.0
RsTALR	TAACTAGTGTACTAAACGGGGGACTGTT	58.5
TAL_trcoreF	TTTGAATTCGAGCTGTTGACAATTGTGAGCGCTCACAATATAATGTGTG GAATAGTGGAGGTTACTAGATGCTGGCTATGAGCCCCCC	57.9
TAL_trc1OF	TTTGAATTCTTGACAATTAATCATCCGGCTCGTATAATGTGTGGAATTGT GAGCGGATAACAATTTCACACATAGTGGAGGTTACTAGATGCTGGCTAT GAGCCCCCC	57.9
TAL_trCR	AACTGCAGAAAAAAAACCCCGCCCTGTCAGGGGCGGGGTTTTTTTTTTT ATTACTTCTCGAACTGAGGATGACTCCAACTTCCGCTACCAACGGGGGA CTGTTGTAATAAGTGAG	58.0
TAL_rtR	TGGGCACAGCGGGAGCCAATTCA	60.6
Vv4CLF	ATCTAGATCTATGGAAGTGAAAAAAGAAGAAC	56.7
Vv4CLR	TAACTAGTGTATTAGTTGGGAACGCC	56.4
4CL_trcoreF	TTTGAATTCGAGCTGTTGACAATTGTGAGCGCTCACAATATAATGTGTG GAATAGTGGAGGTTACTAGATGGAAGTGAAAAAAGAAGAACAACCCC A	57.3
4CL_trc1OF	TTTGAATTCTTGACAATTAATCATCCGGCTCGTATAATGTGTGGAATTGT GAGCGGATAACAATTTCACACATAGTGGAGGTTACTAGATGGAAGTGA AAAAAGAAGAACAACCCCA	57.3
4CL_trCR	AACTGCAGAAAAAAAACCCCGCCCTGTCAGGGGCGGGGTTTTTTTTTTT ATTACTTCTCGAACTGAGGATGACTCCAACTTCCGCTACCGTTGGGAAC GCCCACAGCCA	57.9
4CL_rtR	GGCTTTACCGGAATAGCAGGCCTG	60.8
VvSTSF	ATCTAGATCTATGGCTAGTGTGGAAG	56.4
VvSTSR	TAACTAGTGTACTAATTGGTCACCATGG	57.0

STS_trcoreF	TTTGAATTCGAGCTGTTGACAATTGTGAGCGCTCACAATATAATGTGTG GAATAGTGGAGGTTACTAGATGGCCTCTGTGGAAGAATTTCGCA	57.7
STS_trc1OF	TTTGAATTCTTGACAATTAATCATCCGGCTCGTATAATGTGTGGAATTGT GAGCGGATAACAATTTCACACATAGTGGAGGTTACTAGATGGCCTCTGT GGAAGAATTTCGCA	57.7
STS_trCR	AACTGCAGAAAAAAAACCCCGCCCTGTCAGGGGCGGGGTTTTTTTTTTT ATTACTTCTCGAACTGAGGATGACTCCAACTTCCGCTACCGTTAGTCAC CATGGGAATAGAATGCAG	58.2
STS_bcdF	TTTGAATTCGGGCCCAAGTTCACTTAAAAAGGAGATCAACAATGAAAG CAATTTTCGTACTGAAACATCTTAATCATGCTAAGGAGGTTTTCTAATG GCCTCTGTGGAAGAATTTCGCA	57.7
STS_p3F	TTTTCTAGAATGTGGAGTCATCCTCAGTTCGAGAAGGCCTCTGTGGAAG AATTTCGCA	57.7
STS_p3R	AACTGCAGTTATTAGTTAGTCACCATGGGAATAGAATGCAG	57.7
STS_rtR	CAATTTATAATCAGCACCGGGCAT	54.0
trcore_F	TTTGAATTCGAGCTGTTGACAATT	50.6
Ptrcore_midF	TATAATGTGTGGAATAGTGGAGGT	52.3
trc1O_F	TTTGAATTCTTGACAATTAATCAT	45.4
trc_R	AACTGCAGAAAAAAAACCCCGCCC	57.4
VF2_BBa	TGCCACCTGACGTCTAAGAA	51.8
VR_Bba	ATTACCGCCTTTGAGTGAGC	51.8
pPMQAK1_F	GGCGTATCACGAGGCAGAATTTCA	57.4
pPMQAK1_R	AGGGTGGTGACACCTTGCCCTT	58.6
pJET_F	CGACTCACTATAGGGAGAGCGGC	60.6
pJET_R	AAGAACATCGATTTTCCATGGCAG	54
cat_r	GGTATATCCAGTGATTTTTTTCTCCAT	53.7

Strep_R	CTTCTCGAACTGAGGATGACTCCA	57.4
Fused_midF	AGTGACTAGCGTTGCCCAACA	54.4
Fused_midR	GCTAGTCACTTGGCCCCGAT	55.9
16S_uniF	GGGGGATCCGCTCAGATTGAACGCTGGCG	68.6
16S_uniR	CCCAAGCTTACATTTCACAACACGAGCTG	61.5
16s_F	CACACTGGGACTGAGACAC	53.2
16s_R	CTGCTGGCACGGAGTTAG	52.6
27F1	AGAGTTTGATCCTGGCTCAG	51.8
809R	GCTTCGGCACGGCTCGGGTCGATA	64.2

APPENDIX D

Reagent preparations

1. Preparation for media

1.1 Luria-Bertini (LB) broth 1 L

Tryptone	10	g
Yeast extract	5	g
NaCl	10	g

All components were dissolved in 1L distilled water and then autoclaved at 121° C, 15 1b/in^2 for 15 min.

1.2 LB agar 1 L

Tryptone	10	g
Yeast extract	5	g
NaCl	10	g
Agar	15	g

All components were dissolved in 1L distilled water and then autoclaved at 121° C, 15 1b/in^2 for 15 min.

1.3 BG-11 1 L

Stcok solution 1L

(1) $NaNO_3$	150	g
(2) K_2HPO_4	40	g
(3) $MgSO_4$.7H2O	75	g
(4) $CaCl_2$.2H_2O	36	g
(5) Citric acid	6	g

(6) Ammonium ferric citrate green	6	g
(7) $EDTANa_2$	1	g
(8) Na_2CO_3	20	g
(9) Trace metal solution:		
H_3BO_3	2.86	g
$MnCl_2.4H_2O$	1.81	g
$ZnSO_4.7H_2O$	0.22	g
$Na_2MoO_4.2H_2O$	0.39	g
$CuSO_4.5H_2O$	0.08	g
$Co(NO_3)_2.6H_2O$	0.05	g

10 mL stock solution 1 was mixed with 1.0 mL Stock solutions 2-9. The distilled water was added for making up volume to 1L and its pH was adjusted to 7.1 by using 1M NaOH or HCl. For agar, BG-11 was added with 15.0 g per liter of Bacteriological Agar. Then, it was autoclaved at 121° C, 15lb/in^2 for 15 min. and stored at room temperature

2 Preparation for agarose electrophoresis

2.1 50X Tris-acetate-EDTA buffer (TAE buffer) 1 L

Tris base	242.5	g
Glacial acetic acid	57	mL
0.5M EDTA (pH 8.0)	100	mL

The distilled water was added for making up volume to 1L and its pH was adjusted to 8.3 by using HCl. Then, it was autoclaved at 121° C, 15lb/in^2 for 15 min. and stored at room temperature.

2.2 50X Tris-boratate-EDTA buffer (TBE buffer) 1 L

Tris base	540	g
Boric Acid	275	mL
Na- EDTA	46.88	mL

The distilled water was added for making up volume to 1L and its pH was adjusted to 8.3 by using HCl. Then, it was autoclaved at 121° C, 151b/in^2 for 15 min. and stored at room temperature.

2.3 1% Agarose gel

Agarose	1	g
1X TAE or TBE buffer	100	mL

3. Preparation for SDS-PAGE

3.1 Stock reagent

3.1.1 30 % Acrylamide, 0.8 % bis-acrylamide 100 mL

Acrylamide	29.2	mg
N,N–methylene-bis-acrylamide	0.8	g

3.1.2 1.5 M Tris-HCl, pH 8.8

Tris (hydroxymethyl)-aminomethane	18.17	g

The pH of solution was adjusted to 8.8 by HCl and brough the volume up to 100 mL distilled water.

3.1.3 1 M Tris-HCl, pH 6.8

Tris (hydroxymethyl)-aminomethane	12.1	g

The pH of solution was adjusted to 6.8 by HCl and brough the volume up to 100 mL distilled water.

3.1.4 10 % Ammonium persulfate

Ammonium persulfate	0.1	mg
Distilled water	1	mL

3.1.5 10 % SDS

SDS	0.1	mg
Distilled water	1	mL

3.2 5X Sample buffer

1M Tris-HCl, pH 6.8	0.6	mL
Glycerol	2.5	mL
10 % SDS	2	mL
2-mercaptoethanol	0.5	mL
1 % bromophenol blue	1	mL
Distilled water	3.4	mL

One part of 5X sample buffer is added to four parts of sample. The mixture is heated at 95°C for 5 min and centrifuged at 12,000 rpm for 5 min before loading to the gel.

3.3 10X Electrophoresis running buffer 1 L

Tris (hydroxymethyl)-aminomethane	30.3	g
Glycine	144	g
SDS	10	g

The distilled water was used for adjusting volume to 1 liter.

3.4 SDS gel

3.4.1 12 % separating gel

Distilled water	3.3	mL
1.5 M Tris-HCl, pH 8.8	2.5	mL
30 % acrylamide solution	4	mL
10 % SDS	0.1	mL
10 % Ammonium persulfate	0.1	mL
TEMED	0.004	mL

3.4.2 5.0 % stacking gel

Distilled water	1.4	mL
1. M Tris-HCl, pH 6.8	0.25	mL
30 % acrylamide solution	0.33	mL
10 % SDS	0.02	mL
10 % Ammonium persulfate	0.02	mL
TEMED	0.002	mL

3.5 Staining solution

Coomassie brilliant blue R-250	0.5	g
Methanol	250	mL
Glacial acetic acid	50	mL

The distilled water was used for adjusting volume to 500 mL and mixed well.

3.6 Destaining solution

Methanol	100	mL
Glacial acetic acid	100	mL

Add distilled water to 1000 mL and mix.

4. Western blot analysis buffer solutions

4.1 10X Phosphate-buffered saline (PBS), pH 7.4

NaCl	80	g
KCl	80	g
Na_2HPO_4	14.4	g
KH_2PO_4	2.4	g

The pH of solution was adjusted to 7.4 by HCl and the volume was brought up to 1,000 mL distilled water.

4.2 1X PBST buffer 1 L

NaCl	8	g
KCl	8	g
Na_2HPO_4	1.44	g
KH_2PO_4	0.24	g
Tween 20	1	mL

The pH of solution was adjusted to 7.4 by HCl and the volume was brought up to 1,000 mL distilled water.

4.3 Blocking buffer for strep-tagged protein 20 mL

BSA	0.6	g
Tween 20	0.1	mL
1X PBS	19.9	mL

4.4 10X Tris-buffered saline (TBS) , pH 7.4

Tri-base	24.2	g
NaCl	87.8	g

The pH of solution was adjusted to 7.4 by HCl and the volume was brought up to 1,000 mL distilled water.

4.5 10X TBST buffer 1 L

Tris-base	24.2	g
NaCl	87.8	g
Tween 20	0.5	mL

The pH of solution was adjusted to 7.4 by HCl and the volume was brought up to 1,000 mL distilled water.

4.6 Blocking buffer for flag-tagged protein 20 mL

Skim milk	1	g
1X TBST	20	mL

4.7 Antibody dilution buffer 1 mL

BSA	2	mg
Tween 20	1	µL
1X PBS	1	mL

5. Competent cell preparation

5.1 0.1M $CaCl_2$ 1L

$CaCl_2$	14.7	g

Add distilled water to 1L and mix

5.2 CCMB80 buffer 1L

80 mM $CaCl_2 .2H_2O$

20 mM $MnCl_2 \cdot 4H_2O$

10 mM $MgCl_2 \cdot 6H_2O$

19 mM KOAc pH 7.0

10% glycerol

The pH of solution was adjusted to 6.4 by 0.1N HCl and the volume was brought up to 1L distilled water and then sterillesed filter in hood.

APPENDIX E

Methods

1. Phenol/Chloroform Extraction

1) Add an equal volume of phenol: chloroform (1:1) (at least 200 µL) to digestion reaction

2) Mix well, spin at 13000 rpm for 5 min.

3) Carefully remove the aqueous layer (upper phase) to a new tube, avoid the interface

4) Repeat step 1-3 until an interface is no longer visible

5) To remove traces of phenol, add an equal volume of chloroform to the aqueous layer

6) Spin at 13000 rpm for 2 min.

7) Remove aqueous layer (upper phase) to new tube

8) Clean sample by ethanol precipitation

2. Ethanol Precipitation

1) Add 10% volume of 3M NaOAc pH 4.6

2) Add 3.5 volume of 95% ethanol

3) Spin at 13000 rpm for 20 min

4) Wash with 200 µL of 70% ethanol

5) Air dry

6) Resuspend with 10-20 µL sterile distilled water

3. Competent cells preparation

1) Inoculate single colonies in 30 mL of LB and grow at 37°C over night

2) Transfer cells to 250 mL LB, and incubate till OD_{600} = 0.3

3) Centrifuge at 3000g at 4°C for 10 min.

4) Gently resuspend in 80 mL ice cold CCBM buffer

5) Incubate on ice for 20 min.

6) Centrifuge at 3000g at 4°C for 10 min. and resuspend in 10 mL ice cold CCBM buffer

7) Incubate on ice for 20 min.

8) Aliquot 100 uL into microcentrifuge tube

9) Store at -80^{o}C

APPENDIX F

Protein determinations

1. Preparation of solutions for protein assays

Bradford's reagent

Distilled water

Bradford' reagent was diluted with distilled water at 1:4 volume ratio. Then solution was filtered by filter paper, What man No. 1, and kept at 4 ^{o}C in the brown bottle. (only for 4 weeks)

2. Standard curve of BSA

The standard curve of BSA was constructed using Bradford protein assay method for protein determination. The method is as follows;

1. 1 μg μL^{-1} BSA was diluted with distilled water as 0.1-0.6 μg (**Table C-1**)

2. 5 μL BSA from stock solution was added into 96 wells microplate.

Table F-1 Standard curve BSA

BSA (μg)	Reagent volume (μL)	
	1 μg μL^{-1} of BSA	dH_2O
0	-	1000
0.1	100	900
0.2	200	800
0.3	300	700
0.4	400	600
0.5	500	500
0.6	600	400

3. 300 μL of Bradford's reagent was added and incubated for 5 minutes

4. The product was measured by an increase in the absorbance at 595 nm.

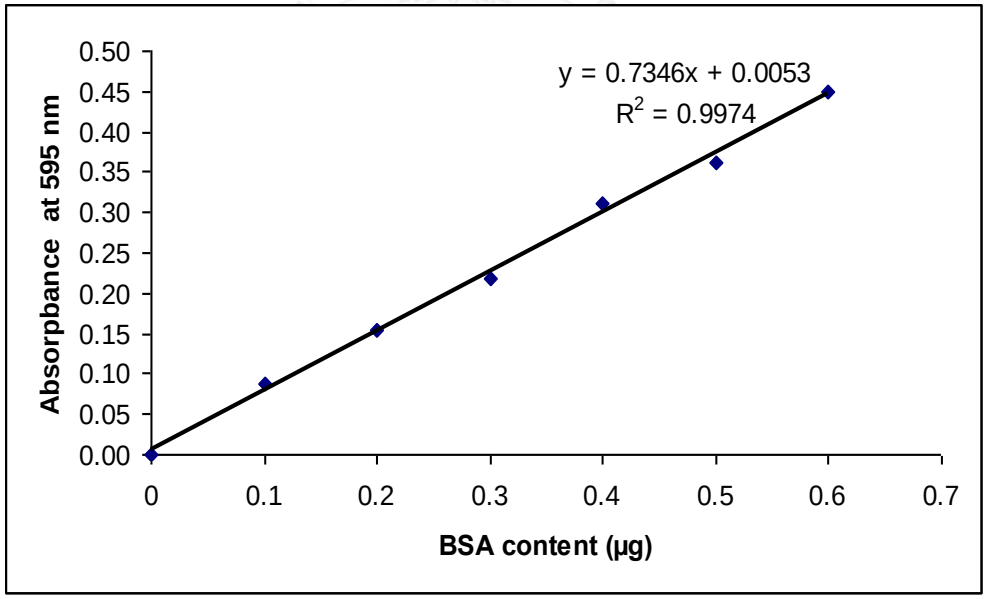

Fig. F-1 Standard curve of BSA

APPENDIX G

Calculation methods

1. Calculation of PCR (insert) volume for ligation

Molar ratio of insert and vector = 3:1

$$\text{volume of insert (ng)} = \frac{\text{volume of vector (ng)} \times \text{size of insert} \times \text{molar ratio}}{\text{size of vector}}$$

2. Calculation of chlorophyll *a* concentration

From $A_{665} = \varepsilon lc$

An extinction coefficient of 78.74 liter/gram/cm for Chl *a* in 90% methanol

So $\varepsilon = 78.74 L\ g^{-1}cm^{-1}$ (Meeks and Castenholz, 1974)

$l = 1$ cm

$$\text{Chlorophyll } a \text{ concentration (mg mL}^{-1}) = \frac{A_{665}}{(78.74\ L\ g^{-1}cm^{-1} * 1\ cm)}$$

$$\text{Chlorophyll } a \text{ concentration (}\mu g\ mL^{-1}) = 12.7 * A_{665}$$

3. Calculation of total cyanobacterial cells (Eaton-Rye, 2004)

An OD_{730} of 0.25 = 1×10^8 cells mL^{-1}

Total cell = $(OD_{730}/0.25) \times 10^8$ cells

VITA

Miss Supaluk Tantong was born on March 27, 1985 in Bangkok, Thailand. She graduated with the Bacherlor Degree of Science in Biochemistry from Department of Biochemistry, Faculty of Science, Chulalongkorn University in 2006 and her Master's Degree of Science in Biotechnology from Program in Biotechnology at the same institution in 2008. She has participated in several conferences during 2011-2015. In 2015, she took parts of her thesis to publish entitle "Two novel antimicrobial defensins from rice identified by gene coexpression network analysis" by Supaluk Tantong, Onanong Pringsulaka, Kamonwan Weerawanit, Rakrudee Sarnthima, and Supaart Sirikantaramas. She also submitted a manuscript entitled "Potential of Synechocystis PCC 6803 as a novel cyanobacterial chassis for heterologous expression of enzymes in the trans-resveratrol biosynthetic pathway" by Supaluk Tantong, Aran Incharoensakdi, Supaart Sirikantaramas, and Peter Lindblad.